TECHNISCHE UNIVERSITÄT MÜNCHEN

Professur für Biochemie

# Negative Regulation of HIF1$\alpha$ by the E3 Ligases RNF8 and TRAF6

**Larissa Rebecca Ringelstetter**

Vollständiger Abdruck der von der Fakultät für Chemie
der Technischen Universität München zur Erlangung des akademischen Grades eines
Doktors der Naturwissenschaften
genehmigten Dissertation.

Vorstizende/-r: Prof. Dr. Johannes Buchner

Prüfende/-r der Dissertation:
1. Prof. Dr. Michael Groll
2. Prof. Dr. Franz Hagn

Die Dissertation wurde am 26.06.2020 bei der Technischen Universität München eingereicht und durch die Fakultät für Chemie am 20.10.2020 angenommen.

## Table of Contents


**1. Summary ..... 1**

**1. Zusammenfassung ..... 2**

**2. Introduction ..... 4**

**2.1 Ubiquitination - a post-translational modification ..... 4**

2.1.1 The ubiquitin cycle ..... 4

2.1.2 Types of ubiquitination and their function ..... 5

2.1.3 E3 Ubiquitin Ligases ..... 7

**2.2 The RING E3 Ligase RNF8 ..... 10**

2.2.1 RNF8 structure ..... 10

2.2.2 RNF8 in DNA double strand break repair ..... 11

2.2.3 Functions of RNF8 in chromosome end protection, cell divison and transcriptional control ..... 12

2.3.4 RNF8 in diseases ..... 14

**2.3 HIF1α and hypoxia ..... 15**

2.3.1 HIF1α structure ..... 16

2.3.2 Post-translational modifications of HIF1α ..... 16

2.3.4 HIF1α in diseases ..... 19

**2.4 TRAF6 in cellular signaling ..... 20**

2.4.1 TRAF6 in hypoxia ..... 21

**3. Aim of this study ..... 22**

**4. Results ..... 23**

**4.1 Identification of new interaction partners of RNF8 ..... 23**

4.1.1 Establishing a genome-wide yeast-two-hybrid screen ..... 23

4.1.2 Hit identification and verification ..... 25

**4.2 HIF1α - a new interaction partner of RNF8 ..... 30**

4.2.1 Full length HIF1α interacts with RNF8 in Y2H ..... 30

4.2.2 HIF1α and RNF8 interact in human cells ..... 31

4.2.3 Mapping of the protein-protein interaction domains of HIF1α and RNF8 ..... 32

**4.3 RNF8 counteracts the HIF1α stabilization mediated by the E3 Ligase TRAF6 ..... 36**

4.3.1 TRAF6 interacts with HIF1α and stabilizes HIF1α protein levels ..... 36

4.3.2 RNF8 counteracts the TRAF6 derived stabilization of HIF1α, independent of its catalytic activity ..... 37

4.3.3 Hypoxia vs. Normoxia – TRAF6 leaves the complex ..... 39

4.3.4 RNF8 and TRAF6 overexpression reduce HIF1 transcriptional activity ..... 40

**5. Discussion ..... 43**

**5.1 Finding new interaction partners of RNF8 using a Y2H screen ..... 43**

5.1.1 The Y2H approach as a tool to identify new interactors of RNF8 ..... 43

5.1.2 Hit verification and selection ..... 45

**5.2 HIF1α – a new interaction partner of RNF8 ..... 48**

5.2.1 HIF1α specifically interacts with RNF8 ..... 48

5.2.2 RNF8 interacts with HIF1α independent of its catalytic activity ..... 49

5.2.3 RNF8 interacts with HIF1α via its FHA domain ..... 50

**5.3 The HIF1α/TRAF6/RNF8 complex ..... 51**

5.3.1 HIF1α, TRAF6 and RNF8 interact among each other ..... 51

5.3.2 Destabilization of HIF1α by TRAF6 and RNF8 ..... 52

5.3.3 The complex of TRAF6 and RNF8 with HIF1α and its functional relevance ..... 56

**6. Conclusion and perspectives ..... 58**

**7. Material and Methods ..... 60**

**7.1 Material ..... 60**

7.1.1 Instruments and Equipment ..... 60
7.1.2 Chemicals ..... 63
7.1.3 Antibodies ..... 65
7.1.4 Enzymes and Kits ..... 65
7.1.5 Bacterial Strain ..... 66
7.1.6 Yeast strains ..... 66
7.1.7 Eukaryotic cell lines ..... 67
7.1.8 Plasmids ..... 67
7.1.9 Oligonucleotides ..... 68
7.1.10 Buffers and Solutions ..... 68
7.1.11 Software ..... 70

**7.2. Methods ..... 70**

7.2.1 Molecular biology methods ..... 70
7.2.1.1 Polymerase chain reaction (PCR) ..... 70
7.2.1.2 Agarose gel electrophoresis and DNA gel extraction ..... 71
7.2.1.3 Restriction Digest ..... 71
7.2.1.4 Ligation ..... 72
7.2.1.5 Transformation of *E.coli* ..... 72
7.2.1.6 Isolation of plasmid DNA from *S.cerevisiae* ..... 72
7.2.1.7 RNA extraction ..... 72
7.2.1.8 cDNA synthesis and Quantitative Realtime PCR ..... 73
7.2.2 Cell biological methods ..... 74
7.2.2.1 Storage of human cell lines ..... 74
7.2.2.2 Cultivation of human cell lines ..... 74
7.2.2.3 Inducing hypoxia or hypoxia mimicking conditions ..... 75
7.2.2.4 Transfection of human cells ..... 75
7.2.2.5 Storage and cultivation of *S. cerevisiae* ..... 76
7.2.2.6 Yeast colony PCR ..... 76
7.2.2.7 Preparation of competent yeast ..... 77
7.2.2.8 Trichloroacetic acid (TCA) protein precipitation ..... 77
7.2.2.9 Yeast-two-hybrid (Y2H) assay ..... 77
7.2.2.10 Transformation of yeast cells ..... 78
7.2.2.11 Yeast-two-hybrid (Y2H) – Screening approach ..... 78
7.2.3 Biochemical and immunological methods ..... 79
7.2.3.1 SDS-Polyacrylamid Gelelektrophoresis (SDS-PAGE) ..... 79
7.2.3.2 Western Blot and immunodetection ..... 80
7.2.3.3 GFP-TRAP Assay ..... 80

**8. References ..... 82**

**9. Abbreviations ..... 97**

**10. Supplement ..... 100**

**11. Appendix ..... 101**

**11.1 Publications ..... 101**
**11.2 Acknowledgement ..... 102**

# 1. Summary

Ubiquitination plays an essential role in almost all cellular functions of eukaryotic cells. It is a reversible post-translational modification that determines the fate of its substrates concerning localization, activation or degradation. The E3 ligase RNF8 belongs to the RING finger family of ligases and is able to modify targets with Lys48-linked, Lys63-linked as well as Lys11-linked ubiquitin chains, determined by the interacting E2 enzyme. Due to its roles in cell division, chromosome end protection and DNA double strand break (DSB) repair, RNF8 is a crucial factor to maintain genomic stability. Thus, it has been closely related with tumorigenesis as well as cancer progression and metastasis. We used a genome-wide yeast-two-hybrid (Y2H) screen, to identify new interaction partners of RNF8, thereby getting new insights in its role in tumor development. 1600 hits were initially identified and verified in several validation steps. With the help of follow up Y2H assays, PCR and western blot analysis we finally isolated 138 remaining hit plasmids from yeast and submitted the samples for sequencing analysis. The most frequent shows in the screen were counted as final hits. Full-length proteins were generated and tested again in yeast, concluding HIF1$\alpha$ as top hit and new interaction partner of RNF8.

As the $O_2$ labile subunit of the transcription factor HIF1, HIF1$\alpha$ is known as the master regulator of cellular adaption to low oxygen tension (hypoxia). HIF1$\alpha$ overexpression is associated with poor patient prognosis in a variety of cancers, including triple negative breast cancer (TNBC). Also RNF8 is known to be upreguated in this most aggressive subtype and treatment resistant form of breast cancer. Therefore, this new protein-protein interaction displays a highly interesting, possible new therapeutic target in TNBC treatment. We were able to prove the specificity of the interaction of RNF8 and HIF1$\alpha$ by a bait dependency test in yeast as well as co-IP assays in human embryonal kidney cells. Several truncations were used to map the interaction of both proteins, revealing that the FHA domain of RNF8 is mandatory for a positive interaction; the FHA domain enables the E3 ligase to bind the TAD domain of HIF1$\alpha$. This is independent of oxygen-dependent modifications of the latter protein. Further interaction studies revealed the additional binding of TRAF6 to RNF8 and of TRAF6 to HIF1$\alpha$. TRAF6 stabilizes HIF1$\alpha$ protein levels, whereas RNF8 has no obvious effects on

its own. However, if RNF8 joins the complex, the stabilizing effect is not only reverted, but HIF1α levels are also decreased to no detection limit. This is independent of the oxygen status of the cell; nevertheless, we observed less TRAF6 in the complex with RNF8 and HIF1α under low oxygen conditions. Interestingly, the down regulation of HIF1α is independent of the catalytic activity of RNF8, which raises the question whether TRAF6 gains the function to bind Lys48 or Lys11 specific E2 enzymes with the help of RNF8, to promote the degradation of the alpha subunit. Importantly, HIF1α dependent target gene activation is significantly decreased as soon as RNF8 is co-expressed with TRAF6 and HIF1α. This study proves a functional consequence of the down regulation of HIF1α and unravels a possible new tumor suppressor role of RNF8 by counteracting the HIF1α-driven cancer progression through TRAF6.

# 1. Zusammenfassung

Die Ubiquitinierung von Proteinen ist eine essentielle, post-translationale Modifikation, die beinahe alle zellulären Vorgänge in Eukaryoten beeinflusst. Diese reversible Markierung kann über die Lokalisation, Aktivierung oder auch Degradierung ihrer Substrate entscheiden. Die E3 Ligase RNF8 gehört zu der Familie der RING Finger E3 Ligasen und ist in der Lage drei verschiedenartige Ubiquitin-Ketten zu bilden. Mit Hilfe eines spezifischen E2 Enzyms, kann RNF8 Proteinsubstrate mit Lys48-, Lys63- und Lys11-verknüpften Ubiquitin-Ketten modifizieren. Aufgrund seiner elementaren Funktionen in der zellulären Signaltransduktion, wie dem Schutz der Chromosomenden und der DNA Doppelstrangbruchreparatur, ist RNF8 ein entscheidender Faktor für die Stabilität des Genoms und damit eng verknüpft mit Karzinogenese und Tumorprogression.

Durch die Identifizierung bislang unbekannter Interaktionspartner von RNF8 sollten neue Einblicke in dessen Rolle in der Krebsentstehung gewonnen werden. Mit Hilfe eines Genom-weiten Hefe-zwei-hybrid Screens wurden insgesamt 1600 initiale Hits ermittelt und einem mehrstufigen Validierungsprozess unterzogen. 138 dieser Hits wurden in weiteren Hefe-zwei-hybrid Tests sowie PCR und Westernblot Analysen bestätigt, ihre DNA Sequenz wurde nach erfolgreicher Extraktion aus Hefezellen durch einen Sequenzierservice ermittelt. Die am häufigsten gezählten Hits wurden

anschließend als Volllängenproteine hergestellt und abermals im Hefe-zwei-Hybrid-System getestet. Auf diesem Weg konnte HIF1α als neuer Interaktionspartner von RNF8 identifiziert werden.

Bei HIF1α handelt es sich um die sauerstofflabile Untereinheit des Transkriptionsfaktors HIF1, dem Hauptregulator für die Anpassungsmechanismen der Zelle an Sauerstoffarmut (Hypoxie). In vielen Tumoren ist HIF1α überexprimiert und korreliert mit einer schlechten Prognose für die Patienten. Im triple-negativ Mammakarzinom (TNBC) ist nicht nur HIF1α sondern auch RNF8 überexprimiert, die Hochrisikoerkrankung ist die aggressivste Form von Brustkrebs und vermehrt thereapieresistent. Die Identifizierung von HIF1α als neuem Interaktionspartner von RNF8 ist somit ein interessanter Ansatzpunkt für neue Therapiemöglichkeiten. Wir konnten die Spezifität der Interaktion in Hefe sowie in humane Zellen mittels Pull-down Experimenten nachweisen. Zelluläre Analysen zeigten, dass die RNF8-HIF1α Bindung unabhängig vom Sauerstoffgehalt der Zelle ist und auf der FHA Domäne von RNF8 beruht, welche mit der C-terminalen TAD Domäne von HIF1α interagiert. Zelluläre Bindungsstudien zeigten außerdem, dass TRAF6 ebenfalls mit RNF8 und HIF1α interagiert. TRAF6 alleine stabilisiert HIF1α, dieser Prozess wird nach zusätzlicher Bindung von RNF8 umgekehrt und somit HIF1α nach Komplexbildung von TRAF6/HIF1α/RNF8 degradiert. Dieser Effekt ist unabhängig vom Sauerstoffgehalt der Zelle, wobei unter hypoxischen Bedingungen weniger TRAF6 im Komplex zu finden ist. Funktionell konnten gezeigt werden, dass die Regulation von HIF1α unabhängig von der katalytischen Aktivität von RNF8 ist. Dies wirft die Frage auf, ob TRAF6 die für die Degradierung erforderliche Ubiquitinierung von HIF1α katalysiert. Des Weiteren ist die Aktivierung der Zielgene von HIF1α nach co-Expression von RNF8 und TRAF6 signifikant vermindert. Diese Funktion lässt auf eine neue Tumorsuppressorrolle von RNF8 schließen. Die E3 Ligase wirkt der TRAF6 bedingten, Tumor induzierenden Wirkung von HIF1α entgegen.

# 2. Introduction

## 2.1 Ubiquitination - a post-translational modification

Ubiquitination is a key regulatory process in almost all cellular functions of eukaryotic cells (Komander and Rape 2012). The reversible post-translational modification determines the fate of its substrates ranging from protein degradation, subcellular localization as well as cell signaling capacities, DNA repair or transcription (Komander and Rape 2012). Ubiquitin (Ub) is a small, 76 residue protein, that is highly conserved from yeast to human. Its compact globular structure consists of an exposed c-terminal tail that can be covalently linked to lysine (Lys) residues of other ubiquitin molecules as well as substrate proteins (Husnjak and Dikic 2012). These targets of the ubiquitination process can either be modified by monoubiquitination at one or multiple sites (monoubiquitination vs. multiple monoubiquitination), or they become polyubiquitinated. The type of ubiquitin linkage determines different outcomes in the cell (Komander and Rape 2012).

### 2.1.1 The ubiquitin cycle

The ubiquitination process itself, is a reversible covalent modification catalyzed by three enzymatic steps involving enzymes referred to as E1, E2 and E3s. So far, two E1 enzymes named UBA1 and UBA6, about 40 E2s and more than 600 E3 enzymes are described in the human proteome (Husnjak and Dikic 2012). The large number of E2 and E3 enzymes underlines the diversity and complexity but also the great specificity of the ubiquitination cascade (Zinngrebe et. al. 2014). The first step involves the ubiquitin-activating enzyme E1, which activates the C-terminal glycine residue of ubiquitin in an ATP dependent reaction, thereby forming a thioester linkage between its active site cysteine and the C-terminus of the ubiquitin. In a second step, activated ubiquitin is transferred to the E2 enzyme, the ubiquitin-conjugating enzyme. Again, the active site cysteine forms a thioester bond with the C-terminus of ubiquitin. Finally, with the help of an ubiquitin-protein ligase E3, ubiquitin gets attached to the target protein by forming an isopeptide bond between the C-terminal glycin of

ubiquitin and the ε-aminogroup of the substrate lysine or the α-aminogroup of the substrate methionine (Berndsen and Wolberger 2014, Kwon and Ciechanover 2017). Repeating the Ub conjugation process generates polyubiquitinated substrates. As mentioned above, ubiquitination is considered a reversible process, about 100 human deubiquitinating enzymes (DUBs) can again remove ubiquitin from the substrate. DUBs often determine the ubiquitin signal by trimming Ub-chains. They rescue proteins from degradation by removing ubiquitin molecules or recycle ubiquitin after successful degradation of marked proteins. Additionally, DUBs are needed to cleave freshly transcribed linear ubiquitin-fusion-chains into monoubiquitin (Nijman et. al. 2005, Komander et. al. 2009).

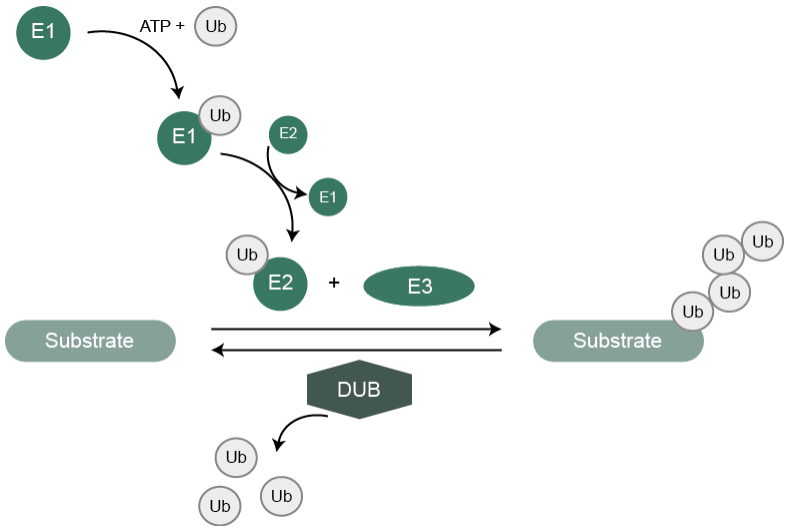


**Figure 2.1: The ubiquitin cycle.** The ubiquitination process has three enzymatic steps. First, the E1 enzyme activates and binds ubiquitin in an ATP dependent manner. Activated ubiquitin is then transferred to the E2 enzyme, the ubiquitin-conjugating enzyme. Finally, E3 ligases transfer ubiquitin from the E2 to the substrate. Deubiquitinating enzymes (DUBs) can revert the ubiquitination process by removing ubiquitin from the substrate.

### 2.1.2 Types of ubiquitination and their function

Monoubiquitination or multiple monoubiquitination of target proteins was shown to regulate endocytosis, cell signaling as well as DNA repair (Husnjak and Dikic 2012). Cellular substrates are primarily modified at Lys residues, but ubiquitin can also bind to the ε-amino group at the N-terminus of the target as well as to cysteine, serin and threonine residues (Husnjak and Dikic 2012). Except for substrates in the cell also

ubiquitin itself can be ubiquitinated. Polyubiquitin (polyUb) chains can be formed at all seven lysine residues (Lys6, Lys11, Lys27, Lys29, Lys33, Lys48, Lys63) within the Ub molecule or at the N-terminal methionine (Met1). Thus, eight different linkage types between two ubiquitin molecules can be formed, generating a wide variety of possible chains. Additionally there exist homotypic ubiquitin chains, where all molecules are connected by the same linkage type and heterotypic chains (or branched chains) that contain multiple linkage types (Komander and Rape 2012). This further increases the complexity of the ubiquitin code. The most extensively studied chains are Lys48-linked and Lys63-linked chains. Lys48-linked polyUb chains serve as degradation signal for the 26S-proteasome (Kwon and Ciechanover 2017), whereas Lys-63 polyUb chains mark targets for proteasome independent processes, as changes in substrate activity, localization or binding partner affinity. Prominent examples are the IKK complex in NF-κB signaling (Taniguchi and Karin 2018) or the recruitment of regulators during DNA double strand break (DSB) repair (Behrends and Harper 2011, Scully et. al. 2019). The remaining ubiquitin linkage types were often referred to as atypical, this has changed in the past few years especially for Lys11 and Met-1 linked chains. They have become more and more subject of investigation. In 2008, Jin et.al. showed that Lys11-linked Ub chains mark substrates for proteasomal degradation during cell cycle progression. In 2014, Meyer and Rape described the extension of these Lys11 chains from homotypic to branched Lys11 chains resulting in a most powerful degradation signal, being more potent than homotypic Lys11 or Lys48 linked ubiquitin chains. Except for its role in cell cycle control, Lys11-linked ubiquitin chains have also been implicated in hypoxic signaling in the cell. A connection of the Lys11 specific DUB OTUD7B and the stability of the transcription factor HIF1$\alpha$ were shown, however the exact regulatory mechanism is not yet fully understood (Bremm et. al. 2014).

Met-1 linked linear ubiquitin chains have attracted increasing attention in the last decade since becoming a key regulator in NF-κB signaling (Akutsu et. al. 2016). The multi-subunit E3 Ligase LUBAC utilizes the N-terminal methionine for ubiquitin chain formation and is the only known E3 ligase to catalyze linear Ub chains. In response to the stimulation of several immune receptors like TNFR, IL-1R or TLR, LUBAC is recruited and facilitates the activation of the transcription factor NF-κB (Ikeda 2015).

Except for its role in innate immune signaling through NF-κB, linear Ub has also been connected to Wnt signaling during embryonic development (Rivkin et. al. 2013, Takiuchi et. la. 2014). Lys29 linked ubiquitin chains are also involved in Wnt signaling, harboring an inhibitory role (Fei et. al. 2013). Lys27 polyubiquitin chains are reported to mediate DNA damage response through the E3 ligase RNF168 (Gatti et. al. 2015), additionally they were shown to be involved in innate immune response (Wang et. al. 2014). The role of Lys6 and Lys33 chain assembly in cell signaling is not yet fully understood (Akutsu et. al. 2016), whereas Lys33 chains have been connected to protein trafficking (Yuan et. al. 2014).

### 2.1.3 E3 Ubiquitin Ligases

E3 ligases are the most heterogeneous type of enzymes in the ubiquitination cascade, as they determine substrate specificity. They can be divided into three main classes depending on their conserved structural domains and the mechanism of ubiquitin transfer to the substrates: the RING, the HECT and the RBR E3 ligases (Lorick et. al. 1999). An additional fourth class has been identified just recently, the RCR E3 Ligases (Pao et. al. 2018). A summary of all classes is shown in Figure 2.2.

The RING (really interesting new gene) E3 ligases are the most abundant group of ubiquitin ligases and are characterized by a RING domain containing two zinc ions or by a U-box domain, which adopts the same RING fold but without zinc. The RING or U-Box domain respectively, mediates the binding of the ubiquitinated E2 enzyme. Importantly, as RING E3 ligases do not contain an intrinsic catalytic cysteine ubiquitin is directly transferred from the E2 to the substrate. The E2-E3 interaction is described rather transient and appears to compete with the E2-E1 interaction, depending of the presence or absence of an E2-bound ubiquitin (Lorick et. al. 1999, Xie et. al. 1999, Eletr et. al. 2005, Ye and Rape 2009). RING E3 ligases can function as monomers, homodimers or heterodimers, U-box containing ligases function as monomers or homodimers respectively (Metzger et. al. 2014). Homodimeric RING E3 ligases, for example RNF4 or cIAP, can bind two E2 enzymes, one per monomer. This is not the case for heterodimeric RING E3 ligases as BRCA1-BARD1 or RING1B-BM1, where only one of the E3s binds the E2 enzyme. Heterodimerization of RING ligases appears to

enhance the catalytic activity due to primed E2 interaction or increased substrate specificity (Metzger et. al. 2014). Additionally, there are multi-subunit E3s composed of the RING E3 ligase and several adaptor proteins. Prominent examples are the cullin-RING Ligases (CRLs) and the anaphase-promoting complex (APC). CRLs are characterized by a cullin scaffold that binds a RING-box protein at its N-terminus and an adaptor protein together with a substrate receptor at its C-terminus (Zimmerman et. al. 2010). The APC complex is a large assembly of 19 subunits including a RING subunit as well as a cullin-like subunit (Primorac et. al. 2013, Metzger et. al. 2014). However, RING E3s are able to synthesize different ubiquitin chain types, whereas the linkage specificity is determined by the bound E2 enzyme (Ye and Rape 2009, Metzger et. al. 2014). Thus, RING E3 ligases generally display the specificity of the particular E2 enzyme they are currently interacting with.

HECT (homologous to the E6AP carboxyl terminus) and RING between RING (RBR) E3 ligases catalyze ubiquitin transfer to the substrate through a two-step mechanism. They first transfer ubiquitin from the bound E2 enzyme to an intrinsic catalytic cysteine on the E3 and then from the E3 to the substrate (Rotin and Kumar 2009, Berndsen and Wolberger 2014). The HECT domain is localized at the C-terminus of the proteins and contains an N-terminal lobe that interacts with the ubiquitin charged E2 enzymes and a C-terminal lobe that harbors the catalytic cysteine. Substrate specificity is determined at the N-terminus of the ligase, outside of the HECT domain (Rotin and Kumar 2009). E6AP as well as SMURF1 and SMURF2 represent well-known members of the HECT E3 ligase family. RBR Ligases are named after the presence of two RING domains (RING1 and RING2) separated by an in-between-RING (IBR) domain. Similar to canonical RING E3 ligases, the RING1 domain binds the ubiquitin-charged E2 enzyme. The RING2 domain on the other hand possesses the catalytic cysteine to generate the E3-Ub intermediate, before targeting the substrate. Since the RING2 does not conform the canonical RING E3 ligase structure it is also called Rcat (required-for catalysis) domain. The IBR domain adopts the same fold as the RING2 (or Rcat) domain, while lacking the catalytic cysteine and therefore the ubiquitination activity. It is therefore also called the BRcat (benign-catalytic-activity) domain (Spratt et. al. 2014, Dove and Klevit 2017). Parkin as well as HOIL-1 and HOIP of the LUBAC complex have been extensively studied to get deeper insights in the mechanism of

RBR E3 ligases (Dove and Klevit 2017). A characteristic feature of all classes of E3 ligases is to catalyze substrate independent autoubiquitination and thus affect their own stability (Lorick et. al. 1999). In addition to the three main classes of E3 ligases, a fourth class, the RING-Cys-Relay (RCR) class has been discovered just recently (Pao et. al. 2018). The RING domain serves again as docking site for the ubiquitin charged E2 enzyme. The ubiquitin is transferred to an upstream catalytic cysteine of the RCR in the tandem cysteine domain (TCD). It is now in a mobile region of the enzyme, close to a mediator loop. This loop is able to relay the ubiquitin molecule to a second catalytic cysteine residue, further downstream. Interestingly, the E3 enzyme is now able to transfer the ubiquitin molecule to a threonine residue and not to the well-established lysine-residue of the substrate. This uncovered a new, distinct mechanism to determine substrate specificity (Pao et. al. 2018). The only known member of this new class of E3 ligases is the neuron-associated protein MYCBP2 (Pao et. al. 2018).

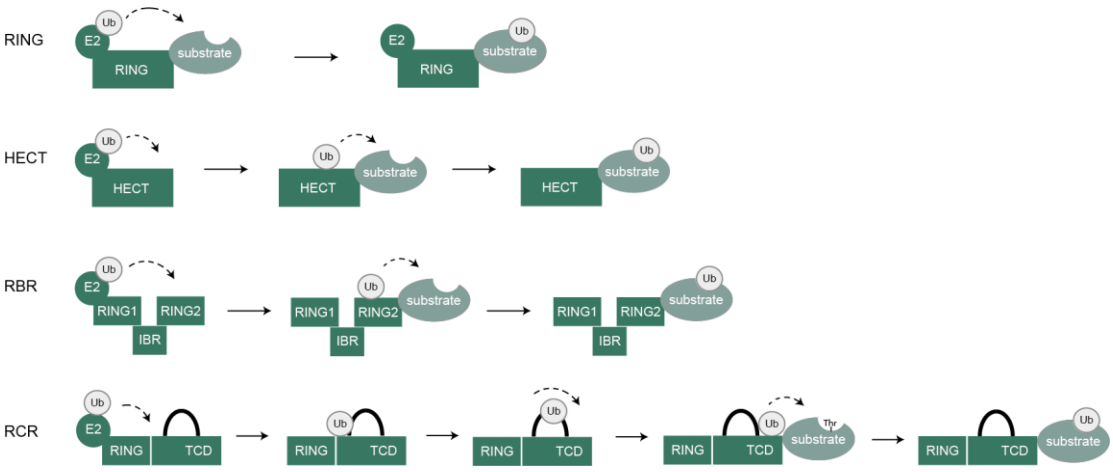


**Figure 2.2: Schematic overview of the ubiquitin-transfer process of four classes of E3 ligases.** E3 ligases can be divided into four classes depending on their conserved structural domains and the mechanism of ubiquitin transfer to the substrates: the RING, the HECT, the RBR and the RCR E3 ligases. RING E3 ligases use a one-step mechanism and bridge the E2-substrate interaction. HECT and RBR ligases use a two-step mechanism and function as E3-Ub intermediate. RCR Ligases use a mediator loop to transfer the ubiquitin molecule from one intrinsic cysteine residue to another, to finally charge the substrate.

## 2.2 The RING E3 Ligase RNF8

### 2.2.1 RNF8 structure

The really interesting new gene (RING) finger protein 8 (RNF8) is a member of the RING finger protein family first described by Seki et. al. in 1998. The ubiquitously expressed RNF8 protein exhibits 485 amino acids and a size of 55.5 kDa. The gene encoding the E3 ligase is located on chromosome 6p21.3, where it clusters with multiple other RING finger proteins (Seki et. al. 1998). RNF8 is primarily described in the nucleus (Kolas et. al. 2007, Mailand et. al. 2007, Huen et. al. 2007) but it has also been found in the cytoplasm - especially under certain stimuli (Fritsch et. al. 2014, Ho et. al. 2015). RNF8 consist of two functional domains, an N-terminal forkhead associated (FHA) domain and a C-terminal RING domain (Fig. 2.3). The FHA domain is important for its subcellular localization, as it is a phospho-protein binding module (Durocher et. al. 2000, Li et. al. 2000). It recognizes a phosphorylated threonine (pThr) with a strong selection for tyrosine (Tyr) and phenylalanine (Phe) in the +3 position. The optimal phosphopeptide binding motif pThr-xx-Tyr/Phe is therefore substantially different to other FHA domains described, which usually have a strong selection for acidic or aliphatic residues in the +3 position (Durocher et. al. 2000, Li et. al. 2000). The high resolution structure of the RNF8 FHA:phosphopeptide complex reveals even more unique features of RNF8 FHA. First, two divergent loops and a C-terminal $\alpha$-helical extension cluster away from the phosphopeptide-interacting surface and could be involved in phospho-independent interactions (Huen et. al. 2007). This would increase the number of potential targets of RNF8, making the RNF8 interaction network even more complex. Second, the observed interaction of RNF8 FHA with the phosphate group is more extensive than in any other FHA domain:phosphopeptide crystal structure. Finally, the strong selection for Tyr/Phe in the +3 position resembles the binding motif of the BRCT domain of BRCA1 and MDC1 proteins. Similar to the DNA damage foci formation of these two proteins, the FHA domain of RNF8 is required for RNF8 foci formation during DNA double strand break (DSB) repair. (Huen et. al. 2007). The C-terminal RING-finger domain of RNF8 harbors the catalytic E3 ligase

activity, it recruits the cognate E2 enzyme and facilitates ubiquitination (Lorick et. al. 1999, Ito et. al. 2001). RNF8 is able to catalyze Lys48-linked or Lys63-linked polyubiquitin chains through its interaction with different classes of E2 enzymes. The interaction with class III E2 ubiquitin enzymes (UBE2E1, UBE2E2, UBE2E3) determines Lys48-linked ubiquitin chains whereas RNF8 in conjungtion with the E2 enzyme complex UBE2N/Uev1a mediates Lys63-linked polyubiquitination (Ito et. al. 1999, Plans et. al. 2006). The RING domain has the intrinsic property of regulating the interaction with different E2s. The single point mutation I405A was shown to disrupt the RNF8-UBE2E2 but not the RNF8-UBE2N/Uev1a interaction. Thereby the RING domain is able to uncouple its Lys48-linked and Lys63-linked ubiquitination activities (Lok et. al. 2012).

Additionally, RNF8 was shown to generate Lys11-linked polyubiquitin chains by interacting with the E2 enzyme UBE2S (Paul and Wang 2017). *In vitro* analyses showed that RNF8 is also able to associate with the E2 UBE2W. However, the role of this E2 in the cell remains unknown and so does its functioning with RNF8 (Wang et. al. 2016).

### 2.2.2 RNF8 in DNA double strand break repair

The best-known function of RNF8 is its role in DNA double strand break (DSB) repair. DSBs are one of the most toxic lesions in the cell that directly result in genomic instability, if not repaired by nonhomologous end joining (NHEJ) or homologous recombination (HR). The damage is initially recognized by the Mre1-Rad50-Nbs1 (MRN) complex, which recruits the serine/threonine kinase ataxia telangiectasia mutated (ATM). ATM autoactivates itself and phosphorylates the histone variant H2A (γH2AX). This enables MDC1 to come to the sight, which is subsequently phosphorylated by ATM as well (Kim et. al. 2006, Kolas et. al. 2007). RNF8 recognizes phosphorylated MDC1 through its FHA domain and is now able to build UBE2N-dependent Lys63-linked ubiquitin chains at linker histone H1 (Mailand et. al. 2007, Thorslund et. al. 2015). The preference for UBE2N, rather than any other E2 enzyme, appears to be dependent on the E3 ligase HERC2. HERC2 binds RNF8 and stabilizes the interaction between the RING domain of RNF8 and UBE2N to generate Lys63-linked ubiquitination at DSB repair sights (Bekker-Jensen et. al. 2010). RNF168 recognizes the

RNF8 mediated Lys63 chains and catalyzes H2A-type histone ubiquitination to further promote the DNA damage response. The sequential action of RNF8 and RNF168 leads to the recruitment of the downstream repair factors 53BP1 and BRCA1, which determine either NHEJ or HR.

In 2017, it was demonstrated that RNF8 is also able to facilitate Lys11-linked polyubiquitin chains by interacting with the E2 enzyme UBE2S (Paul and Wang 2017). RNF8 and UBE2S mediate Lys11-linked ubiquitination of the histone H2A/H2AX thus promoting transcriptional silencing during DNA DSB repair. The exact regulation of Lys11 polyUb chains at DNA damage sites is not yet fully understood, it appears to be a non-proteolytic signal though (Paul and Wang 2017). Just recently, RNF8 was shown to not only promote DNA damage repair by the efficient recruitment of repair factors but also by inhibiting the pro-apoptotic function of p53. P53 is a well-characterized tumor suppressor factor, acetylated by the acyltransferase Tip60. RNF8 decreases Tip60 activity thereby inhibiting p53 dependent activation of apoptosis-related genes (Chen et. al. 2020).

Together, it is obvious that RNF8 is a major factor to transduce the DNA damage response signal, making it a key regulator to maintain genomic stability.

### 2.2.3 Functions of RNF8 in chromosome end protection, cell divison and transcriptional control

RNF8 sustains genomic stability not only through its role in promoting DNA DSB repair, but also by protection of chromosome end integrity (Jacobs 2012). Chromosome ends present natural challenges to genomic integrity. First, due to the inability of DNA polymerases to replicate the very end of chromosomes, second, to protect it from DNA DSB repair and the resulting improper ligation or fusion of chromosome ends (Jacobs 2012). The telomere is a protective structure specialized to handle these problems together with the shelterin complex. RNF8 was found to increase the stability of certain proteins in the shelterin complex, thereby suppressing telomere fusion (Rai et. al. 2011). Additionally it stabilizes the poly (ADP-ribose) polymerase tankyrase-1 by Lys63 ubiquitination, which is an essential factor during telomere replication, again sustaining chromosome end integrity (Tripathi and Smith 2017).

However, if the telomere is already uncapped, RNF8 promotes NHEJ of chromosome ends and generates genomic instability (Peuscher and Jacobs 2011).

Cell division needs to be precisely controlled to transmit the genetic information faithfully from parental to daughter cells. RNF8 participates in mitosis and cytokinesis progression discovered by its localization to centrosomes and cell division sites (Plans et. al. 2008, Chahawan et. al. 2013). The E3 ligase was shown to ubiquitinate the septin SEPT7. All septins are critical factors for cell division and the interference with their regulation by RNF8-inactivation results in cytokinesis defects (Mostowy and Cossart 2012). Additionally, RNF8 shows a cell-cycle dependent turn over, its expression reaches a peak in mitosis followed by a striking decrease in late mitotic stages (Plans et. al. 2008). The exact roles of RNF8 in cell cycle progression are not yet fully understood, thus, RNF8 expression and regulation seems to be a key factor to maintain cellular homeostasis.

Apart from its roles in DNA DSB repair, chromosome end protection and regulation of mitosis and cell divison to sustain genomic stability and prevent tumorigenesis, RNF8 was also found to act in transcriptional regulation in a tumor-promoting fashion (schemed in Figure 2.3). The epithelial-mesenchymal transition (EMT)-related transcription factor TWIST mainly regulates cell lineage determination and differentiation in the early vertebrate embryo (Acloque et. al. 2009, Morel et. al. 2012). As known for all EMT inducers, TWIST is silent in differentiated adult cells, however its reactivation is observed in numerous human cancers linked to poor clinical outcome (Ansieau et. al. 2010). RNF8 was identified as a direct TWIST activator by catalyzing Lys63-linked ubiquitination of TWIST. The stabilization of the transcription factor resulted in its nuclear translocation thereby enabling EMT and cancer stem cell like (CSC) functions leading to disease progression and chemoresistance (Lee et al. 2016). A tumor promoting role of RNF8 is also described by Wang et. al., where RNF8 co-activates and stabilizes the estrogen-receptor $\alpha$ (ER$\alpha$) transcription factor. RNF8 triggers ER$\alpha$ monoubiquitination, which results in increased target gene activation and promotes breast cancer progression (Wang et. al. 2017).

Altogether, RNF8 has divers roles in the cell, mostly as critical factor to maintain genomic stability.

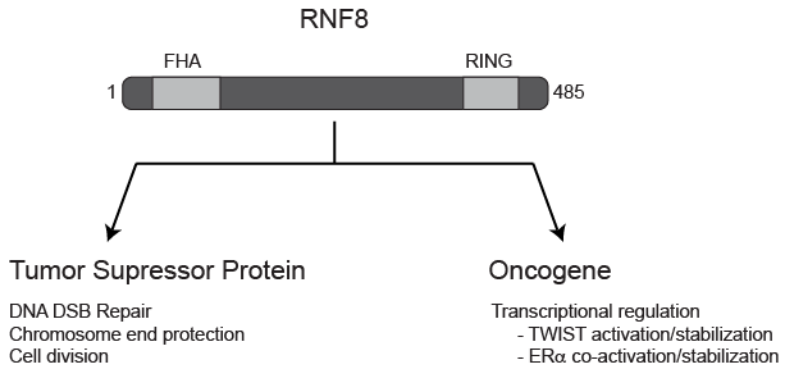


**Figure 2.3: RNF8 as tumor suppressor protein vs. Oncogene.** Domain structure of the E3 Ligase RNF8 and its divers roles inside the cell. The N-terminal FHA domain is important for its subcellular localization, as it is a phospho-protein binding module. The C-terminal RING domain harbors the catalytic E3 ligase activity of RNF8 and binds the cognate E2 enzyme. The roles of RNF8 inside the cell are grouped by the indication as tumor suppressor protein or oncogene.

### 2.3.4 RNF8 in diseases

RNF8 is an essential factor in DNA DSB repair, chromosome end protection as well as during cytokinesis (Mailand et. al. 2007, Jacobs 2012, Plans et. al. 2008). Due to these different implications of RNF8, all of them important to maintain genomic stability, the E3 ligase is considered to be a tumor suppressor protein. Indeed, RNF8 knockout mice showed a predisposition for tumorigensis of lymphoma, thymoma, mammary carcinoma, skin tumor as well as sarcoma (Li et. al. 2010, Zhou et. al. 2019). This was confirmed in patient samples, where low expression of RNF8 correlated with poor prognosis for breast cancer patients (Li et. al. 2018). However, RNF8 is also described as tumor promoting factor. Breast cancer is known to be the number one diagnosed cancer and leading cause of cancer death among females (Bray et. al. 2018). RNF8 is overexpressed in highly malignant breast cancer, promoting epithelial-mesenchymal transition (EMT) and cell migration, both central to cancer metastasis (Kuang et. al. 2016). The transcription factor ERα is overexpressed in about 70% of breast cancers and some patients show therapy resistance through activated ERα signaling. RNF8 was shown to be a co-activator of ERα, thereby promoting breast cancer proliferation (Wang et. al. 2017).

Triple negative breast cancer (TNBC) is the most aggressive type of breast cancer, showing worse prognosis than any other subtype known so far. Treatment options for TNBC are very limited due to lack of estrogen receptor expression, progesterone receptor expression and HER2 protein amplification (Bauer et. al. 2007, Dent et. al. 2007, Lee and Djamgoz 2018). RNF8 is involved in the progression of TNBC through its stabilization and activation of the EMT-transcription factor TWIST. Upregulation of RNF8 and TWIST correlate with chemoresistance and poor survival rate (Lee et. al. 2016). Additionally, silencing of RNF8 in nasopharyngeal and bladder cancers increased their sensitivity to irradiation therapy (Zhao et. a. 2016, Wang et. al. 2015). Hence, RNF8 may act as a protector against genomic instability in normal cells, decreasing the risk of cancer, while it has malignant activities in various cancer cells, acting as a tumor promoting factor (Zhou et. al. 2019).

## 2.3 HIF1α and hypoxia

The adaption of cells to oxygen deprivation is mainly controlled by a family of transcription factors known as hypoxia inducible factors (HIFs). HIF proteins induce the expression of genes involved in new blood vessel formation, metabolic rewiring and cell survival. Therefore, HIFs govern the cellular adaption to hypoxia (low oxygen tension) and maintain the growth of rapidly proliferating tissues as in embryonic development but also in tumor progression (Iyer et. al. 1998A, Ryan et. al. 1998, Tang et. al. 2004, Yee Koh et. al. 2008, Wong et. al. 2011). HIF1 transcription factors work as heterodimers, with one of three oxygen-regulated alpha subunits (HIF1$\alpha$, HIF2$\alpha$, HIF3$\alpha$) and a constitutively expressed beta subunit (HIF1$\beta$) (Huang et. al. 1998, O´Rourke 1999). HIF1$\alpha$ is ubiquitously expressed in all tissues whereas HIF2$\alpha$ and HIF3$\alpha$ are only selectively expressed (Bertout et. al. 2008). Under conditions of normal oxygen tension (normoxia), HIF1$\alpha$ is hydroxylated and rapidly ubiquitinated for its proteasomal degradation. The von hippel lindau (VHL) E3 ligase protein complex recognizes hydroxylated proline and asparagine residues and triggers the degradation (Ivan et. al. 2001, Tanimoto et. al. 2000). Under hypoxia, the alpha subunit is stabilized and translocates to the nucleus where it dimerizes with HIF1$\beta$ to build the active transcription factor HIF1 (schemed in Fig 2.4B). HIF1 target genes are activated,

essential for cell survival and proliferation under low oxygen conditions (Ivan et. al. 2001, Majmundar et. al. 2010).

### 2.3.1 HIF1α structure

HIF1$\alpha$ is the $O_2$-labile subunit of the heterodimeric transcription factor HIF1. It belongs to the per-arnt-sim (PAS) family of basic helix-loop-helix (bHLH) transcription factors, named after their N-terminal bHLH domain, necessary for DNA binding as well as their PAS domain that is required for heterodimerization (Semenza and Wang 1992, Wang 1995). Both domains show a strong sequence and functional conservation among the HIF proteins. HIF1α exhibits 826 amino acids and a size of 93 kDa (Dengler et. al. 2014). The C-terminus of HIF1α consists of an oxygen dependent degradation domain (ODD) and a transactivation (TAD) domain that is again divided in its N-terminal and C-terminal part (N-TAD and C-TAD) (schemed in Fig. 2.4A). The oxygen dependent degradation of HIF1α depends on its ODD domain, as it contains the key proline (P402, P564) residues for hydroxylation leading to its ubiquitination and subsequent degradation, under normoxic conditions. The ODD domain spans the N-TAD domain while C-TAD marks the very end of the protein. The TAD domains are required for the selective activation of HIF1 target genes, by recruiting divers transcriptional co-activators (Jiang et. al. 1996, Huang et. al. 1998, O´Rourke et al. 1999, Kaelin and Ratcliff 2008, Ivan et. al. 2001). CBP and p300 are two well-characterized examples of HIF1 co-activators. The TAD domains of HIF1α exhibit the functional specificity of the protein compared to its tight relatives HIF2$\alpha$ and HIF3$\alpha$ (Hu et. al. 2007).

### 2.3.2 Post-translational modifications of HIF1α

The post-translational modifications of HIF1α determine its stabilization, degradation as well as its transcriptional program. HIF1α is constantly transcribed and translated under normoxic and hypoxic conditions. Due to its hydroxylation by prolyl-4-hydroxylases (PHD1-4) it is subsequently marked for degradation as long as oxygen is available. The key proline residues P402 and P564 are mainly hydroxylated by PHD2 and initiate its ubiquitination by the E3 ligase complex von Hippel Lindau (VHL), followed by its proteasomal degradation (Berra et. al. 2003, Landazuri et. al. 2006,

Ivan et. al. 2001, Huang et. al 1998). Another regulatory hydroxylation is carried out by the factor inhibiting HIF (FIH) at asparagine 803 (N803) in the C-TAD domain of HIF1α. Hydroxylated asparagine blocks the binding of cofactors in the C-TAD domain, thereby decreasing the activation of HIF1α target genes (Mahon et. al. 2001, Lando et. al. 2002). HIF1α proteasomal degradation is not only determined by the E3 ligase complex VHL, also other E3 ligase proteins are described to target HIF1α, however independent of oxygen tension. Receptor protein kinase C (RACK1), carboxyl terminus of HSP70-interacting protein (CHIP) and hypoxia associated factor (HAF) all catalyze Lys48 linked polyubiquitination of HIF1α to mark it for degradation (Liu et. al. 2007, Koh et al. 2008, Bento et. al. 2010). In contrast, the E3 ligase TRAF6 is known to positively regulate HIF1α. TRAF6 stabilizes the alpha subunit through Lys63 linked poly ubiquitination and increases its transcriptional activity (Sun et. al. 2013).

Except for hydroxylation and ubiquitination, also phosphorylation events are key mediators for the regulation of HIF1α (schematically depicted in Fig. 2.4). They can enhance target gene activation by disrupting the interaction of HIF1α and VHL or through enhanced co-activator binding to HIF1α (Richard et. al. 1999). The kinase ERK1 phosphorylates HIF1α at its C-terminus, resulting in a masked nuclear export signal of the latter. The nuclear accumulation of HIF1α is followed by increased transcriptional activity of HIF1 (Mylonis et. al. 2006). Nevertheless, other phosphorylation events are described to negatively regulate HIF1α. The caseine kinase 1 (CK1) phophorylates HIF1$\alpha$ within the PAS domain, thereby inhibiting its binding to HIF1$\beta$ in the nucleus (Kalousi et. al. 2010). Another example is the glycogen synthase kinase 3 $\beta$ (GSK3$\beta$) and the polo-like kinase 3 (PLK3) both destabilizing HIF1α protein levels, independent of the VHL E3 ligase complex (Flügel et. al. 2007, Xu et. al. 2010).

Further post-translational modifications as S-nitrosylation and sumoylation have been described for HIF1α as well, however the exact role is not yet fully understood and needs further investigation (Dengler et. al. 2014). The downstream effect of HIF1α acetylation appears to be dependent on the location of the modified residue. N-terminal acetylation sites are decreasing HIF1α stability as well as inhibiting the activation of several target genes. Is the modification located at the C-terminus of the protein, enhanced co-activator binding as well as increased HIF1α levels lead to induced target gene activation (Lim et. al. 2010, Geng et. al. 2011, Geng et. al. 2012).

All in all, the importance of HIF1α in cellular adaption to hypoxia makes it a highly regulated protein, therefore being targeted by numerous post-translational modifications (illustrated in Fig. 2.4A).

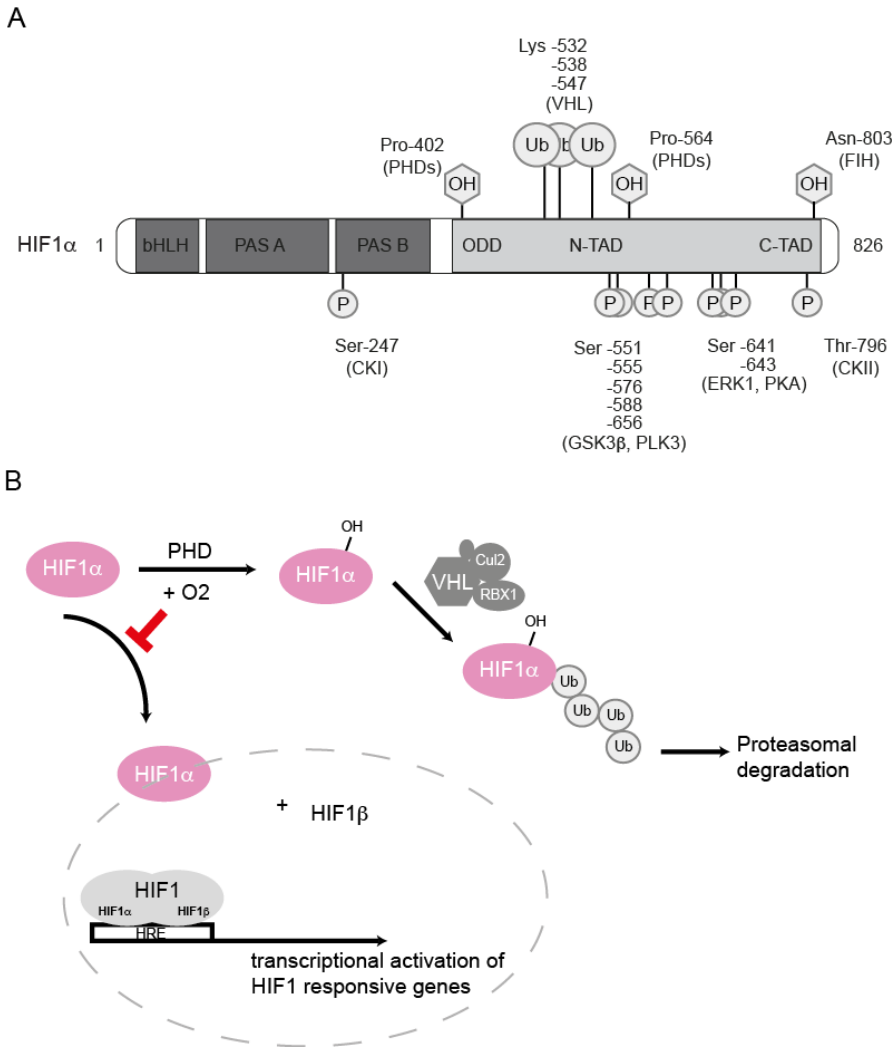


**Figure 2.4: Domain structure and cellular function of HIF1α.** (A) HIF1α protein domains and selected post-translational modifications. The N-terminal basic helix-loop-helix domain (bHLH) is necessary for DNA binding, the PAS domain is required for heterodimerization. The C-terminus of HIF1α consists of an oxygen dependent degradation domain (ODD) and a transactivation (TAD) domain that is again divided in its N-terminal and C-terminal part (N-TAD and C-TAD). Selected post-translational modifications are shown here, including the responsible enzymes. (B) $O_2$ dependent regulation of HIF1α. HIF1α is hydroxylated (by PHDs) and rapidly ubiquitinated (by VHL) for its proteasomal degradation under normoxic conditions. Under hypoxia, the alpha subunit is stabilized and translocates to the nucleus where it dimerizes with HIF1β to build the active transcription factor HIF1.

### 2.3.4 HIF1α in diseases

HIF1 transcription factor is known as the master regulator of oxygen homeostasis in mammalian cells, inducing adaptive responses to hypoxic stress. Thereby, it maintains energy metabolism, proliferation and cell survival (Zhong et. al. 1999, Semenza 2000, Semenza 2003). Low oxygen tension (hypoxia) can be part of the normal physiology but is mainly related to pathological conditions. In acute hypoxic conditions as ischemic heart diseases, lung injuries or acute liver failure, HIF1α stabilization was shown to have a protective role by ensuring ischemic tolerance (Lee et. al. 2019). However, in chronic conditions as congestive heart failure or fibrosis of the lung and liver, HIF1α appears to contribute to the pathogenesis of the disease. There is no easy categorization though, since the complex role of HIF1α in different organs generating different diseases is not yet fully understood and needs more detailed future investigation. HIF1α stabilization has also been linked to innate and adaptive immune activation. Hypoxia as well as bacterial infections activate the key transcription factor in immune responses, nuclear factor-kappa B (NF-κB). In turn, HIF1α mRNA transcription is activated. The crosstalk between both transcription factors enables the expression of pro-inflammatory cytokines and motility in macrophages (Cramer et. al. 2003, Peyssonnaux et. al. 2005). In adaptive immunity, HIF1α promotes Th17 T-cell differentiation as well as the expression and release of cytolytic molecules. Due to its critical role in IL-10 production in B-cells, it is also considered an interesting target in autoimmune diseases (Dang et. al. 2011, Meng et. al. 2018).

Research underlining the implication of HIF1α in cancer biology, has grown immensely since its identification by Semenza et. al. in 1992. Due to their fast proliferation, cancer cells usually have a highly impaired oxygen balance and become hypoxic as a result. The correlation between enhanced HIF1α levels and poor patient survival, treatment resistance and metastasis, made HIF1α an important cancer drug target (Masoud and Li 2015). HIF1α target genes are involved in many pathways important for cancer progression, as angiogenesis, migration, invasion as well as glucose metabolism. In the latter, hypoxic tumor cells need HIF1α to switch from the efficient oxidative phosphorylation to the less efficient glycolysis (Warburg effect) to maintain energy

production as well as control reactive oxygen species (ROS) excess (Masoud and Li 2015, Samanta and Semenza 2018). Another example is the activation of pro-angiogenic factors as vascular endothelial growth factor (VEGF), to stimulate new blood vessel formation and enhance oxygen distribution throughout the tumor (Conway et. al. 2001). Breast cancer is the most common cancer type among women, whereas triple negative breast cancer (TNBC) displays the most aggressive subtype. TNBC is associated with high rate of recurrence, distant metastasis and poor overall survival (Elias 2010, Cancer genome atlas 2012, Gilkes and Semenza 2013, Dong et. al. 2019). HIF1α is hyperactivated in TNBC and is thereby one of the main reasons for its malignancy (Motagner et. al. 2012, Samanta et. al. 2014). The poor patient survival rate is due to many HIF1α target gene pathways, especially to its association with metastasis. HIF1α was shown be required for breast cancer metastasis, for example to the lungs (Semenza 2012b, Gilkes and Semenza 2013). Zhong et. al. described the overexpression of HIF1α in human cancers as well as their metastases already in 1999. They identified HIF1α in 13 tumor types, including lung, prostate, breast and colon carcinoma. A more recent example is HIF1α in renal carcinoma, in about 90% of the aggressive clear cell renal cell carcinoma (ccRCC) patients, HIF1α is accumulated due to a *VHL* mutation (Sato et. al. 2013). Because of the poor prognosis associated with HIF1α overexpression in a variety of human cancers, it is still highly investigated, as most recent publications show (Swiatek et. al. 2020, Fu et. al. 2020).

## 2.4 TRAF6 in cellular signaling

TRAF6 belongs to the TRAF protein family and works as signal transducer to activate the NF-κB transcription factor. Either as adaptor protein or through its E3 ligase activity, mediated by an N-terminal RING domain. Proinflammatory stimuli as cytokines, tumor necrosis factor $\alpha$ (TNF$\alpha$), lipopolysaccharides (LPS) or antigens stimulate NF-κB signaling through the activation of several receptors. Toll-like receptor (TLR), interleukin-1 receptor (IL-1R), T-cell receptor as well as IL-17 receptor signaling are all mediated through TRAF6 to activate NF-κB (Xie et. al. 2013). TRAF6 is mainly involved in TLR/IL-1R signaling, where bacterial lipopolysaccharides (LPS) or virus RNAs are recognized by the receptor followed by a signaling cascade including

Lys63 linked polyubiquitination of target substrate through TRAF6 (Walsh et. al. 2015). The mediated NF-κB activation results in cytokine production, which enables the innate immune response to many pathogens (Xie et. al. 2013, Taniguchi and Karin 2018). Additionally, TRAF6 is implicated in DNA damage repair. Upon DNA damage, the activated serine/threonine kinase ATM translocates to the cytoplasm, interacts with TRAF6 and builds the ATM-TRAF6-cIAP complex mediated through Lys63 ubiquitination of TRAF6. The complex initiates another phosphorylation and ubiquitination event, which finally results in genotoxic activation of NF-κB (Hinz et. al. 2010). Several other signaling pathways, including NOD, RIG-I, IFN, TGF-β, IL-2 and C-leptin receptors have been described for TRAF6 as well (Xie et. al. 2013).

### 2.4.1 TRAF6 in hypoxia

TRAF6 is involved in a variety of signaling pathways to activate NF-κB, nevertheless, it has also been described in NF-κB independent signaling. Together with the E2 enzyme complex UBE2N/Uev1a, TRAF6 was found to stabilize the main regulator for $O_2$ homeostasis in human cells, HIF1α (Sun et. al. 2013, Semenza 2000). Independent of oxygen tension, TRAF6 mediates Lys63 linked poly ubiquitination of the alpha subunit to increase HIF1α protein levels. TRAF6 associates with HIF1α to stabilize the protein, thereby promoting tumor growth and angiogenesis (Sun et. al. 2013). Consistently, Rezaeian and colleges found that TRAF6 overexpression enhanced breast tumor growth as well as cancer cell migration and invasion through its effects on HIF1α (Rezaeian et. al. 2017). However they propose a more indirect mechanism. TRAF6 appears to be autoubiquitinated and activated in hypoxia to generate monoubiquitination of the histone H2AX (mUbH2AX), which enables its subsequent phosphorylation (γH2AX) by the kinase ATM. γH2AX is supposed to mediate HIF1α enrichment in the nucleus, thus leading to HIF1α activation resulting in enhanced tumorigenesis, glycolysis and metastasis (Rezaeian et. al. 2017). The tumor promoting function of TRAF6 in hypoxic signaling seems to be HIF1α dependent, however the exact mechanism needs further investigation.

# 3. Aim of this study

The E3 ligase protein RNF8 is involved in a variety of signaling pathways inside the cell, being a crucial factor to maintain genomic stability. While its critical role in DNA DSB repair has been extensively studied so far, its mechanisms in cell cycle control as well as chromosome end protection are still largely unclear. Additionally, RNF8 is strongly correlated with cancer cell migration, metastasis and disease progression indicating a tumor-promoting function. However its deficiency in mice was shown to cause increased tumorigenesis, therefore suggesting a tumor suppressor role.

The strong correlation between RNF8 and cancer together with its poor understanding in signaling pathways except for DNA double strand break repair, make it an appealing target for further investigation. In this study we aimed at identifying new interaction partners of RNF8 in a genome-wide yeast-two-hybrid (Y2H) screen. After validating the hits by western blot and PCR analyses, the most promising interaction partner should be verified in follow up Y2H assays, as well as co-IP assays in human cells. We identified the main regulator of $O_2$ homeostasis, HIF1α, as new interactor of RNF8. Using truncation constructs the mapping of the interaction should be accomplished. The further aim of this study was to investigate the function of the RNF8-HIF1α interaction, by taking into account the catalytic activity of RNF8 as well as additional binding partners of both proteins.

# 4. Results

## 4.1 Identification of new interaction partners of RNF8

### 4.1.1 Establishing a genome-wide yeast-two-hybrid screen

For establishing a genome-wide yeast-two-hybrid (Y2H) screen the Clontech Matchmaker Gold System was used. It provided a toolbox containing the pGBKT7 vector, the pGADT7 vector as well as the yeast strains Y2HGold and Y187. Both strains are haploid and able to mate with each other to form a diploid cell, thus, providing a straightforward way to introduce a prey cDNA library to the bait. Full length RNF8 (aa 1 - 485) was used as bait and cloned into the pGBKT7 vector, fusing it to the DNA binding domain of the transcription factor Gal4 (pGBKT7-RNF8). The first step to establish the screen was to test pGBKT7-RNF8 for autoactivation and toxicity. Figure 4.1A shows these necessary control experiments. Growing colonies on media lacking tryptophane (-Trp) prove a lack of toxicity as well as the successful transformation of pGBKT7-RNF8 in haploid Y2HGold strain. Y2HGold is auxotrophic for tryptophane and only able to grow on -Trp media upon pGBKT7-RNF8 transformation, due to the Trp1 marker on pGBKT7. Growth on media lacking leucin (-Leu) on the other hand ensures pGADT7-empty transformation, which contains a Leu2 marker, rescuing the haploid Y187 strain that is auxotrophic for leucin. Finally, there is the -Leu/-Trp/-His control, only if bait and prey interact the Gal4 DNA binding domain (DNA-BD) and the Gal4 activation domain (AD) are brought into close proximity to activate transcription of the reporter gene *HIS3*. Thus, a positive protein-protein interaction enables mated yeast to grow on media lacking the essential amino acid histidine (-His). In contrast, autoactivation enables pGBKT7-RNF8 and pGADT7-empty control to activate the GAL4 promotor without any AD-fusion protein. We mated the MATa Gal4 reporter strain Y2HGold transformed with the bait pGBKT7-RNF8 and the MAT$\alpha$ Gal4 reporter strain Y187 transformed with pGADT7 (Fig. 4.1A). pGBKT7-RNF8 as well as pGADT7-empty were successfully transformed and showed no autoactivation or toxicity (Fig 4.1A).

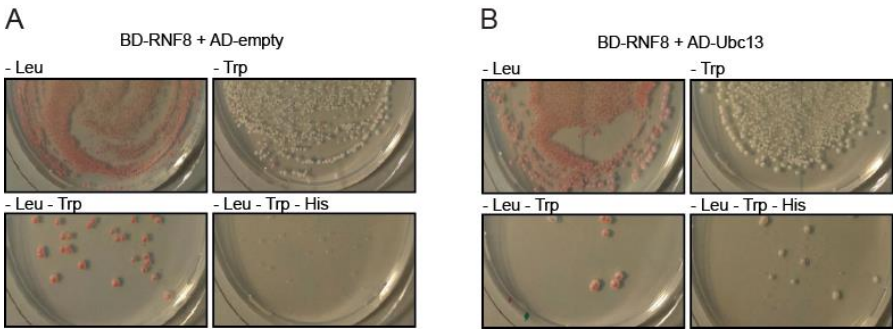


**Figure 4.1: Establishing a genome-wide yeast-two-hybrid screen.** (A) BD-RNF8 is well tolerated by the mated diploids containing of haploid Y2HGold strain and haploid Y187 strain (growing colonies on -Trp and -Leu/-Trp medium) and shows no signs for autoactivation (no viable colonies on -Leu/-Trp/-His). (B) BD-RNF8 and AD-UBE2N interact in the Y2H assay (colonies on -Leu/-Trp/-His selection medium). AD-UBE2N shows no toxicity to mated yeast of Y2HGold strain and Y187 strain. Cells were plated on minimal medium as indicated and incubated for 3 days at 30°C.

As positive control, we used the well-characterized interaction of RNF8 with its cognate E2 enzyme UBE2N (Fig. 4.1B) (Plans et. al. 2006, Kolas et. al. 2007, Mailand et. al. 2007). We cloned UBE2N (aa 1 - 151) in the pGADT7 vector and transformed it in the haploid Y187 strain. Haploid Y2HGold transformed with pGBKT7-RNF8 was mated with haploid Y187 transformed with pGADT7-UBE2N; generated diploids were plated on four different selection plates (-Leu, -Trp, -Leu/-Trp, -Leu/-Trp/-His). Figure 4.1B shows growing colonies on -Leu/-Trp/-His media, caused by the interaction of BD-RNF8 and AD-UBE2N. The number of colonies growing on -Leu/-Trp selection plates and the number of colonies due to the transformed bait only (BD-RNF8, -Trp media), were used to calculate the mating efficiency (percentage of diploids):

$$\left(\frac{No.of\frac{cfu}{ml}\,of\ diploids}{No.of\frac{cfu}{ml}of\ limiting\ partner}\right)x\ 100 = mating\ efficiency$$

A mating efficiency between 2-5% is considered good for a screening (MatchmakerGold user Manual), in our case an efficiency of 2.3% was achieved. Due to the calculation as well as the good signal to noise ratio of the RNF8-UBE2N interaction (>3 biological replicates, no false positives, data not shown), we established the screen with histidine lacking (-His) media, which is a considerably low stringency screen (Clontech manual, Caufield et. al. 2012).

### 4.1.2 Hit identification and verification

For the identification of new protein-protein interactions, full length RNF8 as bait and a normalized human cDNA library (Clontech) as prey, were screened for new interactions (screening procedure summarized in Fig. 4.2).

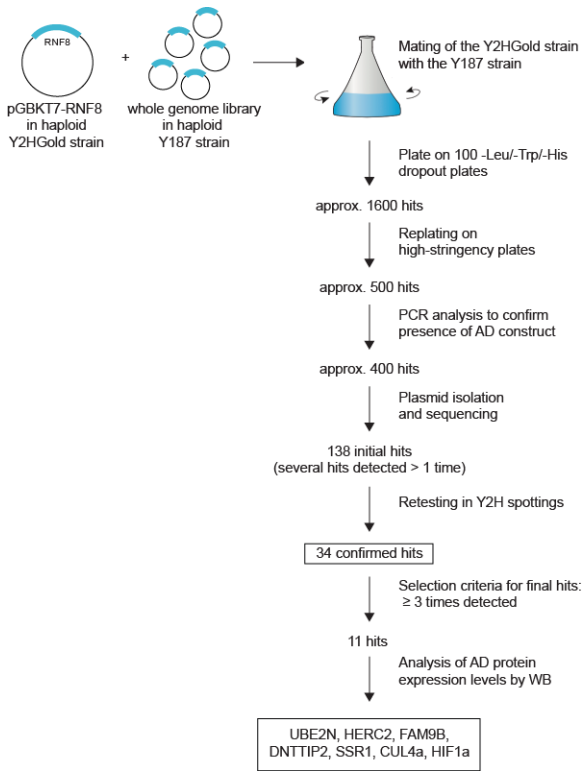


**Figure 4.2: Scheme for hit selection**. Including hit verification methods and conditions for exclusion.

After transforming pGBKT7-RNF8 in the Y2HGold strain, it was mated with the MATα Gal4 reporter strain Y187, which has been transformed with a normalized human c-DNA library beforehand (Clonetech). Thereby we used the ability of haploid yeast strains to form diploid cells containing bait and prey plasmids. -Leu/-Trp/-His dropout supplement was used to select for the activation of the *HIS3* reporter gene as a results of the reconstitution of a functional transcription factor Gal4 upon interaction of RNF8 with any AD-labeled library protein.

We were able to pick 1600 colonies from -Leu/-Trp/-His selection plates; all of these preliminary hits were replated on high-stringency plates (Fig. 4.3A). High-stringency-plates consist of quadruple dropout medium (-Leu/-Trp/-His/-Ade) supplemented with X-α-Gal and Aureobasidin A. Thereby, we made use of four different reporter

genes (*HIS3*, *Ade2*, *AURI-C*, *MEL1*) controlled by three unrelated Gal4-responsive promotors. Except for the short Gal4 DNA-BD binding site, there is no similarity in the three used promotors, ensuring that library proteins that interact with unrelated regions are automatically screened out. The Y2HGold strain is auxotrophic for histidine and adenine. Therefore, when two proteins interact, the two reporter genes *HIS3* (encoding histidine) and *Ade2* (encoding adenine) are expressed, allowing Y2HGold to grow on -His/-Ade minimal medium. The expression of the reporter gene *AUR1-C* ensures resistance to the otherwise toxic drug Aureobasidin A. The forth reporter gene, *MEL1*, encodes $\alpha$-galactosidase. If $\alpha$-galactosidase is expressed, yeast cells turn blue in the presence of the substrate X-$\alpha$-Gal. This very high stringency of four reporter genes (*HIS3*, *Ade2*, *AURI-C*, *MEL1*) controlled by three unrelated promotors, eliminated background activity as false or weak interactions, finally resulting in 500 hits (representative selection plate shown in Fig. 4.3A). To eliminate false positives within these 500 hits yeast colony PCR of all 500 colonies was performed. Figure 4.3B illustrates a representative of 40 PCR analyses. Hits that contained multiple AD-plasmids (#) as well as hits that contained no AD-plasmid (##) were eliminated, an example of both is marked in Fig 4.3B. We excluded 100 Hits by this validation step, resulting in 400 remaining hits. It is important to mention that the size of the amplicons is not necessarily matching the predicted size of the particular prey cDNA. The library approach is mostly based on cDNA fragments of unknown sizes, which decreases the chance for false negatives compared to other Y2H assays (Brückner et. al. 2009). It can therefore not be associated with the DNA size of the unknown hit protein.

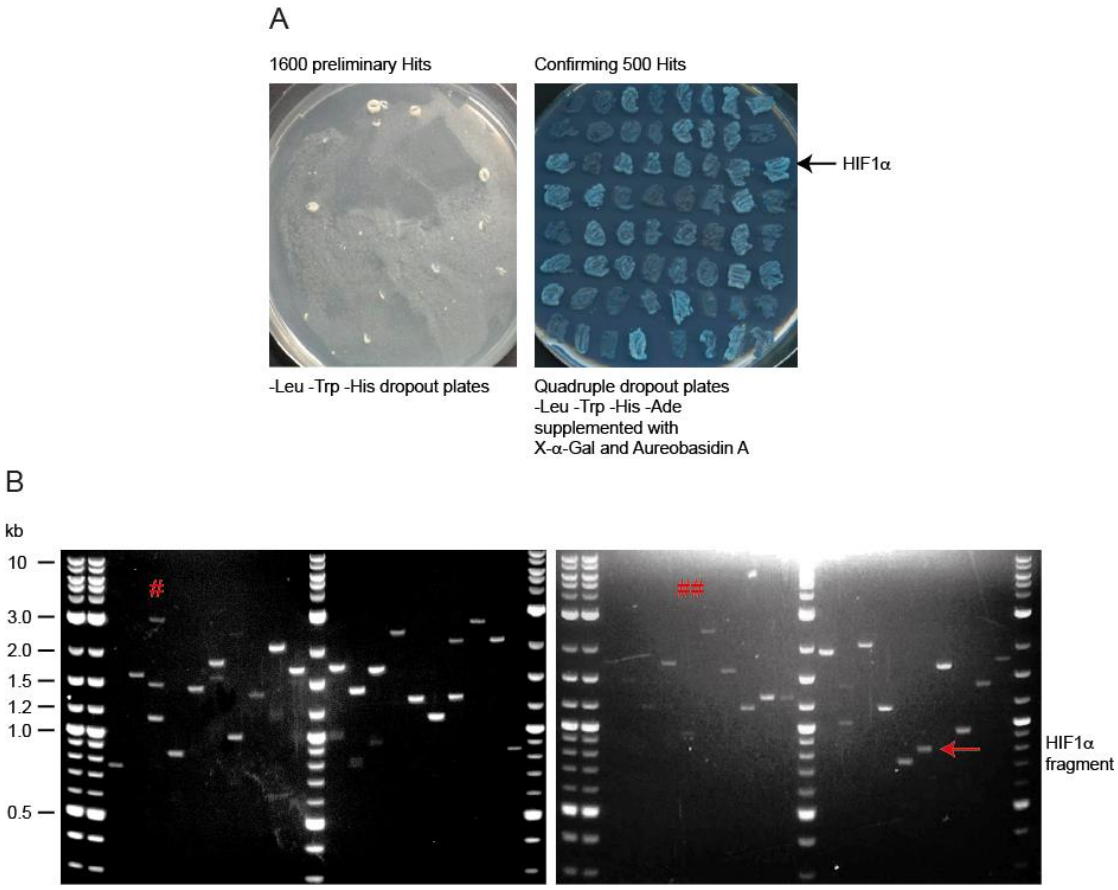


**Figure 4.3: Hit identification and first validation.** (A) Left: Representative image of 100 -Leu/-Trp/-His dropout plates of mated yeast, growing colonies imply a positive interaction with the bait RNF8. 1600 hits were picked and replated (right panel). Right: Representative image of 24 quadruple dropout plates supplemented with X-α-Gal and Aureobasidin A. 500 Hits could be validated, here visible as blue growing colonies. ???1α represents a new interactor of RNF8. (B) Representative image of 40 out of 500 PCR analyses. An example of multiple amplified AD plasmids is marked with #, an example of no amplicon is marked with ##. HIF1α shows a defined PCR product and was proceeded as hit.

Next, we did a plasmid isolation of the remaining 400 hits and submitted the isolated plasmids for sequencing analysis. Due to hits that appeared multiple times, we were able to decrease the number to 138 putative new interaction partners of RNF8. As expected, the positive control UBE2N was the most frequent hit; it came up >30 times. As an additional confirmation step a yeast-two-hybrid (Y2H) assay on individual hits was performed. We co-transformed the bait BD-RNF8 with each of 138 isolated prey plasmids into the haploid yeast strain pJ69-7a. BD-RNF8 and the empty prey vector (AD-empty) were used as negative control. Growing yeast on -Leu/-Trp/-His selection medium shows protein interaction, illustrated in Fig. 4.4.

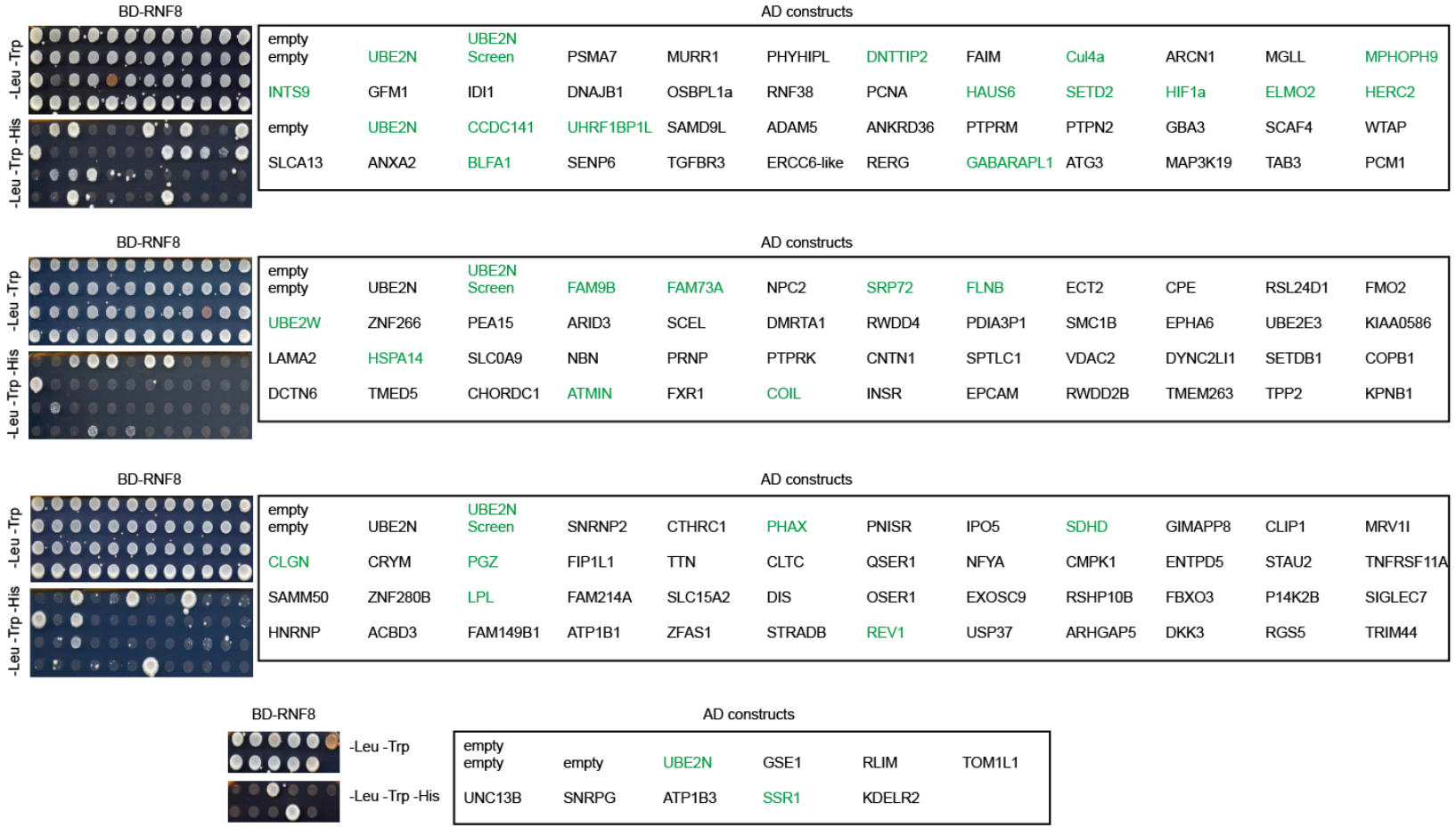


**Figure 4.4: Hit validation in yeast-two-hybrid.** Yeast-two-hybrid (Y2H) assay to re-test 138 isolated AD-Plasmids from the c-DNA library together with BD-RNF8 in pJ69-7a for interaction. Yeast was plated on -Leu/-Trp selection medium to monitor successful transformation of both plasmids. Growth on -Leu/-Trp/-His medium shows protein interaction. 34 verified interaction partners are highlighted in green. Cells were plated on minimal medium as indicated and incubated for 3-5 days at 30°C.

We could confirm 34 hits by this evaluation method, summarized in Fig. 4.5A according to their frequency in the screen. To choose the most promising interaction partners we checked the expression levels of BD-RNF8 as well as the expression levels from all 34 hit plasmids by western blot analysis (Supplement 1). BD-RNF8 was detected in every sample, however in some cases the expression was rather low. The AD-Plasmids showed a wide range of expression levels. The positive control UBE2N was prominently expressed in all tested samples (Supplement 1) whereas several hits showed no AD-plasmid expression, even after very long exposure times. We decided to choose the final hits not only due to their expression levels, but also due to the frequency they came up in the screen. Hence, we eliminated all hits that came up less than three times in the screen or showed no obvious AD plasmid expression (Fig. 4.2). Based on this approach, we identified 13 interaction partners, including HERC2 and UBE2N as positive control and 11 putative new interaction partners of RNF8 (bold in Fig. 4.5A).

As mentioned above, the c-DNA library obtained by clontech only presents fragments of the prey DNA, so no full-length proteins are translated. Therefore we wanted to generate clones expressing full-length proteins of all 13 hits, to verify the putative interactions with RNF8. However, only 5 of the remaining hits were cloned successfully as full-length vectors due to size and cellular expression issues. In Fig. 4.5B we used the Y2H approach to investigate the physical interaction between the E3 Ligase RNF8 as bait and FAM9B, DNTTIP2, SSR1, CUL4a and HIF1$\alpha$ as prey proteins. Bait and prey constructs were transformed into the yeast strain Y2HGold, auxotrophic for leucin and tryptophane allowing the selection for successfully transformed cells on leucin and tryptophane lacking media (-Leu/-Trp). If bait and prey interact, Gal4 is able to transcribe the reporter gene *HIS3* enabling cells to grow on histidine lacking media (-His). As positive control we used UBE2N and HERC2, well-known interaction partners of RNF8 (Mailand et. al. 2007, Bekker-Jensen et. al. 2010), as both were prominent hits in the screen (Fig 4.5A). Due to its size, we were not able to use full length HERC2, instead we tested the C-terminal HECT domain of HERC2. Notably, RNF8 was able to interact with UBE2N, Fam9B, Cul4a and HIF1α (Fig. 4.5B). However, we could not reproduce the interaction with DNTTIP2 or SSR1 in this setting. It appears that HERC2-HECT is not sufficient to interact with RNF8 in this approach. Reasons could be

problems with the construct, since the screen showed a positive interaction of RNF8 with a C-terminal fragment of HERC2. Nevertheless, common examples for false negatives in Y2H assays are large proteins, which cannot be reliably expressed in yeast (Nakayama et. al. 2002).

Summarizing the screening, out of 1600 initial hits, we found 11 promising new interaction partners. We finalized on FAM9B, Cul4a and HIF1α by showing that they are reliably able to interact with RNF8 in yeast.

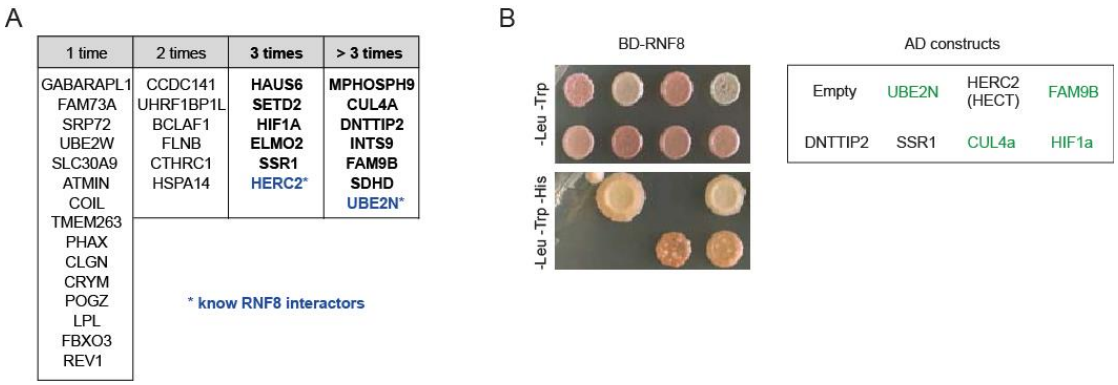


**Figure 4.5 Final hit selection.** (A) Summary of 34 verified interaction partners of RNF8, listed by frequency in the screen. HERC2 and UBE2N are highlighted as positive controls. (B) Full length UBE2N, FAM9B, CUl4a and HIF1α are interacting with RNF8 in Y2H (highlighted in green). Cells were plated on minimal selection medium as indicated and incubated at 30°C for 3 days.

## 4.2 HIF1α - a new interaction partner of RNF8

### 4.2.1 Full length HIF1α interacts with RNF8 in Y2H

We next reasoned to pick one interactor out of FAM9B, Cul4a and HIF1α to pursue in-depth validation and functional studies. FAM9B (Family with sequence similarity 9 member B) is a largely uncharacterized protein, while Cul4a is part of a well-known cullin-Ring Family of E3 Ligases. With RNF8 being a RING E3 Ligase, we argued that this might not be a best-fit candidate. Thus, our attention was drawn to HIF1α, the α-subunit of the hypoxia induced transcription factor HIF1 (details in introduction), being a putative substrate for the E3 ligase RNF8. To analyze the specificity of the interaction we tested whether HIF1α interacted with RNF8 only, or also another member of the RING Finger protein family, RNF168. The RING E3 Ligase RNF168 acts in close proximity to RNF8 during the DNA double strand break (DSB) repair and is

structural, functional and locational wise very similar to RNF8 (Mailand et. al. 2007, Kolas et. al. 2007, Doil et. al. 2009). In a Y2H assay, RNF8 or RNF168 were used as bait proteins, HIF1α was used as prey. Bait and prey were transformed into the yeast strain pJ69-7a, auxotrophic for leucin, tryptophane and histidine. Figure 4.6 shows successful transformation of bait and prey proteins with growing colonies on -Leu/-Trp media, as well as HIF1α being able to interact with RNF8 but not RNF168 on -Leu/-Trp/-His media plates. HIF1α has a specificity for RNF8 in Y2H assays.

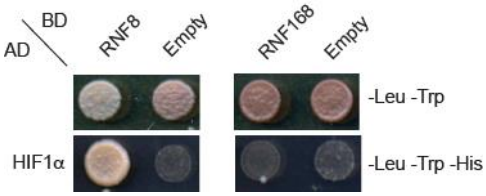


**Figure 4.6: HIF1α interacts with RNF8 but not RNF168 in Y2H.** Cells were plated on minimal medium as indicated and incubated at 30°C for 3 days.

### 4.2.2 HIF1α and RNF8 interact in human cells

The Y2H analyses indicate that HIF1α and RNF8 interact in yeast cells. To learn more about the interaction in human cells, RNF8 and HIF1α were cloned into the mammalian expression vectors pEGFPC1 and pEF4 fusing the proteins to an N-terminal GFP-tag or Flag-tag, respectively. We overexpressed GFP-RNF8 and Flag-HIF1α fusion proteins in human embryonal kidney cells (HEK293T). Using agarose beads coupled to GFP-nanobodies (Chromotek, GFP-TRAP assay) we were able to immunoprecipitate the GFP labeled protein, GFP-RNF8 and analyzed its interaction with HIF1α (Fig. 4.7A). To control for unspecific binding of Flag-HIF1α to the GFP-tag or agarose beads, we included GFP-empty as a negative control. Actin proves similar loading of all samples while Flag-HIF1α, GFP-empty as well as GFP-RNF8 are expressed evenly, shown in the input samples (Fig. 4.7A). In the upper panel, the GFP TRAP samples show the evident co-immunoprecipitation of Flag-HIF1α with GFP-RNF8 compared to GFP-empty. In order to decrease the chance for assay-derived artifacts, we repeated the TRAP experiment while using flipped protein tags. In Figure 4.7B, GFP-HIF1α is pulled by the GFP-nanobodies as well as GFP-empty as control. As expected, overexpressed Flag-RNF8 specifically co-immunoprecipitates with GFP-HIF1α and not with the empty control.

The results in Figure 4.7 confirmed an interaction between HIF1α and RNF8 in human cells.

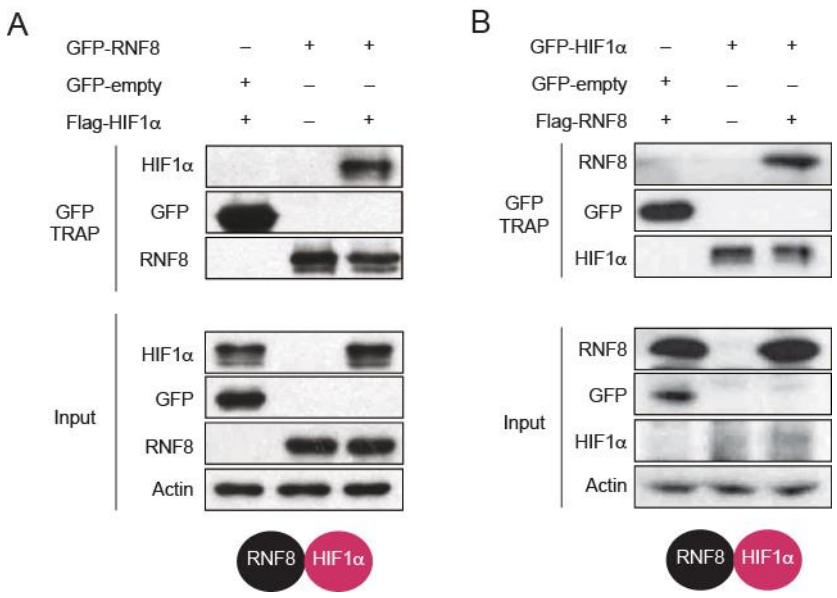


**Figure 4.7: RNF8 interacts with HIF1a in human cells.** (A) GFP-RNF8 was co-expressed with Flag-HIF1α in HEK293T cells, GFP-empty was used as negative control. Cells were harvested 24 h post transfection. Flag-HIF1α co-immunoprecipitates with GFP-RNF8 but not the GFP-empty control. (A-B) In the GFP-TRAP assay agarose beads coupled to GFP-nanobodies were used to pull GFP-tagged proteins from the lysate (Input), protein levels were analyzed via immunoblotting. (B) GFP-HIF1α was co-expressed with Flag-RNF8, GFP-empty was used as negative control. Flag-RNF8 co-immunoprecipitates with GFP-HIF1α but not with the empty control.

### 4.2.3 Mapping of the protein-protein interaction domains of HIF1α and RNF8

It is well established, that certain protein domains determine the structure of the protein as well as reveal the protein function (Todd et. al. 2001, Bashton and Chothia 2007). In order to get new insights in the functional relationship of HIF1α and the RING E3 Ligase RNF8 we created several truncations of both proteins to do further interaction studies by mapping the binding domains. All protein variants are summarized in Figure 4.8A. For RNF8 we focused on the N-terminal FHA domain, important for its subcellular localization as well as the C-terminal RING domain, harboring the catalytic E3 Ligase activity (Durocher et. al. 2000, Ito et. al. 2001, Huen et. al. 2007). We either deleted one of two domains to investigate the rest of the protein (RNF8ΔFHA, RNF8ΔRING) or used the domains only (RNF8 (FHA), RNF8 (RING)). HIF1α on the other hand, can be divided in its N-terminal and C-terminal part, the latter one (TAD domain) known to be the target for numerous post-translational

modifications (Jiang et. la. 1997). We created HIF1α (TAD) together with the WT protein (HIF1α WT). Next, RNF8 wild type (RNF8 WT), RNF8 (FHA), RNF8 (RING), RNF8 ΔFHA and RNF8 ΔRING were used as bait in an Y2H assay together with HIF1α WT and HIF1α (TAD) as prey. UBE2N was used as control. Bait and prey were transformed into the yeast strain pJ69-7a as shown in Figure 4.8B. The -Leu/-Trp media selects for successful transformation (upper panel), whereas the -Leu/-Trp/-His plates show positive interaction of bait and prey. The -Leu/-Trp/-His medium shows colonies growing with an empty prey plasmid as well (middle panel, bottom line), which can be a sign for false positives in Y2H assays. To eliminate this common technical problem, we increased the stringency of the assay by using adenine deficient media instead of histidine (lower panel). Only if bait and prey interact, the Gal4 transcription factor is able to transcribe the reporter gene *Ade* enabling cells to grow on adenine lacking media (-Ade). Interestingly, we found that HIF1α selectively interacts with the FHA domain of RNF8 and not its catalytically active RING domain. HIF1α WT as well as HIF1α (TAD) is able to interact with RNF8 WT, RNF8 (FHA) as well as the RNF8 ΔRING truncation (Fig. 4.8B). As expected, the E2 enzyme UBE2N interacts with RNF8 WT, RNF8 (RING) and RNF8 ΔFHA, since it needs the RING domain of RNF8 for interaction (Plans et. al. 2007). Thus, the interaction of RNF8 with HIF1α seems to be independent of its catalytic E3 Ligase activity. To verify this finding in human cells we overexpressed Flag-HIF1α WT together with GFP-RNF8 WT, GFP-RNF8 ΔFHA and GFP-RNF8 I439D. I439D is a point mutation in the catalytic center of the RING domain of RNF8, causing its inactivation. Using the GFP Trap assay we analyzed the binding to HIF1α WT and the RNF8 mutants (Fig. 4.8C). The input control shows equal sample loading by comparing the actin levels, and ensures successful transfection as well as expression of GFP-RNF8 WT, GFP-RNF8 I439D, GFP-RNF8 ΔFHA, GFP-empty and Flag-HIF1α. As illustrated in the upper panel of Figure 4.8C, HIF1α WT is co-precipitated with GFP-RNF8 WT as well as its catalytically inactive mutant GFP-RNF8 I439D. However, RNF8 without FHA domain (GFP-RNF8 ΔFHA) does not bind HIF1α WT. Flag-HIF1α did not unspecifically bind to the GFP tag or the agarose beads (Figure 4.8C)

As mentioned in the introduction, HIF1α is constitutively expressed and subsequently degraded under normoxic conditions, due to modifications by prolyl-4-hydroxylases

(PHDs). HIF1α is known to be subsequently ubiquitinated by the E3 Ligase VHL and targeted for proteasomal degradation after hydroxylation by PHDs (Huang et. al. 1998, O´Rourke et. al. 1999, Tanimoto et. al. 2000). To test whether the interaction of RNF8 and HIF1α is also oxygen dependent, as shown for VHL, we created three point mutations in the TAD domain of HIF1α (P402A, P564A, N803A), resulting in stable non-hydroxylated HIF1α (HIF1α ΔΔΔ). In Figure 4.8D, the input samples control for equal loading (Actin) as well as positive transfection and expression of all protein variants (GFP-empty, GFP-RNF8 WT, Flag HIF1α WT, Flag- HIF1α ΔΔΔ). The GFP-TRAP samples illustrate that pulled GFP-RNF8 WT interacts with Flag-HIF1α WT as well as its mutation Flag-HIF1α ΔΔΔ. GFP-empty was used as negative binding control for Flag-HIF1α WT and Flag-HIF1α ΔΔΔ.

Together, these results indicate, that the interaction of RNF8 and HIF1α is dependent on the FHA domain of RNF8, enabling it to bind to the TAD domain of HIF1α. This interaction is independent of oxygen-dependent modifications of HIF1α.

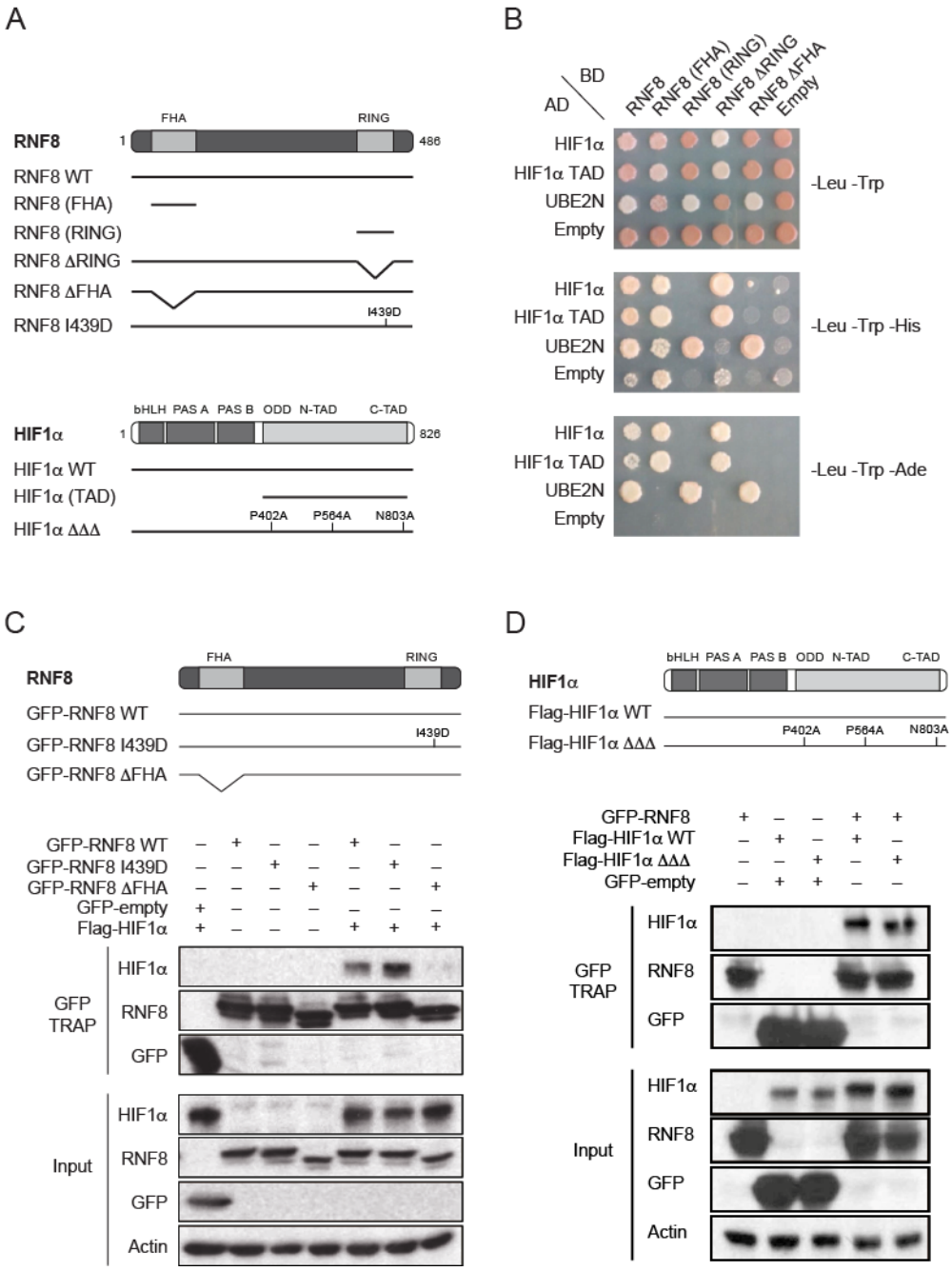


**Figure 4.8: Mapping of the interaction of HIF1α and RNF8.** (A) Schematic of RNF8 and HIF1α protein variants used in Fig. B-D. (B) Y2H assay in pJ69-7a yeast strain, BD and AD plasmids were transformed as indicated and grown on -Leu/-Trp selection plates to monitor the uptake of both plasmids. Growth on -Leu/-Trp/-His or -Leu/-Trp/-Ade medium shows protein interaction, whereas -Leu/-Trp/-Ade has a higher stringency. AD-UBE2N was used as positive control. HIF1α WT as well as HIF1α (TAD) needs the FHA domain of RNF8 for interaction. (C) GFP tagged protein variants of RNF8 (GFP-RNF8 WT, GFP-RNF8 I439D, GFP-RNF8 ΔFHA) were overexpressed and pulled from HEK293T cell lysates. Overexpressed Flag-HIF1α was co-precipitated with GFP-RNF8 WT as well as GFP-RNF8 ΔFHA, detected via western blot analysis. (D) Flag-HIF1α WT as well as Flag-HIF1α ΔΔΔ are able to co-immunoprecipitate with GFP-RNF8 WT after overexpression in HEK293T cells, analysis via western blot. (C-D) GFP-empty was used as negative control. GFP tagged proteins were trapped using GFP-nanobodies coupled to agarose beads.

## 4.3 RNF8 counteracts the HIF1α stabilization mediated by the E3 Ligase TRAF6

### 4.3.1 TRAF6 interacts with HIF1α and stabilizes HIF1α protein levels

TRAF6 is a RING E3 Ligase that is involved in a wide variety of cell signaling processes (Xie P. 2013). Nevertheless, its role in hypoxia has just recently come into focus and is not yet fully understood (Sun et. al. 2013, Rezaeian et. al. 2017). TRAF6 and RNF8 are both RING finger E3 Ligases able to build K63 ubiquitin chains, together with the same E2 enzyme complex, UBE2N/Uev1a. Also, they both play a role in the DNA damage DSB repair (Hinz et. al. 2010, Kolas et. al. 2007, Mailand et. al. 2007). To elucidate the role of these two E3 Ligases together with HIF1α, we investigated the interplay of all three proteins. Figure 4.9A illustrates the interaction between HIF1α and TRAF6 in human embryonal kidney cells (HEK293T). GFP-HIF1α and GFP-empty as control were overexpressed together with Flag-TRAF6. Successful transfection as well as equal loading is illustrated in the input samples. GFP-HIF1α and GFP-empty were pulled from the cell lysate by agarose beads coupled to GFP-nanobodies (GFP-TRAP assay) and co-immunoprecipitated Flag-TRAF6 could be detected with GFP-HIF1α. In addition to that, the lysate samples of the assay reveal a stabilization of HIF1α after overexpression of TRAF6, which is consistent with results obtained in previous studies (Sun et. al. 2013). In Figure 4.9B we use the same GFP-TRAP approach, but this time we co–express GFP-RNF8 or GFP-empty together with Flag-TRAF6. Interestingly, Flag-TRAF6 was co-immunoprecipitated also with GFP-RNF8. These data indicate that not only HIF1α interacts with RNF8 and TRAF6 (Fig. 4.7, Fig. 4.9A) but also RNF8 and TRAF6 interact among each other (Fig. 4.9B).

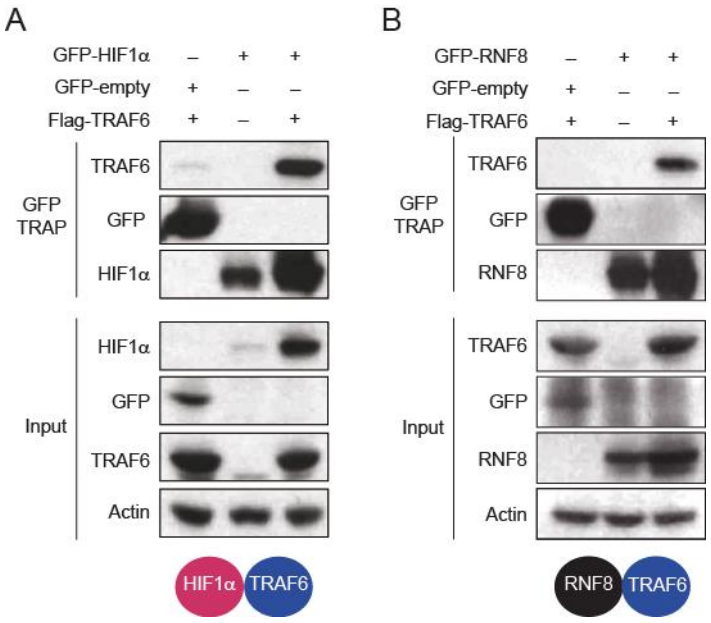


**Figure 4.9: TRAF6 interacts with RNF8 and HIF1a in human cells.** (A-B) Flag-TRAF6 co-immunoprecipitates with GFP-HIF1α (A) and GFP-RNF8 (B) in HEK293T cells after overexpression of both proteins. GFP-tagged proteins were overexpressed and pulled from HEK293T cell lysates using GFP-nanobodies coupled to agarose beads. Cells were harvested 24 h post transfection, subsequently protein levels were analyzed via immunoblotting. GFP-empty was used as negative control.

### 4.3.2 RNF8 counteracts the TRAF6 derived stabilization of HIF1α, independent of its catalytic activity

In order to understand the interplay between the two E3 Ligases RNF8 and TRAF6 together with the transcription factor HIF1α, we investigated the effects on endogenous HIF1α. Therefore we needed to induce HIF1α protein levels by mimicking hypoxic conditions using $CoCl_2$. We overexpressed and subsequently pulled GFP-RNF8 and checked for co-precipitated endogenous HIF1α (induced by $CoCl_2$), via western blot analysis. In Figure 4.10A we show that endogenous HIF1α binds GFP-RNF8 but not the GFP-empty control. This indicates that RNF8 and HIF1α interact also under physiological conditions in the cell, suggesting a role of RNF8 in hypoxia. Additionally we investigated the role of TRAF6 in this setting. Surprisingly, after overexpressing Flag-TRAF6 together with GFP-RNF8 in hypoxia mimicking conditions (+$CoCl_2$), we detected less HIF1α in the whole cell lysate (Input sample). The co-immunoprecipitated HIF1α protein with GFP-RNF8 is also drastically decreased (Fig. 4.10A) if TRAF6 is present. We used actin to control for equal loading in the lysate samples, staining for GFP, HIF1α, RNF8 and TRAF6 illustrates positive transfection and

expression of all protein variants in the input sample. Next, we wanted to investigate whether the destabilization of HIF1α depends on the catalytic activity of RNF8. Therefore we overexpressed GFP-RNF8 WT, GFP-RNF8 ΔFHA (ΔF) or GFP-RNF8 ΔRING (ΔR) together with Flag-HIF1α and Flag-TRAF6. As shown in the first two lanes of Figure 4.10B Flag-HIF1α gets stabilized after $CoCl_2$ treatment (-$CoCl_2$ vs. +$CoCl_2$), supporting previous studies (O´Rourke et. al. 1999, Wong et. al. 2013). In lane 3 and 4 we can observe, that the HIF1α protein level decreases to no-detection limit in western blot analysis, if Flag-TRAF6 is co-expressed with GFP-RNF8 WT. This is also true under hypoxia mimicking conditions (+$CoCl_2$, lane 4). The same happens if TRAF6 and RNF8 ΔRING are expressed. However, HIF1α levels are stabilized again if RNF8 looses its FHA domain (RNF8 ΔFHA). This is in line with our interaction studies from Figure 4.8B-C, suggesting that the interaction of RNF8 and HIF1α is necessary to see a destabilizing effect on HIF1α in the presence of RNF8 and TRAF6.

Taken together, we observed that HIF1α induced by hypoxia mimicking conditions decreases if RNF8 and TRAF6 are both overexpressed and this observation is dependent on the presence of the FHA domain of RNF8.

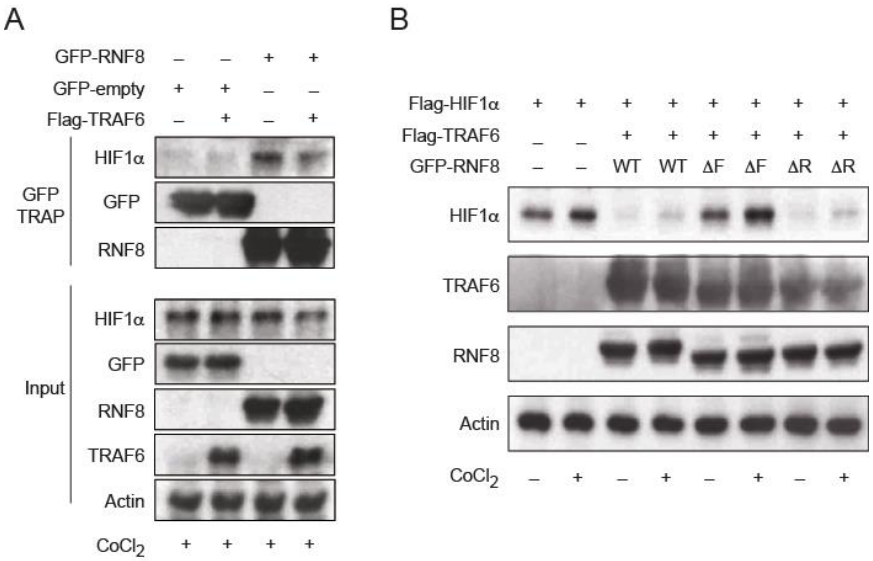


**Figure 4.10: Interaction studies between RNF8, TRAF6 and HIF1α.** (A) GFP-RNF8 and Flag-TRAF6 were overexpressed in HEK293T cells under hypoxia mimicking conditions (+ $CoCl_2$, 300µM for 24 h). HIF1α was induced by $CoCl_2$ and co-purified with GFP-RNF8. Flag-TRAF6 expression decreases the amounts of co-purified HIF1α with GFP-RNF8. (B) Flag-HIF1α was overexpressed in HEK293T cells together with Flag-TRAF6 and GFP-RNF8 WT, GFP-RNF8 ΔFHA (ΔF) or GFP-RNF8 ΔRING (ΔR) as indicated. Cells were incubated with (+) or without (-) 300 µM $CoCl_2$ for 24 h. Protein levels were analyzed via western blot, Flag-HIF1α levels are destabilized if Flag-TRAF6 is co-expressed with GFP-RNF8 WT or GFP-RNF8 ΔR.

### 4.3.3 Hypoxia vs. Normoxia – TRAF6 leaves the complex

We have shown that RNF8 and TRAF6 each interact with HIF1α, as well as that HIF1α protein levels decrease after overexpression of both E3 Ligases. Next, we wanted to understand if there is a prioritization between the interactions of all three proteins, under hypoxic vs. normoxic conditions. Flag-HIF1α and Flag-TRAF6 fusion proteins were overexpressed in HEK293T cells, together with GFP-RNF8. In line with our previous experiments (Fig. 4.10), in Figure 4.11A we demonstrate that HIF1α gets stabilized after $CoCl_2$ treatment and is significantly reduced after additional co-expression of TRAF6 together with RNF8 in the cell lysate (Input). GFP-empty, GFP-RNF8 and Flag-TRAF6 expression levels are not affected by $CoCl_2$ treatment. By pulling GFP-RNF8 we could co-immunorecipitate and thereby enrich the remaining Flag-HIF1α protein level (TRAP). The co-pulled HIF1α seems to even slightly increase after $CoCl_2$ treatment. Interestingly, also TRAF6 is able to co-purify with GFP-RNF8 under normoxic conditions (-$CoCl_2$) together with Flag-HIF1α (GFP TRAP, lane 3) giving rise to a complex. Nevertheless, co-immunoprecipitated TRAF6 amount decreases under hypoxic conditions (Fig. 4.11A, lane 3-4), whereas co-pulled HIF1$\alpha$ stays unaffected.
These findings suggest that stabilization of HIF1α by TRAF6 is not only reverted by RNF8, but RNF8 even decreases HIF1α levels in the cell lysate. HIF1α and TRAF6 are both binding RNF8, however, after inducing hypoxia (+$CoCl_2$) the amount of co-pulled TRAF6 decreases. The quantity of TRAF6 in the complex has no effect on the destabilization of HIF1$\alpha$.

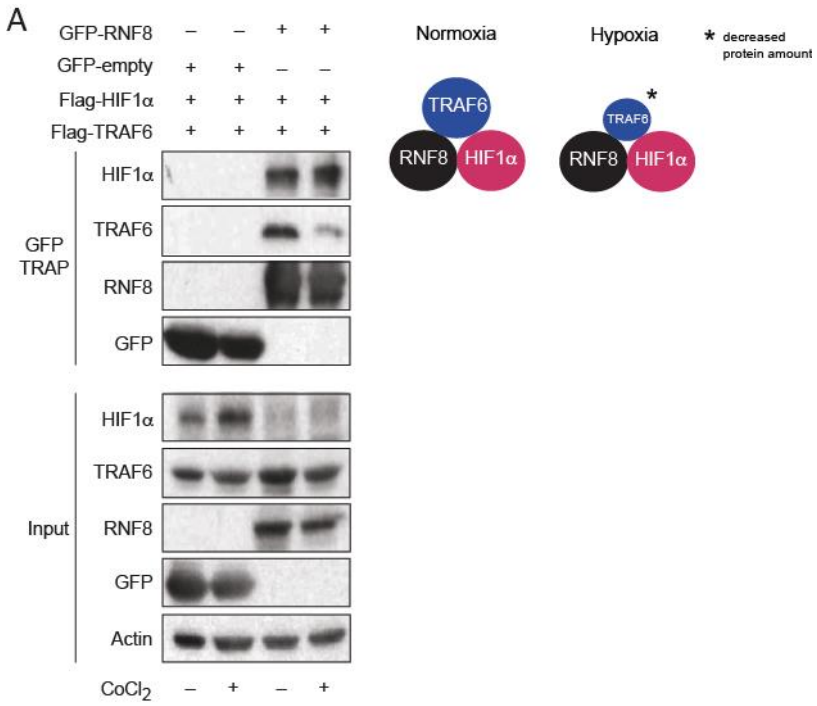


**Figure 4.11: The complex of HIF1α, RNF8 and TRAF6 under hypoxic vs. normoxic conditions.** (A) GFP-RNF8 was co-expressed with Flag-TRAF6 and Flag-HIF1α in HEK293T cells under normoxic (-$CoCl_2$) vs. hypoxic mimicking (+300 µM $CoCl_2$ for 24 h) conditions. GFP-proteins were trapped by GFP-nanobodies coupled to agarose beads. Co-immunoprecipitated TRAF6 and HIF1α were analyzed via immunoblotting. Co-pulled TRAF6 amount decreases under hypoxic conditions, whereas co-pulled HIF1α stays unaffected. The size of the circles illustrates protein quantity.

### 4.3.4 RNF8 and TRAF6 overexpression reduce HIF1 transcriptional activity

After establishing the interaction between RNF8 and HIF1α and finding the unusual destabilization of the transcription factor together with the E3 Ligase TRAF6, we aimed at investigating the functional outcome of this effect.

HIF1α is a highly regulated subunit, which under hypoxic or hypoxic mimicking conditions translocates to the nucleus and heterodimerizes with HIF1β to build the active transcription factor HIF1 (Semenza and Wang 1992, Wang et. al. 1995). We used two established target genes of HIF1 encoding the vascular endothelial growth factor (VEGF) as well as the Glucose transporter GLUT1, both ensuring cell survival under low oxygen conditions, thereby playing a major role in tumor progression (Tsuzuki et. al. 2000, Hayashi et. al. 2004). VEGF is one of several growth factors, controlled by HIF1, known as major regulator of angiogenesis increasing the distribution of the remaining oxygen under hypoxic conditions (Takeda et. al. 2004). GLUT1 ensures cell survival under low oxygen conditions by promoting anaerobic metabolism in the cell (Lum et.

al. 2007). HIF1α as well as RNF8 has been shown to be overexpressed in the most aggressive subtype of breast cancer, triple negative breast cancer (TNBC) (Lee et. al. 2016, Cancer Genome Atlas Network 2012), which is why we chose to use the TNBC model cell line MDA-MB231 for further functional analysis. In Figure 4.12A we investigated the mRNA levels of HIF1α after overexpression of Flag-RNF8 and Flag-TRAF6 under hypoxic conditions (0.1% $O_2$). All hypoxic samples were normalized to their normoxic control samples. As described in the literature, overall HIF1α mRNA levels decrease under low oxygen conditions (Uchida et. al. 2004, Chamboredon et. al. 2011), however Flag-TRAF6 overexpression increases HIF1α mRNA levels again. Overexpression of Flag-empty control, Flag-RNF8 as well as Flag-RNF8 together with Flag-TRAF6 show similar levels of HIF1α mRNA under hypoxic conditions (Fig. 4.12A). Finally we investigated the mRNA levels of the HIF1 target genes VEGF and Glut1 after overexpression of Flag-TRAF6, Flag-RNF8 or the combination of both of them. As expected, we found that Flag-TRAF6 overexpression results in higher levels of Glut1 and VEGF compared to the Flag-empty control in 0.1% $O_2$. Interestingly, the target gene levels are significantly decreased after co-expression of Flag-RNF8. These results underline our previous findings, RNF8 together with TRAF6 reverts the stabilizing effect on HIF1α by TRAF6, and as illustrated in Fig. 4.12B, results in diminished target gene activation of the transcription factor HIF1. This shows that the decreased protein level of HIF1α due to co-expression of RNF8 and TRAF6, actually has a functional consequence on target gene level. A scheme in Figure 4.12C summarizes these new findings.

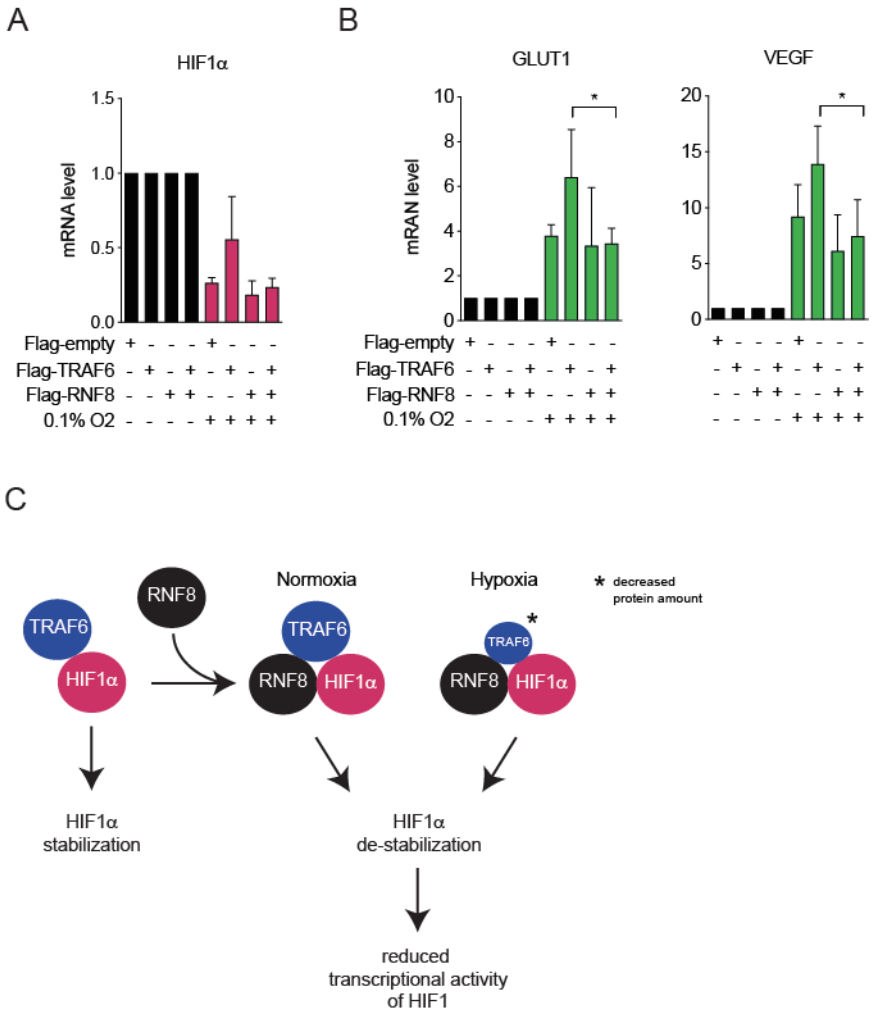


**Figure 4.12: RNF8 and TRAF6 co-expression reduce HIF1α transcriptional activity.** (A-B) MDA-MB-231 cells were cultured in normoxia (- 0,1% O2) vs. hypoxia (+ 0.1% O2) for 24 h post transfection with Flag-empty, Flag-TRAF6 and Flag-RNF8 (transfected as indicated). Cells were harvested for mRNA analysis of HIF1α (A), GLUT1 and VEGF (B) (n=3, biological independent extracts). Means and standard deviation are shown. Significances are calculated using Students t-test (p-value < 0.05). (C) Scheme of the interaction studies of RNF8 together with HIF1α and TRAF6 and their effect on HIF1 transcriptional activity. The size of the circles illustrates protein quantity.

# 5. Discussion

## 5.1 Finding new interaction partners of RNF8 using a Y2H screen

### 5.1.1 The Y2H approach as a tool to identify new interactors of RNF8

The Really Interesting New Gene (RING) Finger Protein 8 (RNF8) is implicated in a variety of cellular processes, best known for its role in DNA double strand break (DSB) repair (Kolas et. al. 2007, Mailand et. al. 2007). DSB is the most toxic form of DNA damage caused by endogenous stress (for example reactive oxygen species) or exogenous stress (for example ionizing radiation), leading to genomic instability. RNF8 plays a central role in transducing the DSB signal, enabling the main repair mechanisms, non-homologous end joining (NHEJ) and homologous recombination (HR) repair (Thorslund et. al. 2015, Mailand et. al. 2007). RNF8 has also been shown to play important roles in cell cycle progression, protection of chromosome ends and transcriptional activation (Chahwan et. al. 2013, Lee et. al. 2016, Wang et. al. 2017). All these functions are critical to prevent tumorigenesis and cancer progression and RNF8 was therefore described as an important tumor suppressor protein (Li et. al. 2010). However, recent studies illustrate that the E3 ligase is correlated with cancer cell migration, metastasis and disease progression in breast cancer, indicating a tumor-promoting function of RNF8 (Lee et. al. 2016, Wang et. al. 2017). The described implication of RNF8 in the most aggressive subtype of breast cancer, triple negative breast cancer (TNBC), makes it an interesting target, since there is a high need of new therapeutic strategies in this treatment-resistant form of cancer. Therefore, deciphering the diverse roles of RNF8 in cell signaling is an appealing strategy to find new ways of cancer therapy. Protein-protein interactions are crucial for all levels of cellular function. New interaction partners facilitate the understanding of biological functions of the protein of interest (POI), and may be useful for therapeutic purposes (Brückner et. al. 2009). For the identification of unknown interaction partners of RNF8, we performed a genome-wide yeast-two-hybrid (Y2H) screen, using RNF8 as bait and a human normalized c-DNA library as prey.

In 1989, Fields and Song described the Y2H approach for the first time, inventing the detection of new protein-protein interactions *in vivo*, in a true eukaryotic cellular environment. The technique is accessible for any laboratory, and allows for *in vivo* binary interactions, independent of the protein size in larger throughput. This is an advantage compared to the more classic biochemical *in vitro* interaction assays (for example co-purification, immunoprecitpitation, pulldown experiments) as well as to the commonly applied mass spectrometry (MS) approach. MS has become a powerful tool for the identification of large-scale interactomes. Although Y2H analysis is not able to identify a whole complex of interacting proteins, it is significantly cheaper as well as unbiased towards high affinity interactions compared to MS (Mehla et. al. 2017). However, the technique is only suitable for proteins that have no DNA binding (bait protein) or transcriptional activating (prey proteins) capacity on their own as well as interactions that are not blocked from N- or C-terminal fusions (activating domain (AD) or binding domain (BD)). Unless one is studying proteins that naturally occur in the yeast nucleus, the experimental set up reduces the possibility of indirect interactions. Additionally, the Y2H approach is known to be easily adapted for high throughput analysis, even on a genome wide scale (Rual et. al. 2005, Stelzl et. al. 2005). Two different screening procedures are described, the matrix (or array) and the library approach. The matrix approach is usually used to screen a set of baits versus a set of preys using full-length open reading frames (ORFs). Knowing the exact position of each bait on a matrix allows rapid identification of prey and bait, however the number of ORFs that can be screened is certainly limited. We wanted to screen one defined bait protein against a variety of prey proteins, which is why we chose the library screening approach. RNF8 was used as bait together with a cDNA library of prey proteins. The ability of haploid yeast strains (as Y2HGold and Y187) to mate with each other and form diploid cells provides a straightforward way to introduce the cDNA library (prey) to the bait (RNF8). In this work we made use of the commercially available Matchmaker Gold Y2H System (Clontech), providing us with an advanced Y2H assay version, using a normalized human cDNA mate and plate library. The library represents a broad range of expressed genes, from a collection of adult human tissues, both male and female. Since it contains a variety of cDNA fragments with different sizes, it decreases the rate of false negatives (Brückner et. al. 2009, Mehla et. al. 2017).

To also decrease the number of false positives, we invested in several independent follow up hit validation methods. With all its characteristics mentioned above, the Y2H screening approach seemed to be an excellent tool to identify new protein-protein interactions, revealing unknown tumor related functions of RNF8.

### 5.1.2 Hit verification and selection

To maximize the number of true interactions and minimize the number of false positives in the screen, we combined different validation steps. On the basis of our pilot studies with RNF8 as bait and the cognate E2 enzyme complex UBE2N/Uev1a as prey, we decided to run the screen at low stringency, using only one out of four possible reporter genes, *i.e. HIS3*. Comparing the number of colonies on medium lacking leucin and tryptophane (-Leu/-Trp) and the number of colonies on media additionally lacking histidine (-Leu/-Trp/-His) we concluded, the signal to noise ratio was sufficient on -Leu/-Trp/-His plates. Additionally, we minimized the number of false negatives by this decision (due to low stringency). The common problem in Y2H library screening approaches is the number of false positives. By using three independent promotors that control four reporter genes (*HIS3*, *Ade2*, *Aur1-C* and *Mel1*) we automatically eliminated all library proteins that interact with unrelated sequences in the promotor region enabling the transcription of reporter genes without proper Gal4 activation. We were able to eliminate a high number of false positives by this validation step, decreasing the number from 1600 hits to 500 hits. However, the high stringency of four reporter genes can also result in losing weak or transient interactions, which should not be excluded in our case. The ideal stringency level needs to be decided individually for each screen. Nevertheless, since 500 interactions are still considered a rather high number of hits, we used the highest stringency possible. Unfortunately, hit selection in Y2H assays by the experimenter is a subjective task. Thus, we included the reporter gene *Mel1*, which helped to increase the reproducibility of the screen by adding a systematic approach to monitor gene expression by discriminating between blue and white colonies. To further eliminate false positives, we used yeast colony PCR to determine the presence of AD-constructs and selected only colonies with one AD-construct. Spontaneous mutations as well as

contaminations can be the source for false positives as well. The final step in a library based Y2H screen is the prey identification by sequencing, enabled by plasmid isolation. After eliminating several duplicate hits, we found 138 interaction partners of RNF8. The most frequent hit was UBE2N, the cognate E2 enzyme of RNF8 used as positive control in the pilot experiments. The E3 Ligase HERC2, another well-known interaction partner of RNF8, was identified three times in the screen, together with the E2 conjugating enzymes UBE2E3 and UBE2W. The identification of several established interaction partners of RNF8 supports the high reliability of the screen and expands our confidence in the validity of the remaining hits. However, the high stringency procedure chosen, certainly gave rise to false negatives: both the E2 enzyme UBE2S and the E3 Ligase TRAF6 were not identified.

After identification of the prey proteins, there are several options to further validate these hits. Adapting the stringency and changing the vector system are highly recommended in order to get reproducible results. We were able to increase the stringency as needed by using nutrition markers, an antibiotic resistance marker, or colometric detection. In addition, we decided to test the interactions in a second yeast strain, *i.e.* pJ697a. Out of 138 Hits, we were able to verify 34 interactions in pJ697a, including the positive controls UBE2N and HERC2. True interactions should be reproducible in more than one Y2H assay system, which is why we decided to eliminate 75% of our preliminary hits using this harsh validation step (Caufield et. al. 2017, Brückner et. al. 2009). We recognized the high risk of losing true but weak interactions in this step, but since we were still able to reproduce the interaction of the E3 Ligase RNF8 with the E2 enzyme UBE2N, which is described to be rather transient and unstable itself (Lorick et. al. 1999, Xie et. al. 1999, Ye and Rape 2009), we considered it an acceptable criterion. Additionally, the expression of bait and prey proteins is usually higher after mating (as done in the screen) compared to the used double transfection method here; this could have eliminated possible true hits. Nevertheless, with this strategy the 34 remaining hits can be considered as highly reliable and thus limit the possibility for false positives. Since the library approach uses mostly cDNA fragments for prey expression, it is mandatory to retest all interactions with full-length proteins. On the basis of the frequent detection of the known interaction partners of RNF8 in the screen (UBE2N and HERC2), we decided to use the

cutoff at three shows or higher for interesting new binding partners of RNF8. We further eliminated hits that did not show any prey protein expression in yeast, investigated by western blot analysis.

Eventually, we were able to confirm the interaction of RNF8 with full-length FAM9B, Cul4a and HIF1α and reasoned to pick one new interactor to pursue in-depth validation and functional studies. FAM9B (Family with sequence similarity 9 member B) is a largely uncharacterized protein, shown to be exclusively expressed in testis with its gene product localized to the nucleus (Martinez-Garay et. al. 2002). In addition, FAM9B has been directly implicated in serum testosterone concentration (Ohlsson et. al. 2011). Cul4a is part of a well-known cullin-Ring Family of E3 Ligases implicated in a wide variety of cellular processes and pathologies (Angers et. al. 2006, Liu et. al. 2009). It works as a scaffold protein, thereby able to bind a repertoire of substrate receptors with its N-terminal domain, as well as the small RING-finger protein ROC1 (ring of cullins) with its C-terminal domain. HIF1α is the $O_2$ labile $\alpha$-subunit of the hypoxia induced transcription factor HIF1 (detailed information see introduction), which is overexpressed in TNBC cells resulting in increased invasion, metastasis and resistance to chemotherapy (Zhong et. al. 1999, Vaupel et. al. 2001, Cancer Genome Atlas Network 2012). RNF8 was recently shown to interact and stabilize another transcription factor, TWIST by Lys63 ubiquitination (Lee et. al. 2016) and TWIST and RNF8 were also shown to be highly expressed in triple negative breast cancer (TNBC). By using rigor validation during and after the Y2H screening procedure, we identified HIF1α as promising new interaction partner of RNF8. This finding is a highly interesting new protein-protein interaction that may identify a new therapeutic target for TNBC treatment.

## 5.2 HIF1α – a new interaction partner of RNF8

### 5.2.1 HIF1α specifically interacts with RNF8

To ensure the specificity of the interaction between RNF8 and HIF1α, we wanted to make use of two more validation steps in yeast: the bait dependency test as well as the bait/prey swapping. Both are commonly used and highly recommended verification techniques following a Y2H screen (Möckli et. al. 2007, Brückner et. al. 2009). To see whether HIF1α interacts specifically with RNF8 rather than any E3 ligase, we used RNF168 as control-bait in Y2H. The sequential action of the RING finger E3 Ligases RNF168 and RNF8 in DNA double strand break repair leads to the recruitment of several repair factors to the DNA lesion. Both E3 ligases work in close proximity at the same site, generating Lys63-ubiquitin chains while binding the same E2 enzyme complex, UBE2N/Uev1a (Mailand et. al. 2007, Thorslund et. al. 2015). RNF168 was therefore considered to be the ideal control due to its functional, structural and locational similarity to RNF8. Indeed, we were able to show that HIF1α interacts with RNF8 but not RNF168. Thereby, we proved the specificity of the binding and decreased the risk for an indirect or bridged interaction. However, it was not possible to verify the interaction using a bait/prey swapping as suggested by Caufield et. al. 2012. In this case, RNF8 should get fused to the AD plasmid and HIF1α to the BD plasmid. HIF1α, being a transcription factor, harbors a very high gene activation capacity on its own. By enabling it to bind to the DNA as a DNA-BD fusion it will activate reporter gene transcription without binding of any AD-protein. This limitation of the Y2H assay was already described by Fields and Song in 1989; proteins that have an activating capacity on their own are not suitable as “bait” proteins. Therefore, we finally verified the interaction in human cells, using *in vitro* co-immunoprecipitation assay by pulling GFP tagged proteins and analyzing the co-precipitates for the probable interaction partner. Our results demonstrate that RNF8 and HIF1α also interact in human cells. An RNF8-HIF1$\alpha$ interaction was confirmed by pulling either RNF8 or HIF1$\alpha$. Importantly, we further proved the interaction of GFP-RNF8 with endogenous HIF1α under hypoxic conditions. The interaction between RNF8 and HIF1$\alpha$ seems to be rather strong. Based

on the identification in a Y2H assay, it is likely that HIF1α and RNF8 interact in the nucleus rather than in the cytoplasm. Ongoing experiments may support this hypothesis and are in line with the described localization of active HIF1α (Ivan et. al. 2001, Majmundar et. al. 2010) as well as active RNF8 (Kolas et. al. 2007, Mailand et. al. 2007, Huen et. al. 2007).

Taken together, we could confirm the interaction of HIF1α and RNF8 in yeast and in human cells.

### 5.2.2 RNF8 interacts with HIF1α independent of its catalytic activity

To get a first impression if HIF1α is a substrate of RNF8, we investigated the protein levels in the cell lysate samples of the *in vitro* pull-down experiments in more detail. Surprisingly, we could not detect any change of HIF1α protein level after overexpression of RNF8. This is distinct from the described role of RNF8 in controlling other transcription factors. RNF8 was shown to stabilize the transcription factor TWIST by Lys63-linked poly ubiquitination, revealing a tumor promoting function of RNF8 (Lee et. al. 2016). Wang et. al. 2017 showed that RNF8 stabilizes and transactivates the transcription factor ERα, probably by monoubiquitination. Our results seem to refute the hypothesis that RNF8 is also stabilizing HIF1α by its E3 Ligase activity, similar to the mechanism of action described for TWIST or ERα. Nevertheless, RNF8 is not only capable of modifying substrates with Lys63-linked ubiquitin chains, but also with Lys48-linked ubiquitin chains, the latter marking proteins for subsequent proteasomal degradation (Ito et. al. 2001, Lok et. al. 2012). Under normoxic conditions, HIF1α is hydroxylated by prolyl-4-hydroxylases (PHDs) and thereby recognized by von Hippel Lindau (VHL), which is part of an E3 ligase complex to mark HIF1α with Lys48-linked ubiquitin chains for its fast degradation. Obviously we questioned whether RNF8 could be another E3 Ligase able to ubiquitinate HIF1α with Lys48-linked chains. We therefore would expect decreased protein levels of HIF1α after RNF8 overexpression in HEK293T cells. However, this was not the case as protein levels were stable in the binding studies. Hence, these results suggest a different mechanism behind the interaction of RNF8 and HIF1α, possibly a function independent of its E3 Ligase activity.

To understand whether the hydroxylation status of HIF1a determines the interaction with RNF8, we generated a triple point mutation of HIF1α (P402A, P564A, N803A), to get a non-hydroxable form of the protein. Under hypoxic conditions, the hydroxylation events are prevented as well, therefore von Hippel Lindau (VHL) can no longer recognizes its substrate and HIF1α is stabilized to mediate transcriptional activation. We used the triple point mutation HIF1αΔΔΔ to investigate if the interaction mode with the E3 Ligase RNF8 follows the same pattern. Interestingly, we could show that the interaction of RNF8 and HIF1α is independent of the hydroxylation status of HIF1α supporting our previous observations and the hypothesis that HIF1α is no substrate of RNF8.

### 5.2.3 RNF8 interacts with HIF1α via its FHA domain

To characterize the interaction of HIF1α and RNF8 in more detail, we generated several truncations of both proteins, thereby trying to map the interaction. RNF8 consists of two functional domains: the N-terminal forkhead-associated (FHA) domain and the C-terminal RING domain. The FHA domain is important for its subcellular localization, and the RING domain is involved in ubiquitin ligase activity (Seki et.al. 1998). We found that the FHA domain of RNF8 is mandatory for the interaction with HIF1α, whereas the RING domain is neither necessary nor sufficient to bind HIF1α. We were able to show that the FHA domain alone is capable of binding HIF1α WT as well as the C-terminal TAD Domain, which is the transactivation domain of HIF1α. This was tested in Y2H and confirmed in human cells using an *in vitro* pull-down assay. Our findings compare well with the characteristics of the FHA domain, mediating protein-protein interactions by recognizing phosphopeptide binding motifs (Durocher et. al. 1999, Durocher et. al. 2000). The FHA domain of RNF8 recognizes a short amino acid sequence around a central phospho-Threonin (pThr), with either Tyr or Phe in the +3 position (pTxxY/F) (Huen et. al. 2007). The strong selection for this motif is rather unique compared to all other FHA domains for which x-ray crystal structures are available (Durocher et. al. 2000, Li et. al. 2000, Huen et. al. 2007). We were able to localize the pTxxY/F motif in HIF1α at three different sites, all in the N-terminal region (Fig. 5.1). However, this is rather inconclusive, since we have shown that RNF8 is able

to interact with only the C-terminal TAD domain of HIF1α, thereby lacking all possible interaction motifs. Nevertheless, this was only tested in yeast, not in human cells so far and should therefore be validated with other methods. Noteworthy, there is a described phosphorylation site in the C-terminal TAD domain of HIF1α, at T796 (Gradin et. al. 2002). It is not followed by Tyr or Phe in the +3 position, and is therefore not predicted as a RNF8 interaction motif, but could still govern the interaction motif. This should be analyzed in future studies using point mutation. Interestingly, the unique FHA domain of RNF8 has structural features that are likely involved in phospho-independent interactions as well (Huen et. al. 2007, Durocher 2000). HIF1α could be the first binding partner of RNF8 to use this unique property of the FHA domain. Further work is planned to address the phosphorylation status of HIF1α while interacting with RNF8.

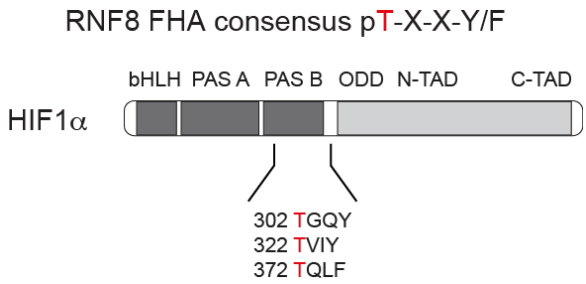


**Figure 5.1: Functional domains of HIF1α and location of the RNF8 consensus motifs**

## 5.3 The HIF1α/TRAF6/RNF8 complex

### 5.3.1 HIF1α, TRAF6 and RNF8 interact among each other

HIF1α was found to be stabilized by Lys63 ubiquitination by TRAF6 (Sun et. al. 2013). A similar mechanism was described for the transcription factor TWIST, which is modified with Lys63 chains by RNF8 (Lee et. al. 2016). In this thesis, we aimed at understanding HIF1α stabilization by TRAF6 and RNF8, respectively, in more detail. First, we were able to confirm binding of HIF1α to TRAF6 as previously described (Sun et. al. 2013) using *in vitro* pull-down assays in human cells, as well as TRAF6 mediated stabilization of HIF1α. Additionally, we could show that TRAF6 interacts with RNF8. This observation is rather surprising; two RING E3 ligases as novel heterodimeric

complex. TRAF6 oligomerization is well established and known to ensure efficient polyubiquitin chain assembly by optimizing the interaction with E2 enzymes (Yin et. al. 2009, Hu et. al. 2017). Heterodimers of RING E3 Ligases have been described, as for example BRCA1-BARD1 and RING1B-Bmi1, in both cases resulting in a promoted catalytic activity. This can be either due to stabilization effects, primed E2 interaction or increased substrate specificity (Metzger et. al. 2014). This could explain our previous findings that HIF1α does not seem to be a substrate of RNF8 even though they strongly interact. We wanted to understand whether TRAF6 and RNF8 in complex are needed to establish an enzyme-substrate relationship with HIF1α. *In vitro* pull-down experiments revealed that after overexpression of GFP-RNF8 and Flag-TRAF6, endogenous HIF1α is still co-pulled with GFP-RNF8 in hypoxic conditions. However, we discovered that endogenous HIF1α levels markedly decreased in the presence of both E3 ligases compared to GFP-RNF8 alone. Thus, our findings demonstrate that HIF1α, TRAF6 and RNF8 all interact among each other and further suggest a novel function for RNF8 and TRAF6, where they act together as E3 ligases to regulate HIF1α levels.

### 5.3.2 Destabilization of HIF1α by TRAF6 and RNF8

TRAF6 stabilizes HIF1α protein levels whereas RNF8 does not affect HIF1α protein levels by its own. Interestingly, when both E3 ligases are overexpressed, decreased level of HIF1α protein was detected. Our results demonstrate very strikingly how HIF1α protein levels decrease almost to no-detection limit if TRAF6 and RNF8 WT or RNF8 ΔRING are co-expressed. If RNF8 loses its FHA domain, HIF1α protein levels are restored. This is in perfect agreement with our interaction studies, the FHA domain of RNF8 is mandatory for the interaction with HIF1α. Our data reveal a compelling contrast between the stabilization of HIF1α by TRAF6 alone, compared to the loss of protein level as soon as RNF8 gets co-expressed and joins the complex. Importantly, this effect is independent of oxygen. Intriguingly, pulling GFP-RNF8 and analyzing binding to HIF1α and TRAF6 under hypoxic and normoxic conditions revealed new and unexpected interaction dynamics. We found HIF1α and TRAF6, both co-precipitated with GFP-RNF8 under normoxic conditions. However, after inducing hypoxia, the amounts of TRAF6 decrease while co-pulled HIF1α stays unaffected. This indicates a

mechanism where RNF8 and TRAF6 can destabilize HIF1α even with low levels of TRAF6. Importantly, TRAF6 has been shown to play a distinct role in hypoxia: it gets recruited to the histone variant H2AX under low oxygen conditions to enrich HIF1α ??ezaeian et. al. 2017). Therefore, a regulatory feedback loop seems possible, in which TRAF6 leaves the complex to stabilize HIF1α again under continuing hypoxic conditions. This would rescue HIF1α in prolonged hypoxia, thereby maintaining cell survival. Target gene experiments, to determine this hypothesis and prove HIF1α re-stabilization are in progress.

To encourage our basic hypothesis, that TRAF6 and RNF8 are modifying HIF1α on a protein level, we investigated the mRNA level as well. In agreement with current literature, we showed that HIF1α mRNA levels are decreased under hypoxic conditions (Chamboredon et. al. 2011). Otherwise, it is rather unaffected by the overexpression of RNF8 and TRAF6. Expression slightly increases after Flag-TRAF6 overexpression, a trend also detected by Sun et. al. 2013; nevertheless there is no significant difference. This underlines the main idea, that TRAF6 and RNF8 regulate HIF1α on a protein level, most likely by ubiquitination. HIF1α is known to be regulated in multiple ways, due to its function as master regulator in $O_2$ homeostasis. Several E3 ligases are described to be involved in this process. Best known is the E3 ligase complex with von Hippel Lindau (VHL), which regulates the stability of HIF1α via Lys48-linked ubiquitination and proteasomal degradation under normoxic conditions (Tanimoto et. al. 2000). Hypoxia-associated factor (HAF) and carboxyl terminus HSP70-interacting protein (CHIP) on the other hand, use the same post-translational modification to induce HIF1α degradation, but independent of oxygen tension (Koh et. la. 2008, Bento et. al. 2010). In 2012, another E3 ligase was discovered to modify the alpha subunit; Sharpin induces proteasomal degradation of HIF1α independent of the ubiquitination machinery (Montagner et. al. 2012). Our data indicate that the regulation of HIF1α is independent of the E3 ligase activity of RNF8. It is possible though, that both RING E3 ligases, (RNF8 and TRAF6) work in concert to promote ubiquitination as described for BRCA1-BARD1 and RING1B-Bmi1 (Metzger 2015). We suggest three possible mechanisms for RNF8/TRAF6 mediated degradation of HIF1α: (i) RNF8 may facilitate the interaction of TRAF6 with Lys48 or Lys11 specific E2 enzymes, which is otherwise not possible for TRAF6 alone (Walsh et. al. 2015). This has never been described for

HIF1α before and thus suggests a novel regulatory mechanism. (ii) RNF8 and TRAF6 enable the association with other regulatory factors enhancing the interaction with VHL to modify HIF1α, or allow other E3 ligases to mark HIF1α for degradation. Accordingly, they could also enable regulatory factors to bind or modify HIF1α, inducing proteasomal independent degradation, as autophagy. (iii) A model according to the mechanism published by Montagner et. al. in 2012, where TRAF6 and RNF8 build a complex with HIF1α to directly present it to the proteasome. A scheme of all mentioned possibilities is illustrated in Figure 5.2. Further work is needed to decipher the exact mechanism behind the regulation of HIF1α by TRAF6 and RNF8, including ubiquitination assays as well as proteasomal inhibition assays. By using a small molecule inhibitor of TRAF6, which is able to selectively inhibit TRAF6 activity by interfering with the E3-E2 protein-protein interaction, we hope to determine whether TRAF6 is catalytically active and ubiquitinates HIF1a with the help of RNF8. The compound C25-140 (Brenke et. al. 2018) will be an excellent tool to understand the role of TRAF6 in this new ternary complex of HIF1$\alpha$, RNF8 and TRAF6.

In this work, we revealed the new interaction of RNF8 and HIF1α, resulting in downregulation of HIF1α levels after co-expression of TRAF6.

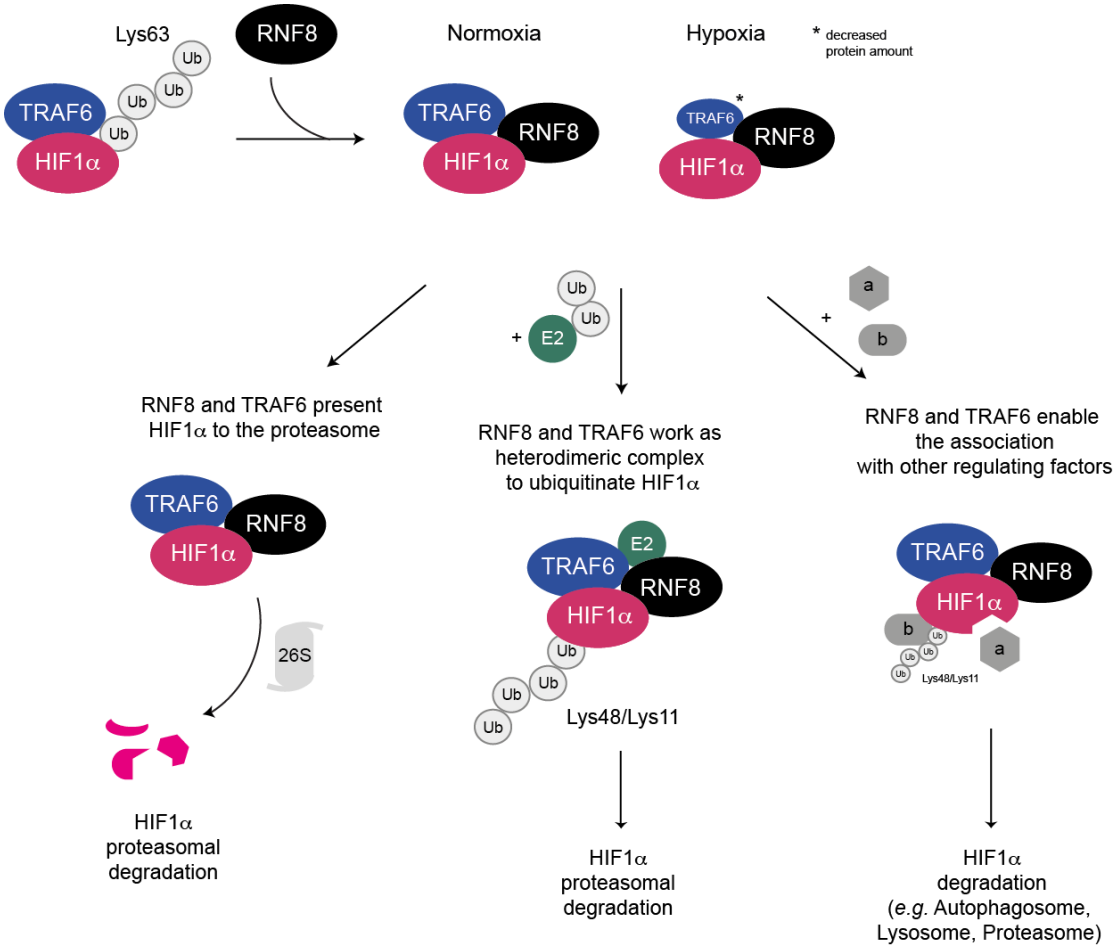


**Figure 5.2: Model for the regulation of HIF1α by TRAF6 and RNF8.**

### 5.3.3 The complex of TRAF6 and RNF8 with HIF1α and its functional relevance

To prove the relevance of our findings, we investigated the effect on HIF1α dependent target gene expression. In response to oxygen deprivation, HIF1α gets stabilized to bind HIF1β in the nucleus and form the active transcription factor HIF1. HIF1 target genes are involved in diverse biological pathways including proliferation, apoptosis, redox homeostasis, inflammation as well as metastasis and invasion (Semenza 2012a, Wenger et. al. 2005). However, the largest group of target genes is important for maintaining oxygen homeostasis and supply. Vascular endothelial growth factor (VEGF) is known as a major regulator of angiogenesis, and is responsible for increasing the distribution of the available oxygen throughout the cell (Takeda et. al. 2004). Together with glucose transporter 1 (Glut-1), which helps to rewire the metabolism from oxidative phosphorylation to glycolysis, we choose two well-characterized targets that play a major role in cell survival under hypoxic conditions in many different cell types (Takeda et. al. 2004, Hayashi et. al. 2004, Dengler et. al. 2014). As expected, we could show that TRAF6 overexpression increases the mRNA levels of VEGF and Glut-1, since TRAF6 increases HIF1α signaling (Sun et.al. 2013, Rezaeian et. al. 2017). Most notably, we were able to show that co-expression of RNF8 together with TRAF6 indeed reverts the expression levels of *VEGF* and *Glut1* back to basal levels. Our study reveals that HIF1α protein levels are decreased after expression of TRAF6 together with RNF8 causing a significant reduction of target gene activation compared to TRAF6 alone. These data prove a functional consequence of the downregulation of HIF1α and unravel a possible new tumor suppressor role of RNF8 by counteracting the HIF1α-driven cancer progression through TRAF6 (Rezaeian et. al. 2017). Angiogenesis and glucose metabolism play a crucial role in cancer biology and so does HIF1α regulation. It is well established that HIF1α overexpression is associated with increased patient mortality in numerous cancer types of different organs (Zhong et. al. 1999, Semenza 2003). Triple negative breast cancer (TNBC) is associated with high rate of recurrence, distant metastasis and poor overall survival (Elias 2010). HIF1α as well as RNF8 are known to be overexpressed in TNBC; nevertheless, there is no study connecting both proteins to our knowledge. Our findings reveal the reduction of HIF1α

by RNF8 and TRAF6, which should be further analyzed in tumorigenesis. Indeed, the downregulation of HIF1α was shown to reduce tumor growth in xenograft models (Bharti et. al. 2018). The interplay of RNF8, TRAF6 and HIF1α should be investigated in a variety of tissues to increase the chance to identify new therapeutic targets. Not only breast cancer, but also cancers of the brain, cervix, oropharynx, ovary and uterus are associated with HIF1α overexpression and should be included in future studies (Zhong et. al. 1999, Semenza 2003).

# 6. Conclusion and perspectives

The E3 Ligase RNF8 has been closely related with tumorigenesis and cancer progression through its role in DNA damage response as well as telomere protection, cell cycle control and transcriptional regulation. Deciphering these functions of RNF8 may help identify new strategies for cancer treatment. Using a genome-wide Y2H screen, we could identify HIF1α as new interaction partner of RNF8. The interaction of HIF1α and RNF8 was verified by Y2H dependency tests and co-IPs in human embryonic kidney cells. It could be demonstrated that the interaction is independent of the catalytic activity of RNF8 and relies on its N-terminal FHA domain as well as the TAD domain of HIF1α. Further binding studies revealed the additional binding of TRAF6 to RNF8 and of TRAF6 to HIF1α. The interaction of all three proteins seemed oxygen independent, nevertheless, TRAF6 binding is diminished in hypoxia compared to normoxic conditions. Functional analysis revealed that RNF8 counteracts the stabilization of HIF1α by TRAF6, resulting in significantly decreased target gene activation. Since TRAF6 and HIF1α overexpression are associated with increased patient mortality in a variety of cancers, we suggest this effect could be countered by RNF8 while joining the complex. Taken together, our results suggest a new tumor suppressor role for RNF8 through reverting the stabilization effects of TRAF6 on HIF1α. However, the exact mechanism of RNF8 and TRAF6 reducing HIF1α in the cell needs further investigation.

In a next step, *in vitro* assays should answer the question whether all three proteins build one complex to interact with each other or sequentially interact. Structural and cellular assays will be useful to determine necessary modifications for the interaction of RNF8 and HIF1α. We speculate about the involvement of a phospho-site on HIF1α for successful RNF8 interaction. To shed light into the regulatory mechanism between the three proteins, ubiquitination assays as well as proteasomal inhibitions assays will be helpful. The use of the small molecule inhibitor C25-140, which selectively inhibits the catalytic activity of TRAF6, will also provide insights whether additional regulatory factors are needed for the decreasing effect on HIF1α. Point mutation studies with TRAF6 will address this problem as well. Further work should investigate the

interaction dynamics in different cancer cell lines, since HIF1α overexpression is known to play a role in a variety of human organs.

# 7. Material and Methods

## 7.1 Material

### 7.1.1 Instruments and Equipment

| Instrument / Equipment | Source |
|---|---|
| Agarose Gel chambers | NeoLab, Munich |
| Amersham Hyperfilm ECL | GE Healthcare, Munich |
| Bacterial culture flasks | Schott, Zwiesel |
| Bacterial incubators | Sartorius, Göttingen; Memmert, Schwabach |
| Cell culture flasks/dishes | BD, Heidelberg; Nunc |
| Cell scraper | Sarstedt, Newton in USA |
| Cell viability analyzer – ViCell-XR | Beckman Coulter, Krefeld |
| Centrifuges<br>Cooling centrifuge cell culture 5810R<br>Cooling lab centrifuge 5417R | <br>Eppendorf, Hamburg<br>Eppendorf, Hamburg |
| $CO_2$ Incubator | Binder, Tuttlingen |
| Cover foil qPCR | 4titude, Berlin |
| Cryovials | Greiner, Frickenhausen |
| Cuvettes | Brand, Wertheim |
| Developer Optimas typ TR | MS Laboratory instruments, Wiesloch |
| Eppendorf tubes 1.5mL, 2mL | Eppendorf, Hamburg |
| Falcon Tubes | Neolab, Munich |
| Filter pipette tips – Tip One | StarLab, Hamburg |
| Fridge and freezers (-20°C, -80°C) | Liebherr, Ochsenhausen |
| Glass Bottles | Schott, Zwiesel |
| Heat blocks | Techne, Burlington, USA |
| Hypoxia culture chamber | Baker & Ruskinn, Bridgend in Wales |

| | |
|---|---|
| Ice machine – Scotsman AF20 | Scotsman ICE Systems, Vernon Hills, USA |
| Light Cycler 480 | Roche Diagnostics |
| Light Cycler 96 well plates | 4titude,Berlin |
| Magnetic stirrer | IKA Labortechnik, Staufen |
| Microscopes | Leica, Wetzlar |
| Microwave | SHARP, Hamburg |
| Nanodrop 2000 | Thermo Scientific, Rockford in USA |
| Petri dishes | Greiner Bio-One, Frickenhausen |
| pH meter (PB11) | Sartorius, Göttingen |
| Photometer | Eppendorf, Hamburg |
| Pipettes | Eppendorf, Hamburg |
| Pipette tips | Eppendorf, Hamburg |
| Pipetting aid – accu-jet pro | Brand, Werthiem |
| Plastic pipettes | Greiner Bio-One, Frickenhausen |
| Power supply | Consort, Turnhout in Belgium |
| Precision Scale – New Classic MS | Mettler Toledo, Gießen |
| Rotator – Intelli-Mixer | NeoLab, Heidelberg |
| PVDF Membrane | Millipore, Schwabach |
| Scalpel | B. Braun, Melsungen |
| SDS-PAGE gel chamber | Roth, Karlsruhe |
| Semi-dry blotter | Roth, Karlsruhe |
| Syringes | B. Braun, Melsungen |
| Thermocycler – Mastercycler Gradient | Eppendorf, Hamburg |
| Thermomixer comfort | Eppendorf, Hamburg |
| Tissue culture hoods | Nunc, Wiesbaden |
| Ultra-pure water system – Milli-Q Plus | Merck, Millipore, Darmstadt |
| UV-table | Herolab, Wiesloch |
| Vortexer | Scientific Industries, Bohemia in USA |
| Whatman Paper | Roth, Karlsruhe |
| Water-jet vacuum pump | Schott, Zwiesel |

| | |
|---|---|
| Yeast incubator BM600 | Memmert GmbH and Co.KG,<br>Büchenbach |

### 7.1.2 Chemicals

| Chemical | Source |
|---|---|
| Acrylamide/Bisacrylamid | Roth, Karlsruhe |
| Agarose | Biozym, Hessisch Oldenburg |
| Amino acids for S. cerevisiae media | Roth, Karlsruhe |
| Ammonium persulfate (APS) | BioRad, Munich |
| Ampicillin | Roth, Karlsruhe |
| Aureobasidin A | Clontech, Takara Europe France |
| Bacto Peptone | Roth, Karlsruhe |
| Biotin | Sigma-Aldrich, Taufkirchen |
| Boric Acid | Roth, Karlsruhe |
| Bovine serum albumin (BSA) | Sigma-Aldrich, Taufkirchen |
| Calcium Chloride ($CaCl_2$) | Roth, Karlsruhe |
| Chloramphenicol | Roth, Karlsruhe |
| Deoxycholate | Roth, Karlsruhe |
| Dithiothreitol (DTT) | Sima-Aldrich, Taufkirchen |
| DNA 1 kb plus ladder | Thermo Fisher Scientific, Waltham USA |
| dNTPs | Fermentas, St. Leon-Roth |
| Cobald chloride ($CoCl_2$) | Sigma-Aldrich, Taufkirchen |
| Dulbecco´s modified eagle medium (DMEM) | Life Technologies, Darmstadt |
| Dulbecco´s modified eagle medium, high Glucose (DMEM+GlutaMax) | Life Technologies, Darmstadt |
| Ethanol (EtOH, p. a.) | Merck, Darmstadt |
| Ethidium Bromide (EtBr) | Roth, Karlsruhe |
| Ethylenediaminetetraacetic acid (EDTA) | Roth, Karlsruhe |
| Fetal calf serum (FCS) | Life Technologies, Darmstadt |
| Gel Loading Dye, Purple (6 x) | NEB, Frankfurt |
| GFP-TRAP agarose | Chromotek, Martinsried |

| | |
|---|---|
| Glucose a-Monohydrat | Roth, Karlsruhe |
| Glycerol | Roth, Karlsruhe |
| HEPES | Roth, Karlsruhe |
| Isopropanol p.a. | Merck, Darmstadt |
| Kanamycin | Roth, Karlsruhe |
| LB-Agar | Roth, Karlsruhe |
| LB-medium | Roth, Karlsruhe |
| Lithiumacetate | Roth, Karlsruhe |
| Magnesium Chloride | Roth, Karlsruhe |
| Monopotassium phosphate ($KH_2PO_4$) | Roth, Karlsruhe |
| Non essential amino acids (NEAA) | Life Technologies, Darmstadt |
| Nonidet P40 substitute (NP-40) | Sigma-Aldrich, Taufkirchen |
| Opti-MEM reduced serum media | Life Technologies, Darmstadt |
| PageRuler Prestained Protein Ladder | Thermo Fisher Scientific, Waltham USA |
| Penicillin-Streptomycin (10 000 U/ml) | Thermo Fisher Scientific, Waltham USA |
| Phosphate buffered saline (PBS) 10 x | Applichem, Darmstadt |
| Protease/Phosphatase-inhibitor RocheComplete | Roche Diagnostics, Mannheim |
| Roti-load 4 x SDS loading buffer | Roth, Karlsruhe |
| SOC outgrowth medium | New England Biolabs, Frankfurt |
| Sodium chloride (NaCl) | Roth, Karlsruhe |
| Sodium dodecyl sulfate (SDS) | Roth, Karlsruhe |
| Sodium hydroxide (NaOH) | Roth, Karlsruhe |
| Sorbitol | Roth, Karlsruhe |
| Tetramethylethylenediamine (TEMED) | BioRad, Munich |
| Tris | Roth, Karlsruhe |
| Triton-X-100 | Roth, Karlsruhe |
| Trypsin (0.05%)/EDTA | Life technologies, Darmstadt |
| Tween-20 | Roth, Karlsruhe |
| UltraPure Salmon Sperm DNA solution | Life technologies, Darmstadt |
| Yeast extract | Roth, Karlsruhe |

| | |
|---|---|
| Yeast nitrogen base (Difco) | Roth, Karlsruhe |
| Western blotting detection (ECL substrate) 20x LumiGlo and 20x Peroxide | Cell signaling Technology, Frankfurt |
| X-α-Gal | Clontech, Takara Europe France |
| X-tremeGENE HP Transfection Reagent | Roche Diagnostics, Mannheim |

### 7.1.3 Antibodies

| Primary Antibody | Dilution in Western Blot | Source |
|---|---|---|
| ß-Actin I-19 | 1:1000 | Santa Cruz, Heidelberg |
| Gal4 AD | 1:1000 | Santa Cruz, Heidelberg |
| Gal4 BD | 1:1000 | Santa Cruz, Heidelberg |
| GFP | 1:1000 | Santa Cruz, Heidelberg |
| HIF1α | 1:1000 | Abcam, Cambridge in England |
| RNF8 | 1:1000 | Santa Cruz, Heidelberg |
| TRAF6 EP591Y | 1:2000 | Abcam, Cambridge in England |
| **Secondary Antibody** | **Dilution in Western Blot** | **Source** |
| Anti-Goat | 1:7500 | Dianova, Hamburg |
| Anti-Mouse | 1:7500 | Dianova, Hamburg |
| Anti-Rabbit | 1:7500 | Dianova, Hamburg |

### 7.1.4 Enzymes and Kits

| Enzyme / Kit | Source |
|---|---|
| Alkaline Phosphatase CIP | New England Biolabs, Frankfurt |
| Expand high fidelity kit | Roche Diagnostics, Mannheim |
| Gel extraction Kit | Qiagen, Hilden |
| KAPA SYBR Fast qPCR Kit (optimized for LC480) | VWR, Darmstadt |
| Matchmaker® Gold Y2H System | Clontech, Takara Europe France |

| | |
|---|---|
| Mate & Plate™ Library - Universal Human (Normalized) | Clontech, Takara Europe France |
| Nucleo Spin Plasmid Kit | Macherey-NagelDüern |
| QiaQuick Nucleotide removal kit | Qiagen, Hilden |
| Rapid DNA Ligation Kit | Roche Diagnostics, Mannheim |
| RNeasy Kit | Qiagen, Hilden |
| RQ1 RNase-free DNaseI | Promega, Mannheim |
| Shredder Kit | Qiagen, Hilden |
| Super Script III First Strand cNDA Synthesis System for RT-PCR | Life Technologies, Darmstadt |
| Restriction endonucleases (BamHI, EcoRI, NdeI, NotI, SacI, SalI, XmaI) | New England Biolabs, Frankfurt |

### 7.1.5 Bacterial Strain

TOP 10 *E.coli* — F- mcrA Δ(mrr-hsdRMS-mcrBC) Φ80lacZΔM15 ΔlacX74 recA1 araD139 Δ(ara-leu)7697 galU galK rpsL(StrR) endA1 nupG

### 7.1.6 Yeast strains

pJ697a — MATa trp1-901 LEU2-3,112 ura3-53 his3-200 gal4 gal80 GAL1-HIS3 GAL2-ADE2 met2::GAL7-lacZ

Y187 — MAT$\alpha$, ura3-52, his3-200, ade2-101, trp1-901, leu2-3, 112, gal4Δ, gal80Δ, met–, URA3 : : $GAL1_{UAS}$–$Gal1_{TATA}$–LacZ, MEL1

Y2HGold — MATa, trp1-901, leu2-3, 112, ura3-52, his3-200, gal4Δ, gal80Δ, LYS2 : : $GAL1_{UAS}$–$Gal1_{TATA}$–His3, $GAL2_{UAS}$–$Gal2_{TATA}$–Ade2, URA3 : : $MEL1_{UAS}$–$Mel1_{TATA}$ AUR1-C MEL1

### 7.1.7 Eukaryotic cell lines

| | |
|---|---|
| HEK293T | Human embryonal kidney cell line containing Adenovirus 5 DNA and SV40 large T-antigen |
| MDA-MB-231 | Human epithelial cells from mammary gland/breast, derived from metastatic site, pleural effusion Adenocarcinoma cell line |

### 7.1.8 Plasmids

| Vectors | Information |
|---|---|
| pEGFP-C1 | Clontech, N/A; GFP-tag |
| pEGFP-C1 GFP-RNF8 WT | N-terminal GFP-tag, EcoRI/SalI |
| pEGFP-C1 GFP-RNF8 ΔFHA | N-terminal GFP-tag, EcoRI/SalI |
| pEGFP-C1 GFP-RNF8 I□□□□ | N-terminal GFP-tag, EcoRI/SalI |
| pEGFP-C1 GFP-HIF1α □□ | N-terminal GFP-tag, SacI/SalI |
| pEF Flag | Modified pEF4 backbone (Scharschmidt et al., 2004); N-terminal 2xFlag-tag SEP |
| pEF Flag-RNF8 WT | N-terminal 2xFlag-tag, EcoRI/NotI |
| pEF Flag-RNF8 WT | N-terminal 2xFlag-tag, EcoRI/NotI |
| pEF Flag-TRAF6 WT | N-terminal 2xFlag-tag, EcoRI/NotI |
| pEF Flag-HIF1α WT | N-terminal 2xFlag-tag, BamHI/NotI |
| pEF Flag-HIF1α ΔΔΔ | N-terminal 2xFlag-tag, BamHI/NotI |
| pGBKT7 | Clonetech, Matchmaker Gold System |
| pGBKT7 RNF8 WT | EcoRI/SmaI |
| pGBKT7 RNF8 ΔFHA | EcoRI/SmaI |
| pGBKT7 RNF8 ΔRING | EcoRI/SmaI |
| pGBKT7 RNF8 FHA | EcoRI/XmaI |
| pGBKT7 RNF8 RING | EcoRI/SmaI |
| pGBKT7 RNF168 | EcoRI/SmaI |
| pGADT7 | Clonetech, Matchmaker Gold System |

| | |
|---|---|
| pGADT7 UBE2N WT | EcoRI/BamHI |
| pGADT7 HIF1α ?? | SmaI/BamHI |
| pGADT7 HIF1α TAD | XmaI/BamHI |
| pGADT7 SSR1 | EcoRI/XmaI |
| pGADT7 HERC2 HECT | EcoRI/SmaI |
| pGADT7 DNTTIP2 | NdeI/BamHI |
| pGADT7 Cul4a | XmaI/BamHI |
| pGADT7 Fam9B | EcoRI/XmaI |

### 7.1.9 Oligonucleotides

| qPCR oligonucleotides | Sequence |
|---|---|
| HIF1α for | 5´ CGT CGA AAA GAA AAG TCT CGA GAT 3´ |
| HIF1α rev | 5´ AGG CCT TAT CAA GAT GCG AAC T 3´ |
| VEGF for | 5´ CTC TAC CTC CAC CAT GCC AAG T 3´ |
| VEGF rev | 5´ GCT GCG CTG ATA GAC ATC CA 3´ |
| Glut1 for | 5´ GCG GGT TGT GCC ATA CTC AT 3´ |
| Glut1 rev | 5´ ACT TCA AAG AAG GCC ACA AAG C 3´ |
| RPL27 for | 5´ TCG CCA AGA GAT CAA AGA TAA 3´ |
| RPL27 rev | 5´ CTG AAG ACA TCC TTA TTG ACG 3´ |

### 7.1.10 Buffers and Solutions

| Buffer / solution | Composition |
|---|---|
| Blocking buffer | 3% BSA (PAA) in PBS-Tween20 (0.1%) |
| Blotting buffer (10 x) | 48 mM Tris; 39 mM Glycin; 0.037% SDS; 20% Methanol |
| GFP-TRAP wash buffer | 10 mM Tris/Cl, pH 7.5 at 4°C; 150 mM NaCl; 0.5 mM EDTA |
| HU sample buffer | 8 M Urea; 5% SDS; 1 mM EDTA; 1.5% DTT; 0.04% bromophenol blue |
| LB Agar | 40 g/l |

| | |
|---|---|
| LB medium | 25 g/l |
| PEG | 100 mM Lithiumacetate; 10 mM Tris/Cl, pH 8.0; 1 mM EDTA, pH 8.0; 40% (w/v) PEG-3350 |
| RIPA buffer | 10 mM Tris/Cl, pH 7.5 at 4°C; 150 mM NaCl; 0.5 mM EDTA; 0.1% SDS; 1% Triton-X-100; 1% Deoxycholate; Complete protease inhibitor |
| *S. cerevisiae* agar plates | 0.67% yeast nitrogen base (Difco); 0.2% dropout amino acid mix, 2% glucose; 2% agar dropout amino acid mix; 20 mg Try, His; 30 mg Leu; 50 mg Phe; 100 mg Glu, Asp; 150 mg Val; 200 mg Thr; 400 mg Ser |
| *S. cerevisiae* high-stringency agar plates | -Leu/-His/-Trp/-Ade yeast agar plates supplemented with 200 ng/ml Aureobasidin A and 40 µg/ml X-α–Gal |
| SDS buffer (10x) | 250 mM Tris; 2 M Glycine; 1% SDS |
| Separation gel buffer (5x) | 1.88 mM Tris/Cl, pH 8.8 |
| Separation gel | 375 mM Tris/Cl, pH 8.8; 10-12.5% Acrylamide; 0.1% SDS; 0.075% APS; 0.05% TEMED |
| SORB | 100 mM Lithiumacetate; 10 mM Tris/Cl, pH 8.0; 1 mM EDTA, pH 8.0; 1 M Sorbitol |
| Stacking gel buffer (4x) | 0.5 M Tris/Cl, pH 6.8 |
| Stacking gel | 125 mM Tris/Cl, pH 6.8; 5% Acrylamide; 0.1% SDS; 0.1% APS; 0.1% TEMED |
| TBE Buffer (20x) | 1 M Tris; 1 M Boric Acid; 20 mM EDTA; pH 8.3 |
| Yeast lysis buffer | 2 M NaOH + 7.5% β-mercaptoethanol |
| YPD medium for *S. cerevisiae* | 0.1 % Yeast extract; 0.2% Bacto Peptone; autoclave before adding 2% Glucose |

### 7.1.11 Software

| Software | Company |
|---|---|
| Adobe software CS5 | Adobe Systems incorporated, San Jose in USA |
| CLC Sequence Viewer | Qiagen, Hilden |
| Gene construction Kit | Textco BioSofteare, Raleigh in USA |
| LabImage 1D | Kapelan, Leipzig |
| LightCycler 480 Software | Roche Diagnostics, Mannheim |
| Micrososft Office 2011 | Microsoft, Redmond in USA |
| Nanodrop 2000 Software | Thermo Scientific, Rockford in USA |
| PRISM 6 | Graph Pad Software, La Jolla in USA |

## 7.2. Methods

### 7.2.1 Molecular biology methods

#### 7.2.1.1 Polymerase chain reaction (PCR)

For the amplification of DNA sequences by polymerase chain reaction (PCR), complementary DNA (cDNA) (for cDNA synthesis see 7.2.1.7) or plasmid DNA (Weber et. al. 2017) were used as templates. The samples were prepared as follows:

5 µl 10x Expand High Fidelity Buffer

1 µl dNTPs (10 mM)

1 µl forward primer (20 µM)

1 µl reverse primer (20 µM)

100 ng template DNA

1 µl DNA Polymerase (Expand High Fidelity Mix)

ad 50 µl $H_2O$

The following standard PCR program was used:

| Step | Temperature | Time | Cycles |
|---|---|---|---|
| Initial denaturation | 95°C | 4 min | 1 |
| Denaturation | 95°C | 30 sec | 30 |
| Annealing | Lowest primer melting temperature - 5°C | 30 sec | 30 |
| Elongation | 72°C | 1 min/kb | 30 |
| Final elongation | 72°C | 7 min | 1 |
| Cooling | 4°C | ∞ | 1 |

To introduce specific mutations or deletions we used site directed mutagenesis. This PCR based method uses two complementary oligonucleotide primers, containing the desired point mutation or deletion plus 10-15 flanking nucleotides complementary to the DNA template. The amplified DNA was assessed by Agarose gel electrophoresis and purified (see 7.2.1.2).

**7.2.1.2 Agarose gel electrophoresis and DNA gel extraction**

Isolation of DNA fragments was performed by gel electrophoresis. DNA samples (PCR product or restriction digest probes) were mixed with 6 x DNA loading buffer and subjected to electrophoresis using 1.5 % agarose gels containing 0.2 µg/ml ethidium bromide (agarose powder in 1 x TBE buffer plus ethidium bromide). Gels were run at 120 V in 1 x TBE buffer. DNA was visualized by UV-excitation due to intercalation of ethidium bromide into DNA. The size of the DNA fragments was estimated by comparison to standard size markers (2 log DNA ladder) and cut from the gel with a scalpel. DNA was extracted from agarose using a *Qiagen gel extraction kit* according to manufacturer´s instructions. Finally, DNA was eluted in 30 µl sterile $H_2O$ and further used for restriction digest and ligation.

**7.2.1.3 Restriction Digest**

Site directed cleavage of PCR products as well as plasmids was done using restriction enzymes and buffers from New England Biolabs. In general, 10-20 Units of the respective restriction enzyme were used to digest ~2 µg DNA for 2h at 37°C. To avoid

religation, the 5´ end of the vector DNA was dephosphorylated with 1 µl calf intestinal phosphatase (CIP) at 37°C, for another 30 minutes. Samples were separated by DNA gel electrophoresis and purified as described in 7.2.1.2. DNA concentration was photometrically determined measuring the absorbance at a wavelength of 260nm using the NanoDrop 2000 spectrophotometer.

#### 7.2.1.4 Ligation

For optimal ligation results, the molar ratio of dephosphorylated vector DNA to insert DNA was adjusted to 1:3. In general, 50 ng vector DNA was used, the amount of insert DNA was calculated by the following formula: ng insert = 3 x (bp insert/bp vector) x 50 ng). Vector DNA, Insert DNA, Ligase and Ligase buffers were mixed according to the manufacturer's instruction of the *Rapid DNA Ligation Kit* (Roche). Ligation was carried out for 30 minutes up to 4 h at room temperature (RT).

#### 7.2.1.5 Transformation of *E.coli*

For transformation, 100 µl competent TOP10 *E.coli* cells were mixed gently with the complete ligation reaction and incubated on ice for 30 minutes. Heat shock was performed at 42°C for 45 seconds followed by cooling the cells for 2 min on ice. Subsequently 900 µl SOC-medium was added and cells were incubated at 37°C for 60 minutes at 900 rpm. Selection of transformants was achieved by plating the cells on LB agar plates, containing the respective antibiotics. After incubation over night at 37°C, single bacterial colonies were picked and inoculated in 5 ml LB-medium. Upon shaking over night at 37°C, plasmid DNA was isolated following the *NucleoSpin plasmid Kit*. Eurofins Genomics (Ebersberg) performed all sequencing reactions.

#### 7.2.1.6 Isolation of plasmid DNA from *S.cerevisiae*

Isolation of plasmid DNA from yeast was done in an automated work-flow at the Max-Planck-Institute of Biochemistry by Jochen Rech.

#### 7.2.1.7 RNA extraction

To obtain RNA as template for cDNA synthesis, 1 x $10^6$ HeLa cells were pelleted and lysed according to the manufacturer instructions of the *Qiashredder kit*. As it is for quantitative realtime PCR experiments, all cells of one sample were lysed according

to the respective protocol. RNA was isolated following the instruction of the *Qiagen RNeasy kit* and subsequently treated with *DNAseI* (Promega) for 30 min at 37°C, to clear all RNA samples from genomic DNA. After inactivating the reaction (65°C for 15 min), RNA probes were stored at -80°C.

#### 7.2.1.8 cDNA synthesis and Quantitative Realtime PCR

RNA was transcribed into cDNA following the manufacturer's instructions of the *SuperScript III First Strand cDNA Synthesis System*. We used the provided random hexamers for reverse transcription. The amount of cDNA per sample was quantified using the LightCycler (LC480) system together with the *KAPA SYBR qPCR Kit* and one specific primer pair for each target gene of interest. The housekeeping gene RPL27 was used to control for the initial RNA level in each sample and normalize all target genes to that.

Sample preparation was done in a 96-well plate as follows:

1 µl forward primer (20 µM)

1 µl reverse primer (20 µM)

10 µl 2 x KAPA SYBRGreen master mix

6 µl $H_2O$

2 µl cDNA

The reaction mix was done for each primer pair per sample.

The 96 well plate was sealed and centrifuged for 2 min at 200 x g before performing the PCR reaction using the LC480 system with the following standardized program:

| Step | Temperature | Time | Cycles |
|---|---|---|---|
| Initial denaturation | 95°C | 10 min | 1 |
| Denaturation | 95°C | 10 sec | 35 |
| Annealing | 60°C | 10 sec | 35 |
| Elongation | 72°C | 10 sec | 35 |
| Generation of melting curves | 65°C – 95°C | 15 sec | 1 |

Melting curves are important to control the amplification of only one certain PCR product. The ΔΔCp method was used for relative quantification (Pfaffl 2001), thereby we normalized the Cp value of the target gene to the Cp value of the house keeping gene, RPL27. All results are from at least three biological replicates, shown as mean, +/- standard deviation of the mean. The statistical analysis was performed by PRISM, using the two-tailed unpaired t-test with statistical significance at p-value <0.05 (*= p-value <0.05).

### 7.2.2 Cell biological methods

#### 7.2.2.1 Storage of human cell lines

For long-term storage of cells, 1 x $10^6$ cells were pelleted (350 x g, 5 min), resuspended in 1 ml storage medium (DMEM, 20% FCS, 1% penicillin-streptomycin, 10% DMSO) and transferred into cryovials. Vials were frozen over night at -80°C in isopropanol containing freezing containers to slow down the freezing process (1°C per min). Frozen cells were stored in liquid nitrogen.

#### 7.2.2.2 Cultivation of human cell lines

All cell lines were maintained at 37°C and 5% $CO_2$ and grown in medium containing 1% penicillin-streptomycin as well as 10% fetal bovine serum (FCS). MDA-MB-231 and HEK293T cells were cultured in 750 ml cell culture flasks containing dulbeccos modified eagle medium high Glucose medium (DEME+GlutaMax) supplemented with 10% FBS, 1% Penicillin/Streptomycin and 1% NEAA (MDA-MB-231) or dulbeccos

modified eagle medium (DMEM) supplemented with 10% FBS, 1% Penicillin/Streptomycin (HEK293T) respectively. When reaching up to 90% confluence, cells were split. They were washed once with 1 x PBS and detached by 2 ml 0.5% Trypsin-EDTA. Trypsination was stopped by adding 8 ml complete culture medium. Finally, cells were diluted and seeded as required for further experiments.

#### 7.2.2.3 Inducing hypoxia or hypoxia mimicking conditions

To induce hypoxia in the cell, HEK293T cells and MDA-MB-231 cells were cultured in 0.1% $O_2$ and 5% $CO_2$ for 24 h. We used the hypoxia chamber (Baker & Ruskinn) to maintain low oxygen conditions. For harvesting, cells were transferred on ice right from the chamber. Fast procedure while washing the cells with PBS and during the final lysis was crucial.

To mimic hypoxic conditions, cells were treated with the hypoxia mimicking reagent $CoCl_2$ for 20 h. $CoCl_2$ powder was diluted in sterile $H_2O$ and 300 µM $CoCl_2$ or sterile water as control, was added to the cells. Cell number and well format differed dependent on the performed assay (summarized in 7.2.2.4).

#### 7.2.2.4 Transfection of human cells

HEK293T cells as well as MDA-MB-231 cells were transfected using *X-tremeGENE HP DNA transfection reagent* according to the manufacturer´s instructions. Opti-MEM reduced serum media was used for the incubation of DNA and transfection reagent. Cell number, well-format and DNA amount differed dependent on the performed assay, summarized in the following:

| Assay | Number of cells | Dish format | Volume (ml) | Transfection reaction mix |
|---|---|---|---|---|
| GFP-TRAP | 2 x $10^6$ | 10 cm | 10 ml | 200 µl Opti-MEM<br>+ 4 µg total DNA<br>+ 10 µl transf. reagent |
| Cell lysate probes | 3 x $10^6$ | 10 cm | 10 ml | 200 µl Opti-MEM +<br>4 µg total DNA<br>+ 10 µl transf. reagent |
| qPCR | 4 x $10^5$ | 6 cm | 3 ml | 200 µl Opti-MEM +<br>6 µg total DNA<br>+ 15 µl transf. reagent |

In general, cells were seeded a day prior to transfection and harvested 24 h post transfection. For the induction of hypoxic conditions, cells were additionally incubated for 24 h under low oxygen conditions, 10 h post transfection. Similar, if treated with the hypoxia-mimicking reagent, 10 h post transfection, cells were treated with 300 µM $CoCl_2$ or sterile water as control for another 20 h (7.2.2.3).

#### 7.2.2.5 Storage and cultivation of *S. cerevisiae*

Yeast cells were stored on agar plates at 4°C for up to two months. For long-term storage of yeast strains, freshly cultivated cells were used. Therefore, a fresh single yeast colony was inoculated in YPD medium and grown at 150 rpm over night at 30°C. Overnight cultures were diluted to 0.1 $OD_{600}$ with fresh medium and again grown at 30°C and 150 rpm till they reached $OD_{600}$ 0.6 - 0.9 (the mid-log phase). Finally, 500 µl yeast culture was gently mixed with 500 µl of 30% glycerol solution and stored at -80°C.

#### 7.2.2.6 Yeast colony PCR

The yeast colony was resuspended in 20 µl 0.02 M NaOH and lysed by mixing vigorously at 1400 rpm and 100°C for 5 min. To pellet all cell debris, the solution was centrifuged at max speed for 1 min. 4 µl of the supernatant was used as PCR template

together with oligonucleotides complementary to the 3´ end of the Gal4-AD gene. PCR reaction was otherwise performed as described in 7.2.1.1.

#### 7.2.2.7 Preparation of competent yeast

Yeast cells were grown to mid-log phase as described in 7.2.2.5 and harvested by centrifugation (500 x g, 5 min, RT). Pelleted cells were washed with ½ volume of sterile $H_2O$ followed by 1/10 SORB. After washing, cells were centrifuged again (500xg, 5 min) and resuspended in 360 µl SORB and 50 µl denatured carrier DNA (salmon sperm DNA solution). Competent yeast cells were stored at -80°C, in 50 µl aliquots.

#### 7.2.2.8 Trichloroacetic acid (TCA) protein precipitation

A total of 1 $OD_{600}$ yeast cells were pelleted and resuspended in 1 ml ice-cold dd$H_2O$ with 150 µl ice-cold yeast lysis buffer and incubated on ice for 15 min. The proteins were precipitated by the addition of 150 µl 55% TCA, followed by incubation on ice for 15 min. The precipitated material was pelleted by two rounds of centrifugation (20,000 g, 15 min, 4°C). The supernatant was removed. Denaturated proteins were then resuspended in 100 µl HU sample buffer and heated at 65°C for 5 min. Proteins were separated by SDS Page and analyzed by antibody detection on western blot membranes.

#### 7.2.2.9 Yeast-two-hybrid (Y2H) assay

Protein-protein interactions were analyzed in living yeast cells using the Gal4 based Yeast-two-hybrid system. By cloning the proteins of interest in the pGBKT7 (bait) or the pGADT7 (prey) vector, the bait protein is expressed as fusion to the Gal4 DNA binding domain (BD domain) while the prey protein is expressed as fusion to the Gal4 activating domain (AD domain). In Y2H, if bait and prey interacted, the Gal4 BD and AD were brought into close proximity to reconstitute the transcription factor Gal4. Active Gal4 was able to activate the transcription of the reporter genes *His3* or *Ade2*. Y2H specific yeast strains, which are auxotrophic for leucin, tryptophane, histidine and adenin were used, allowing the selection for successfully transformed cells on leucin and tryptophane lacking media (-Leu/-Trp) due to TRP1 an LEU2 markers at the respective plasmids. Only if bait and prey interact, Gal4 is able to transcribe the

reporter gene *HIS3* and *Ade2* enabling cells to grow on histidine or adenine lacking media (-His, -Ade).

#### 7.2.2.10 Transformation of yeast cells

For transformation, 1 µl plasmid DNA was added to 10 µl competent yeast (7.2.2.7) and subsequently mixed with 360 µl PEG medium. After incubation for 30 min at room temperature (RT), cells were heated at 42°C for 15 min. Yeast cells were pelleted by centrifugation (200 x g, 5 min, RT) and resuspended in 100 µl sterile $H_2O$. The whole 100 µl were plated on -Leu/-Trp dropout plates to select for successful transformed yeast and incubated at 30°C for 3-5 days. Positive protein-protein interactions were tested on -Leu/-Trp/-His or -Leu/-Trp/-Ade selection plates.

#### 7.2.2.11 Yeast-two-hybrid (Y2H) – Screening approach

A yeast-two-hybrid screen was performed using the Matchmaker Gold System, purchased by Clontech, according to manufacturer's instructions. The DNA coding sequence of RNF8, amino acids 1-486, was amplified via PCR and cloned into the vector pGBKT7. RNF8 was used as bait (RNF8-BD) to screen a human normalized c-DNA library (Library-AD) from Clontech. The library represents a broad range of expressed genes, from a collection of adult human tissues, both male and female. It has been normalized to remove most abundant cDNAs derived from high-copy-number mRNAs and was transformed in the MAT$\alpha$ Gal4 reporter strain Y187 by Clontech. pGBKT7-RNF8 was tested for autoactivation and toxicity in the haploid MATa Gal4 reporter strain Y2HGold, using pGBKT7-empty as control. Further control experiments were done with pGADT7-UBE2N as positive control and PGADT7-empty as negative control, each transformed in the haploid Y187 strain (MAT$\alpha$ mating type), ready for mating with the haploid Y2HGold strain (MATa mating type). Similar amounts of freshly grown colonies of both yeast strains were mixed in 500µl YPD medium and incubated over night at 30°C, 200 rpm for the mating procedure. The next day, 100 µl of a 1/100 dilution was plated on -Leu, -Trp, -Leu/-Trp and -Leu/-Trp/-His agar plates, to select diploid cells. The number of colonies on the -Leu/-Trp/-His selection plate and the number of colonies on the -Trp selection plate were used to calculate the mating efficiency (percentage of diploids):

$$\left(\frac{No.of\frac{cfu}{ml}\,of\ diploids}{No.of\frac{cfu}{ml}of\ limiting\ partner}\right)x\ 100 = mating\ efficiency$$

A mating efficiency between 2-5% is considered good to screen (Matchmaker Gold user manual).

For the actual screen we combined 4-5 ml of a concentrated overnight culture of the bait strain (> 1x10$^8$ cells/ml of pGBKT7-RNF8 in Y2HGold) with 1 ml of the library strain in 45 ml YPD medium, as described in the Matchmaker Gold user manual. Mating was done at 30°C for 24 h at 50 rpm. After pelleting the cells (10 min 1000 x g at RT) and resuspending them in 10 ml fresh YPD medium, they were plated on 100 -Leu/-Trp/-His agar plates, using 100 µl per plate. After 5 days at 30°C, we counted 1600 colonies. All colonies were replated on high-stringency-plates (-Leu/-Trp/-His/-Ade selection plates, supplemented with X-$\alpha$-Gal and Aureobasidin A).

### 7.2.3 Biochemical and immunological methods

#### 7.2.3.1 SDS-Polyacrylamid Gelelektrophoresis (SDS-PAGE)

Proteins were separated according to their size through Sodium dodecyl sulfate polyacrylamide gel electrophoresis (SDS-Page). Proteins heated in presence of SDS denature into their primary polypeptides and gain an overall identical negative charge density. These polypeptides, migrating in an electric field towards the positive anode, can then be separated in a porous gel according to their size with smaller proteins migrating faster than larger ones. Different amounts of acrylamide determined the pore size of the separation gel (10%). To induce polymerization of the gels, ammonium persulfate (APS) and TEMED were added. During the polymerization process, the separation gel was covered with isopropanol to even out the surface. 5% stacking gel was added on top of the fully polymerized separation gel, containing pockets for sample loading. The different samples were mixed with SDS loading buffer (Roti load) and incubated at 95°C for 5 min. Afterwards they were centrifuged at 11000 rpm for 5 minutes. 10 µl of the sample was loaded on 10% SDS gel. As a standard, 4 µl of PageRuler PrestainedPlus Protein Ladder was used. The low pH in the stacking gel and the comparatively high concentration of Acrylamid in running gel concentrates all proteins at a narrow line at the beginning of the running gel, after the voltage was

applied. The gel was run in 1 x SDS gel electrophoresis buffer, at 120 V until the blue gel front reaches the end of the gel (~90 minutes).

#### 7.2.3.2 Western Blot and immunodetection

Following separation by SDS-PAGE, the proteins were transferred to a PVDF-membrane using a semi-dry Western blot system. The PVDF-membrane was activated by hydration in 100% methanol for 10 min and subsequently soaked in blotting buffer together with Whatman filter papers. Upon placing the SDS-gel and the PVDF-membrane in between Whatman papers in the blotting device, the transfer proceeded 55 min at 300 mA for one single blot, and 90 min at 160 mA - 320 mA (80 mA multiplied by the number of blots), for more than one blot. The membrane was blocked in 3% BSA in PBS-Tween20 (PBS-T) for at least one hour, to cover unspecific binding sites. The primary antibody (diluted in 1.5% BSA in PBS-T) was incubated with the membrane over night at 4°C. Having washed the membrane 3 x in PBS-T for 15 min, the horseradish peroxidase (HRP) conjugated secondary antibody (1:7500 in 9 ml PBS-T, 3 ml 3% BSA in PBS-T) was added and incubated for 1 h at room temperature. Membrane was washed 3 x in PBS-T for 15min before the LumiGLO/Peroxide westernblot substrates were used according to the manufacturer's instructions. The blot was exposed to an x-ray film and the film was developed. For detection of another protein on the same membrane, the membrane was incubated in stripping buffer for at least 60 minutes at RT. After washing the membrane 5 x in PBS-T for 10 min, the next primary antibody was applied.

#### 7.2.3.3 GFP-TRAP Assay

For transient overexpression of proteins, 2 x $10^6$ HEK293T cells were seeded in a 10 cm dish and transfected the next day as described in 7.2.2.4. We used 2 µg DNA per construct, transfecting 4 µg total DNA per plate. For lysis, cells were rinsed with PBS before adding 200 µl ice-cold RIPA buffer. After scraping the cells from the plate they were repeatedly passed through a syringe (26G) for sufficient cell disruption. After rotating the cell suspension for 30 min at 4°C end-over-end, all cell debris was pelleted by centrifugation (20 min, 4°C, 20 000 x g). The supernatant was transferred to a new tube and diluted with 300 µl GFP-TRAP wash buffer. 50 µl of the diluted supernatant

was mixed with 20 µl SDS loading buffer as lysate control sample. The remaining solution was incubated with 20 µl of pre-washed GFP-TRAP beads (wash 3 x in 1 ml GFP-TRAP wash buffer at 2500 x g and 4°C for 2 min) on a rotator for 1 h at 4°C end-over-end. To pull down GFP-tagged proteins, samples were centrifuged at 2500 x g for 2 min. Pelleted beads were washed 3 x with 1 ml GFP-TRAP wash buffer. Supernatant was completely removed from the beats before adding 50 µl SDS loading buffer to elute all proteins. TRAP eluates as well as lysate control samples were heated at 100°C for 5 min and separated by SDS-PAGE. Proteins were analyzed by antibody detection on western blot membranes.

# 8. References

Acloque H, Adams MS, Fishwick K, Bronner-Fraser M, Nieto MA (2009). Epithelial-mesenchymal transitions: the importance of changing cell state in development and disease. *J Clin Invest.* 2009;119(6):1438-1449.

Akutsu M, Dikic I, Bremm A (2016). Ubiquitin chain diversity at a glance. *J Cell Sci.* 2016;129(5):875-880.

Angers S, Li T, Yi X, MacCoss MJ, Moon RT, Zheng N (2006). Molecular architecture and assembly of the DDB1-CUL4A ubiquitin ligase machinery. *Nature.* 2006;443(7111):590-593.

Ansieau S, Morel AP, Hinkal G, Bastid J, Puisieux A (2010). TWISTing an embryonic transcription factor into an oncoprotein. *Oncogene.* 2010;29(22):3173-3184.

Bashton M, Chothia C (2007). The generation of new protein functions by the combination of domains. *Structure.* 2007;15(1):85-99.

Bauer KR, Brown M, Cress RD, Parise CA, Caggiano V (2007). Descriptive analysis of estrogen receptor (ER)-negative, progesterone receptor (PR)-negative, and HER2-negative invasive breast cancer, the so-called triple-negative phenotype: a population-based study from the California cancer Registry. *Cancer.* 2007;109(9):1721-1728.

Behrends C, Harper JW (2011). Constructing and decoding unconventional ubiquitin chains. *Nat Struct Mol Biol.* 2011;18(5):520-528.

Bekker-Jensen S, Rendtlew Danielsen J, Fugger K, et. al. (2010). HERC2 coordinates ubiquitin-dependent assembly of DNA repair factors on damaged chromosomes. *Nat Cell Biol.* 2010;12(1):80-12.

Bento CF, Fernandes R, Ramalho J, et. al. (2010). The chaperone-dependent ubiquitin ligase CHIP targets HIF-1α for degradation in the presence of methylglyoxal. *PLoS One.* 2010;5(11):e15062. Published 2010 Nov 29.

Berndsen CE, Wolberger C (2014). New insights into ubiquitin E3 ligase mechanism. Nat *Struct Mol Biol.* 2014;21(4):301-307.

Berra E, Benizri E, Ginouvès A, Volmat V, Roux D, Pouysségur J (2003). HIF prolyl-hydroxylase 2 is the key oxygen sensor setting low steady-state levels of HIF-1alpha in normoxia. *EMBO J.* 2003;22(16):4082-4090.

Bertout JA, Patel SA, Simon MC (2008). The impact of O2 availability on human cancer. *Nat Rev Cancer*. 2008;8(12):967-975.

Bharti SK, Mironchik Y, Wildes F, et. al. (2018). Metabolic consequences of HIF silencing in a triple negative human breast cancer xenograft. *Oncotarget*. 2018;9(20):15326-15339. Published 2018 Feb 24.

Bray F, Ferlay J, Soerjomataram I, Siegel RL, Torre LA, Jemal A (2018). Global cancer statistics 2018: GLOBOCAN estimates of incidence and mortality worldwide for 36 cancers in 185 countries. *CA Cancer J Clin.* 2018;68(6):394–424.

Bremm A, Moniz S, Mader J, Rocha S, Komander D (2014). Cezanne (OTUD7B) regulates HIF-1α homeostasis in a proteasome-independent manner. *EMBO Rep.* 2014;15(12):1268-1277.

Brenke JK, Popowicz GM, Schorpp K, Rothenaigner I, Roesner M, Meininger I, Kalinski C, Ringelstetter L, R'kyek O, Jürjens G, Vincendeau M, Plettenburg O, Sattler M, Krappmann D, Hadian K (2018). Targeting TRAF6 E3 ligase activity with a small-molecule inhibitor combats autoimmunity. *J Biol Chem.* 2018 Aug 24;293(34):13191-13203.

Brückner A, Polge C, Lentze N, Auerbach D, Schlattner U (2009). Yeast two-hybrid, a powerful tool for systems biology. *Int J Mol Sci.* 2009;10(6):2763-2788. Published 2009 Jun 18.

Cancer Genome Atlas Network. Comprehensive molecular portraits of human breast tumours (2012). *Nature.* 2012;490(7418):61-70.

Caufield JH, Sakhawalkar N, Uetz P (2012). A comparison and optimization of yeast two-hybrid systems. *Methods.* 2012;58(4):317-324.

Chahwan R, Gravel S, Matsusaka T, Jackson SP (2013). Dma/RNF8 proteins are evolutionarily conserved E3 ubiquitin ligases that target septins. *Cell Cycle.* 2013;12(6):1000-1008.

Chamboredon S, Ciais D, Desroches-Castan A, et. al. (2011). Hypoxia-inducible factor-1α mRNA: a new target for destabilization by tristetraprolin in endothelial cells. *Mol Biol* Cell. 2011;22(18):3366-3378.

Chen H, Shan J, Liu J, et. al. (2020). RNF8 promotes efficient DSB repair by inhibiting the pro-apoptotic activity of p53 through regulating the function of Tip60. *Cell Prolif.* 2020;53(3):e12780.

Conway EM, Collen D, Carmeliet P (2001). Molecular mechanisms of blood vessel growth. *Cardiovasc Res.* 2001;49(3):507-521.

Cramer T, Yamanishi Y, Clausen BE, et. al. (2003). HIF-1alpha is essential for myeloid cell-mediated inflammation. *Cell.* 2003;112(5):645-657.

Dang EV, Barbi J, Yang HY, et. al. (2011). Control of T(H)17/T(reg) balance by hypoxia-inducible factor 1. *Cell.* 2011;146(5):772-784.

Dengler VL, Galbraith M, Espinosa JM (2014). Transcriptional regulation by hypoxia inducible factors. *Crit Rev Biochem Mol Biol.* 2014;49(1):1-15.

Dent R, Trudeau M, Pritchard KI, et. al. (2007). Triple-negative breast cancer: clinical features and patterns of recurrence. *Clin Cancer Res.* 2007;13(15 Pt 1):4429-4434.

Deshaies RJ, Joazeiro CA (2009). RING domain E3 ubiquitin ligases. *Annu Rev Biochem.* 2009;78:399-434.

Doil C, Mailand N, Bekker-Jensen S, et. al. (2009). RNF168 binds and amplifies ubiquitin conjugates on damaged chromosomes to allow accumulation of repair proteins. *Cell.* 2009;136(3):435-446.

Dong Y, Zhang T, Li X, Yu F, Guo Y (2019). Comprehensive analysis of coexpressed long noncoding RNAs and genes in breast cancer. J Obstet Gynaecol Res. 2019;45(2):428-437. doi:10.1111/jog.13840

Dove KK, Klevit RE (2017). RING-Between-RING E3 Ligases: Emerging Themes amid the Variations. *J Mol Biol.* 2017;429(22):3363-3375.

Durocher D, Henckel J, Fersht AR, Jackson SP (1999). The FHA domain is a modular phosphopeptide recognition motif. *Mol Cell.* 1999;4(3):387-394.

Durocher D, Taylor IA, Sarbassova D, et. al. (2000). The molecular basis of FHA domain:phosphopeptide binding specificity and implications for phospho-dependent signaling mechanisms. *Mol Cell.* 2000;6(5):1169-1182.

Eletr ZM, Huang DT, Duda DM, Schulman BA, Kuhlman B (2005). E2 conjugating enzymes must disengage from their E1 enzymes before E3-dependent ubiquitin and ubiquitin-like transfer. *Nat Struct Mol Biol.* 2005;12(10):933-934.

Elias AD (2013). Triple-negative breast cancer: a short review. *Am J Clin Oncol.* 2010;33(6):637-645.

Fei C, Li Z, Li C, et. al. (2013). Smurf1-mediated Lys29-linked nonproteolytic polyubiquitination of axin negatively regulates Wnt/β-catenin signaling. *Mol Cell Biol.* 2013;33(20):4095-4105.

Fields S, Song O (1989). A novel genetic system to detect protein-protein interactions. *Nature.* 1989;340(6230):245-246.

Flügel D, Görlach A, Michiels C, Kietzmann T (2007). Glycogen synthase kinase 3 phosphorylates hypoxia-inducible factor 1alpha and mediates its destabilization in a VHL-independent manner. *Mol Cell Biol.* 2007;27(9):3253-3265.

Fritsch J, Stephan M, Tchikov V, et. al. (2014). Cell fate decisions regulated by K63 ubiquitination of tumor necrosis factor receptor 1. *Mol Cell Biol.* 2014;34(17):3214-3228.

Fu C, An N, Liu J, et. al. (2020). The transcription factor ZFHX3 is crucial for the angiogenic function of hypoxia-inducible factor 1α in liver cancer cells [published online ahead of print, 2020 Apr 10]. *J Biol Chem.* 2020;jbc.RA119.012131.

Gatti M, Pinato S, Maiolica A, et. al. (2015). RNF168 promotes noncanonical K27 ubiquitination to signal DNA damage. *Cell Rep.* 2015;10(2):226-238.

Geng H, Harvey CT, Pittsenbarger J, et. al. (2011). HDAC4 protein regulates HIF1α protein lysine acetylation and cancer cell response to hypoxia. *J Biol Chem.* 2011;286(44):38095-38102.

Geng H, Liu Q, Xue C, et. al. (2012). HIF1α protein stability is increased by acetylation at lysine 709. *J Biol Chem.* 2012;287(42):35496-35505.

Gilkes DM, Semenza GL (2013). Role of hypoxia-inducible factors in breast cancer metastasis. *Future Oncol.* 2013;9(11):1623-1636.

Gradin K, Takasaki C, Fujii-Kuriyama Y, Sogawa K (2002). The transcriptional activation function of the HIF-like factor requires phosphorylation at a conserved threonine. *J Biol Chem*. 2002;277(26):23508-23514.

Hayashi M, Sakata M, Takeda T, et. al. (2004). Induction of glucose transporter 1 expression through hypoxia-inducible factor 1alpha under hypoxic conditions in trophoblast-derived cells. *J Endocrinol.* 2004;183(1):145-154.

Hinz M, Stilmann M, Arslan SÇ, Khanna KK, Dittmar G, Scheidereit C (2010). A cytoplasmic ATM-TRAF6-cIAP1 module links nuclear DNA damage signaling to ubiquitin-mediated NF-κB activation. *Mol Cell.* 2010;40(1):63-74.

Ho YK, Zhi H, Bowlin T, et. al. (2015). HTLV-1 Tax Stimulates Ubiquitin E3 Ligase, Ring Finger Protein 8, to Assemble Lysine 63-Linked Polyubiquitin Chains for TAK1 and IKK Activation. *PLoS Pathog*. 2015;11(8):e1005102. Published 2015 Aug 18.

Hu CJ, Sataur A, Wang L, Chen H, Simon MC (2007). The N-terminal transactivation domain confers target gene specificity of hypoxia-inducible factors HIF-1alpha and HIF-2alpha. *Mol Biol Cell.* 2007;18(11):4528-4542.

Hu L, Xu J, Xie X, et. al. (2017). Oligomerization-primed coiled-coil domain interaction with Ubc13 confers processivity to TRAF6 ubiquitin ligase activity. *Nat Commun.* 2017;8(1):814. Published 2017 Oct 9.

Huang LE, Gu J, Schau M, Bunn HF (1998). Regulation of hypoxia-inducible factor 1alpha is mediated by an O2-dependent degradation domain via the ubiquitin-proteasome pathway. *Proc Natl Acad Sci U S A.* 1998;95(14):7987-7992.

Huen MS, Grant R, Manke I, et. al. (2007). RNF8 transduces the DNA-damage signal via histone ubiquitylation and checkpoint protein assembly. *Cell*. 2007;131(5):901-914.

Husnjak K, Dikic I (2012). Ubiquitin-binding proteins: decoders of ubiquitin-mediated cellular functions. *Annu Rev Biochem.* 2012;81:291-322.

Ikeda F (2015). Linear ubiquitination signals in adaptive immune responses. *Immunol Rev.* 2015;266(1):222-236.

Ito K, Adachi S, Iwakami R, et. al. (2001). N-Terminally extended human ubiquitin-conjugating enzymes (E2s) mediate the ubiquitination of RING-finger proteins, ARA54 and RNF8. Eur J Biochem. 2001;268(9):2725-2732.

Ivan M, Kondo K, Yang H, et. al. (2001). HIFalpha targeted for VHL-mediated destruction by proline hydroxylation: implications for O2 sensing. *Science.* 2001;292(5516):464-468.

Iyer NV, Kotch LE, Agani F, et. al. (1998). Cellular and developmental control of O2 homeostasis by hypoxia-inducible factor 1 alpha. *Genes Dev.*; 12(2):149-162.

Jacobs JJ (2012). Fusing telomeres with RNF8. *Nucleus.* 2012;3(2):143-149.

Jiang BH, Rue E, Wang GL, Roe R, Semenza GL (1996). Dimerization, DNA binding, and transactivation properties of hypoxia-inducible factor 1. *J Biol Chem.* 1996;271(30):17771-17778.

Jiang BH, Zheng JZ, Leung SW, Roe R, Semenza GL (1997). Transactivation and inhibitory domains of hypoxia-inducible factor 1alpha. Modulation of transcriptional activity by oxygen tension. *J Biol Chem.* 1997;272(31):19253-19260.

Jin L, Williamson A, Banerjee S, Philipp I, Rape M (2008). Mechanism of ubiquitin-chain formation by the human anaphase-promoting complex. *Cell*. 2008;133(4):653-665.

Kaelin WG Jr, Ratcliffe PJ (2008). Oxygen sensing by metazoans: the central role of the HIF hydroxylase pathway. *Mol Cell.* 2008; 30(4):393-402.

Kalousi A, Mylonis I, Politou AS, Chachami G, Paraskeva E, Simos G (2010). Casein kinase 1 regulates human hypoxia-inducible factor HIF-1. *J Cell Sci.* 2010; 123(Pt 17):2976-2986.

Kim JE, Minter-Dykhouse K, Chen J (2006). Signaling networks controlled by the MRN complex and MDC1 during early DNA damage responses. *Mol Carcinog.* 2006;45(6):403-408.

Koh MY, Darnay BG, Powis G (2008). Hypoxia-associated factor, a novel E3-ubiquitin ligase, binds and ubiquitinates hypoxia-inducible factor 1alpha, leading to its oxygen-independent degradation. *Mol Cell Biol.* 2008;28(23):7081-7095.

Kolas NK, Chapman JR, Nakada S, et. al. (2007). Orchestration of the DNA-damage response by the RNF8 ubiquitin ligase. *Science.* 2007;318(5856):1637-1640.

Komander D, Clague MJ, Urbé S (2009). Breaking the chains: structure and function of the deubiquitinases. *Nat Rev Mol Cell Biol.* 2009;10(8):550-563.

Komander D, Rape M (2012). The ubiquitin code. *Annu Rev Biochem.* 2012;81:203-229.

Kuang J, Li L, Guo L, et. al. (2016). RNF8 promotes epithelial-mesenchymal transition of breast cancer cells. *J Exp Clin Cancer Res.* 2016;35(1):88. Published 2016 Jun 4.

Kwon YT, Ciechanover A (2017). The Ubiquitin Code in the Ubiquitin-Proteasome System and Autophagy. *Trends Biochem Sci.* 2017;42(11):873-886.

Landazuri MO, Vara-Vega A, Vitón M, Cuevas Y, del Peso L (2006). Analysis of HIF-prolyl hydroxylases binding to substrates. *Biochem Biophys Res Commun.* 2006; 351(2):313-320.

Lando D, Peet DJ, Gorman JJ, Whelan DA, Whitelaw ML, Bruick RK (2002). FIH-1 is an asparaginyl hydroxylase enzyme that regulates the transcriptional activity of hypoxia-inducible factor. *Genes Dev.* 2002;16(12):1466-1471.

Lee A, Djamgoz MBA (2018). Triple negative breast cancer: Emerging therapeutic modalities and novel combination therapies. *Cancer Treat Rev.* 2018;62:110-122.

Lee HJ, Li CF, Ruan D, et. al. (2016). The DNA Damage Transducer RNF8 Facilitates Cancer Chemoresistance and Progression through Twist Activation. *Mol Cell.* 2016;63(6):1021-1033.

Lee JW, Ko J, Ju C, Eltzschig HK (2019). Hypoxia signaling in human diseases and therapeutic targets. *Exp Mol Med.* 2019;51(6):1-13. Published 2019 Jun 20.

Li J, Lee GI, Van Doren SR, Walker JC (2000). The FHA domain mediates phosphoprotein interactions. *J Cell Sci.* 2000;113 Pt 23:4143-4149.

Li L, Guturi KKN, Gautreau B, et. al. (2018). Ubiquitin ligase RNF8 suppresses Notch signaling to regulate mammary development and tumorigenesis. *J Clin Invest.* 2018;128(10):4525-4542.

Li L, Halaby MJ, Hakem A, et. al. (2010). Rnf8 deficiency impairs class switch recombination, spermatogenesis, and genomic integrity and predisposes for cancer. *J Exp Med*. 2010;207(5):983-997.

Lim JH, Lee YM, Chun YS, Chen J, Kim JE, Park JW (2010). Sirtuin 1 modulates cellular responses to hypoxia by deacetylating hypoxia-inducible factor 1alpha. *Mol Cell.* 2010;38(6):864-878.

Liu L, Lee S, Zhang J, et. al. (2009). CUL4A abrogation augments DNA damage response and protection against skin carcinogenesis. *Mol Cell.* 2009;34(4):451-460.

Liu YV, Baek JH, Zhang H, Diez R, Cole RN, Semenza GL (2007). RACK1 competes with HSP90 for binding to HIF-1alpha and is required for O(2)-independent and HSP90 inhibitor-induced degradation of HIF-1alpha. *Mol Cell.* 2007;25(2):207-217.

Lok GT, Sy SM, Dong SS, et. al (2012). Differential regulation of RNF8-mediated Lys48- and Lys63-based poly-ubiquitylation. *Nucleic Acids Res.* 2012;40(1):196-205.

Lorick KL, Jensen JP, Fang S, Ong AM, Hatakeyama S, Weissman AM (1999). RING fingers mediate ubiquitin-conjugating enzyme (E2)-dependent ubiquitination. *Proc Natl Acad Sci U S A.* 1999;96(20):11364-11369.

Lum JJ, Bui T, Gruber M, et. al. (1999). The transcription factor HIF-1alpha plays a critical role in the growth factor-dependent regulation of both aerobic and anaerobic glycolysis. *Genes Dev.* 2007;21(9):1037-1049.

Mahon PC, Hirota K, Semenza GL (2001). FIH-1: a novel protein that interacts with HIF-1alpha and VHL to mediate repression of HIF-1 transcriptional activity. *Genes Dev.* 2001;15(20):2675-2686.

Mailand N, Bekker-Jensen S, Faustrup H, et. al. (2007). RNF8 ubiquitylates histones at DNA double-strand breaks and promotes assembly of repair proteins. *Cell.* 2007;131(5):887-900.

Majmundar AJ, Wong WJ, Simon MC (2010). Hypoxia-inducible factors and the response to hypoxic stress. *Mol Cell.* 2010;40(2):294-309.

Martinez-Garay I, Jablonka S, Sutajova M, Steuernagel P, Gal A, Kutsche K (2002). A new gene family (FAM9) of low-copy repeats in Xp22.3 expressed exclusively in testis: implications for recombinations in this region. *Genomics.* 2002;80(3):259-267.

Masoud GN, Li W (2015). HIF-1α pathway: role, regulation and intervention for cancer therapy. *Acta Pharm Sin B.* 2015;5(5):378-389.

Mehla J, Caufield JH, Sakhawalkar N, Uetz P (2017). A Comparison of Two-Hybrid Approaches for Detecting Protein-Protein Interactions. *Methods Enzymol.* 2017;586:333-358.

Meng X, Grötsch B, Luo Y, et. al. (2018). Hypoxia-inducible factor-1α is a critical transcription factor for IL-10-producing B cells in autoimmune disease. *Nat Commun.* 2018;9(1):251. Published 2018 Jan 17.

Metzger MB, Pruneda JN, Klevit RE, Weissman AM (2014). RING-type E3 ligases: master manipulators of E2 ubiquitin-conjugating enzymes and ubiquitination. *Biochim Biophys Acta.* 2014;1843(1):47-60.

Meyer HJ, Rape M (2014). Enhanced protein degradation by branched ubiquitin chains. *Cell.* 2014;157(4):910-921.

Montagner M, Enzo E, Forcato M, et. al. (2012). SHARP1 suppresses breast cancer metastasis by promoting degradation of hypoxia-inducible factors. *Nature.* 2012;487(7407):380-384.

Morel AP, Hinkal GW, Thomas C, et. al. (2012). EMT inducers catalyze malignant transformation of mammary epithelial cells and drive tumorigenesis towards claudin-low tumors in transgenic mice. *PLoS Genet.* 2012;8(5):e1002723.

Mostowy S, Cossart P (2012). Septins: the fourth component of the cytoskeleton. Nat Rev *Mol Cell Biol.* 2012;13(3):183-194. Published 2012 Feb 8.

Möckli N, Deplazes A, Hassa PO, et. al. (2007). Yeast split-ubiquitin-based cytosolic screening system to detect interactions between transcriptionally active proteins. *Biotechniques.* 2007;42(6):725-730.

Mylonis I, Chachami G, Samiotaki M, et. al. (2006). Identification of MAPK phosphorylation sites and their role in the localization and activity of hypoxia-inducible factor-1alpha. *J Biol Chem.* 2006;281(44):33095-33106.

Nakayama M, Kikuno R, Ohara O (2002). Protein-protein interactions between large proteins: two-hybrid screening using a functionally classified library composed of long cDNAs. *Genome Res*. 2002;12(11):1773-1784.

Nijman SM, Luna-Vargas MP, Velds A, et. al. (2005). A genomic and functional inventory of deubiquitinating enzymes. *Cell.* 2005;123(5):773-786.

O'Rourke JF, Tian YM, Ratcliffe PJ, Pugh CW (1999). Oxygen-regulated and transactivating domains in endothelial PAS protein 1: comparison with hypoxia-inducible factor-1alpha. *J Biol Chem.* 1999;274(4):2060-2071.

Ohlsson C, Wallaschofski H, Lunetta KL, et. al. (2011). Genetic determinants of serum testosterone concentrations in men. *PLoS Genet.* 2011;7(10):e1002313.

Pao KC, Wood NT, Knebel A, et. al. (2018). Activity-based E3 ligase profiling uncovers an E3 ligase with esterification activity. *Nature.* 2018;556(7701):381-385.

Paul A, Wang B (2017). RNF8- and Ube2S-Dependent Ubiquitin Lysine 11-Linkage Modification in Response to DNA Damage. *Mol Cell.* 2017;66(4):458-472.e5.

Peuscher MH, Jacobs JJ (2011). DNA-damage response and repair activities at uncapped telomeres depend on RNF8. *Nat Cell Biol.* 2011;13(9):1139-1145. Published 2011 Aug 21.

Peyssonnaux C, Datta V, Cramer T, et. al. (2005). HIF-1alpha expression regulates the bactericidal capacity of phagocytes. *J Clin Invest.* 2005;115(7):1806-1815.

Pfaffl MW (2001). A new mathematical model for relative quantification in real-time RT-PCR. *Nucleic Acids Res.* 2001;29(9):e45.

Plans V, Guerra-Rebollo M, Thomson TM (2008). Regulation of mitotic exit by the RNF8 ubiquitin ligase. *Oncogene*. 2008;27(10):1355-1365.

Plans V, Scheper J, Soler M, Loukili N, Okano Y, Thomson TM (2006). The RING Finger Protein RNF8 recruits UBC13 lysine 63-based self ployubiquitylation. *J. Cell. Biochem,* 2006, 97 (3); 572-582

Primorac I, Musacchio A (2013). Panta rhei: the APC/C at steady state. *J Cell Biol.* 2013;201(2):177-189.

Rai R, Li JM, Zheng H, et. al. (2011). The E3 ubiquitin ligase Rnf8 stabilizes Tpp1 to promote telomere end protection. *Nat Struct Mol Biol.* 2011;18(12):1400-1407. Published 2011 Nov 20.

Rezaeian A., Li C., Wu C. et. al. (2017). A hypoxia-responsive TRAF6–ATM–H2AX signalling axis promotes HIF1α activation, tumorigenesis and metastasis. *Nat Cell Biol* 2017;19, 38–51.

Richard DE, Berra E, Gothié E, Roux D, Pouysségur J (1999). p42/p44 mitogen-activated protein kinases phosphorylate hypoxia-inducible factor 1alpha (HIF-1alpha) and enhance the transcriptional activity of HIF-1. *J Biol Chem.* 1999;274(46):32631-32637.

Rivkin E, Almeida SM, Ceccarelli DF, Juang Y.-C., MacLean T. A., Srikumar T., Huang H., Dunham W. H., Fukumura R., Xie G. et. al. (2013). The linear ubiquitin-specific deubiquitinase gumby regulates angiogenesis. *Nature.* 2013;498(7454):318-324.

Rotin D, Kumar S (2009). Physiological functions of the HECT family of ubiquitin ligases. *Nat Rev Mol Cell Biol.* 2009;10(6):398-409.

Rual JF, Venkatesan K, Hao T, et. al. (2005). Towards a proteome-scale map of the human protein-protein interaction network. *Nature*. 2005;437(7062):1173-1178.

Ryan HE, Lo J, Johnson RS (1998). HIF-1 alpha is required for solid tumor formation and embryonic vascularization. *EMBO J.* 1998;17(11):3005-3015.

Samanta D, Gilkes DM, Chaturvedi P, Xiang L, Semenza GL (2014). Hypoxia-inducible factors are required for chemotherapy resistance of breast cancer stem cells. *Proc Natl Acad Sci U S A*. 2014;111(50):E5429-E5438.

Samanta D, Semenza GL (2018). Metabolic adaptation of cancer and immune cells mediated by hypoxia-inducible factors. *Biochim Biophys Acta Rev Cancer.* 2018;1870(1):15-22.

Sato Y, Yoshizato T, Shiraishi Y, et. al. (2013). Integrated molecular analysis of clear-cell renal cell carcinoma. *Nat Genet.* 2013;45(8):860-867.

Scully R, Panday A, Elango R, Willis NA (2019). DNA double-strand break repair-pathway choice in somatic mammalian cells. *Nat Rev Mol Cell Biol.* 2019;20(11):698-714.

Seki N, Hattori A, Sugano S, et. al. (1998). Isolation, tissue expression, and chromosomal assignment of a novel human gene which encodes a protein with RING finger motif. *J Hum Genet.* 1998;43(4):272-274.

Semenza GL (2000). HIF-1 and human disease: one highly involved factor. Genes Dev. 2000;14(16):1983-1991.

Semenza GL (2003). Targeting HIF-1 for cancer therapy. *Nat Rev Cancer.* 2003;3(10):721-732.

Semenza GL (2012a). Hypoxia-inducible factors in physiology and medicine. *Cell.* 2012a; 148(3):399-408.

Semenza GL (2012b). Molecular mechanisms mediating metastasis of hypoxic breast cancer cells. *Trends Mol Med.* 2012b; 18(9):534-543.

Semenza GL, Wang GL (1992). A nuclear factor induced by hypoxia via de novo protein synthesis binds to the human erythropoietin gene enhancer at a site required for transcriptional activation. *Mol Cell Biol.* 1992;12(12):5447-5454.

Spratt DE, Walden H, Shaw GS (2014). RBR E3 ubiquitin ligases: new structures, new insights, new questions. *Biochem J.* 2014;458(3):421-437.

Stelzl U, Worm U, Lalowski M, et. al. (2005). A human protein-protein interaction network: a resource for annotating the proteome. *Cell.* 2005;122(6):957-968.

Sun H, Li XB, Meng Y, Fan L, Li M, Fang J (2013). TRAF6 upregulates expression of HIF1a and promotes tumor angiogenesis. *Cancer Res.* 2013;73(15):4950-4959.

Swiatek M, Jancewicz I, Kluebsoongnoen J, et. al. (2020). Various forms of HIF-1α protein characterize the clear cell renal cell carcinoma cell lines. *IUBMB Life.* 2020;72(6):1220-1232.

Takeda N, Maemura K, Imai Y, et. al. (2004). Endothelial PAS domain protein 1 gene promotes angiogenesis through the transactivation of both vascular endothelial growth factor and its receptor, Flt-1. *Circ Res.* 2004;95(2):146-153.

Takiuchi T, Nakagawa T, Tamiya H, et. al. (2014). Suppression of LUBAC-mediated linear ubiquitination by a specific interaction between LUBAC and the deubiquitinases CYLD and OTULIN. *Genes Cells.* 2014;19(3):254-272.

Tang N, Wang L, Esko J, et. al. (2004). Loss of HIF-1alpha in endothelial cells disrupts a hypoxia-driven VEGF autocrine loop necessary for tumorigenesis. *Cancer Cell*. 2004;6(5):485-495.

Taniguchi K, Karin M (2018). NF-κB, inflammation, immunity and cancer: coming of age. *Nat Rev Immunol. 2018*; 18(5):309-324.

Tanimoto K, Makino Y, Pereira T, Poellinger L (2000). Mechanism of regulation of the hypoxia-inducible factor-1 alpha by the von Hippel-Lindau tumor suppressor protein. *EMBO J.* 2000;19(16):4298-4309.

Thorslund T, Ripplinger A, Hoffmann S, et. al. (2015). Histone H1 couples initiation and amplification of ubiquitin signalling after DNA damage. *Nature.* 2015;527(7578):389-393.

Todd AE, Orengo CA, Thornton JM (2001). Evolution of function in protein superfamilies, from a structural perspective. *J Mol Biol.* 2001;307(4):1113-1143.

Tripathi E, Smith S (2017). Cell cycle-regulated ubiquitination of tankyrase 1 by RNF8 and ABRO1/BRCC36 controls the timing of sister telomere resolution. *EMBO J.* 2017;36(4):503-519.

Tsuzuki Y, Fukumura D, Oosthuyse B, Koike C, Carmeliet P, Jain RK (2000). Vascular endothelial growth factor (VEGF) modulation by targeting hypoxia-inducible factor-1alpha--> hypoxia response element--> VEGF cascade differentially regulates vascular response and growth rate in tumors. *Cancer Res.* 2000;60(22):6248-6252.

Uchida T, Rossignol F, Matthay MA, et. al. (2004). Prolonged hypoxia differentially regulates hypoxia-inducible factor (HIF)-1alpha and HIF-2alpha expression in lung epithelial cells: implication of natural antisense HIF-1alpha. *J Biol Chem*. 2004;279(15):14871-14878.

Vaupel P, Thews O, Hoeckel M (2001). Treatment resistance of solid tumors: role of hypoxia and anemia. *Med Oncol*. 2001;18(4):243-259.

Walczak H, Iwai K, Dikic I (2012). Generation and physiological roles of linear ubiquitin chains. *BMC Biol.* 2012;10:23. Published 2012 Mar 15.

Walsh MC, Lee J, Choi Y (2015). Tumor necrosis factor receptor- associated factor 6 (TRAF6) regulation of development, function, and homeostasis of the immune system. *Immunol Rev.* 2015;266(1):72-92.

Wang B, Merillat SA, Vincent M, et. al. (2016). Loss of the Ubiquitin-conjugating Enzyme UBE2W Results in Susceptibility to Early Postnatal Lethality and Defects in Skin, Immune, and Male Reproductive Systems. *J Biol Chem.* 2016;291(6):3030-3042.

Wang GL, Jiang BH, Rue EA, Semenza GL (1995). Hypoxia-inducible factor 1 is a basic-helix-loop-helix-PAS heterodimer regulated by cellular O2 tension. *Proc Natl Acad Sci U S A*. 1995;92(12):5510-5514.

Wang M, Chen X, Chen H, et. al. (2015). RNF8 plays an important role in the radioresistance of human nasopharyngeal cancer cells in vitro. *Oncol Rep.* 2015;34(1):341-349.

Wang S, Luo H, Wang C, et. al. (2017). RNF8 identified as a co-activator of estrogen receptor α promotes cell growth in breast cancer. *Biochim Biophys Acta Mol Basis Dis.* 2017;1863(6):1615-1628.

Wang Q, Liu X, Cui Y, et. al. (2014). The E3 ubiquitin ligase AMFR and INSIG1 bridge the activation of TBK1 kinase by modifying the adaptor STING. *Immunity*. 2014;41(6):919-933.

Weber E, Rothenaigner I, Brandner S, Hadian K, Schorpp K (2017). A High-Throughput Screening Strategy for Development of RNF8-Ubc13 Protein-Protein Interaction Inhibitors. *SLAS Discov.* 2017; 22(3):316–323.

Wenger RH, Stiehl DP, Camenisch G (2005). Integration of oxygen signaling at the consensus HRE. *Sci STKE.* 2005;2005(306):re12. Published 2005 Oct 18.

Wong BW, Kuchnio A, Bruning U, Carmeliet P (2013). Emerging novel functions of the oxygen-sensing prolyl hydroxylase domain enzymes. *Trends Biochem Sci.* 2013;38(1):3-11.

Wong CC, Gilkes DM, Zhang H, et. al. (2011). Hypoxia-inducible factor 1 is a master regulator of breast cancer metastatic niche formation. *Proc Natl Acad Sci U S A.* 2011;108(39):16369-16374.

Xie P (2013). TRAF molecules in cell signaling and in human diseases. *J Mol Signal.* 2013;8(1):7. Published 2013 Jun 13.

Xie Y, Varshavsky A (1999). The E2-E3 interaction in the N-end rule pathway: the RING-H2 finger of E3 is required for the synthesis of multiubiquitin chain. *EMBO J.* 1999;18(23):6832-6844.

Xu D, Yao Y, Lu L, Costa M, Dai W (2010). Plk3 functions as an essential component of the hypoxia regulatory pathway by direct phosphorylation of HIF-1alpha. *J Biol Chem.* 2010;285(50):38944-38950.

Ye Y, Rape M (2009). Building ubiquitin chains: E2 enzymes at work. *Nat Rev Mol Cell Biol.* 2009;10(11):755-764.

Yee Koh M, Spivak-Kroizman TR, Powis G (2008). HIF-1 regulation: not so easy come, easy go. *Trends Biochem Sci.* 2008;33(11):526-534.

Yin Q, Lin SC, Lamothe B, et. al. (2009). E2 interaction and dimerization in the crystal structure of TRAF6. *Nat Struct Mol Biol*. 2009;16(6):658-666.

Yuan WC, Lee YR, Lin SY, et. al. (2014). K33-Linked Polyubiquitination of Coronin 7 by Cul3-KLHL20 Ubiquitin E3 Ligase Regulates Protein Trafficking. *Mol Cell.* 2014;54(4):586-600.

Zhao MJ, Song YF, Niu HT, et. al. (2016). Adenovirus-mediated downregulation of the ubiquitin ligase RNF8 sensitizes bladder cancer to radiotherapy. *Oncotarget.* 2016;7(8):8956-8967.

Zhong H, De Marzo AM, Laughner E, et. al. (1999). Overexpression of hypoxia-inducible factor 1alpha in common human cancers and their metastases. *Cancer Res.* 1999;59(22):5830-5835.

Zhou T, Yi F, Wang Z, et. al. (2019). The Functions of DNA Damage Factor RNF8 in the Pathogenesis and Progression of Cancer. *Int J Biol Sci.* 2019;15(5):909-918. Published 2019 Mar 9.

Zimmerman ES, Schulman BA, Zheng N (2010). Structural assembly of cullin-RING ubiquitin ligase complexes. *Curr Opin Struct Biol*. 2010;20(6):714-721.

Zinngrebe J, Montinaro A, Peltzer N, Walczak H (2014). Ubiquitin in the immune system. *EMBO Rep.* 2014;15(1):28–45.

# 9. Abbreviations

| | |
|---|---|
| α-gal | alpha-galactosidase |
| AD | Activation Domain |
| Ade | Adenine |
| APC | Anaphase-promoting complex |
| ATM | Ataxia telangiectasia mutated |
| ATP | Adenosin-tri-phosphate |
| BARD1 | BRCA1-associated RING domain protein 1 |
| BD | Binding Domain |
| BRCA1 | Breast Cancer 1 |
| BRcat | benign-catalytic-activity |
| BRCT | BRCA1 C-terminus |
| cDNA | complementary DNA |
| cfu | colony forming unit |
| CHIP | carboxyl terminus of HSP70-interacting protein |
| cIAP | cellular inhibitor apoptosis protein |
| CRL | cullin-RING-Ligases |
| Cl | Chloride |
| C-terminal | carboxy-terminal |
| DNA | Desoxyribonucleic acid |
| DSB | double strand break |
| DUB | Deubiquitinase |
| EMT | epithelial-mesenchymal transition |
| ERα | □□□□□□□□□□□□□□□□□□□□lpha |
| FHA | Forkhead-associated-domain |
| Fig. | Figure |
| for | forward |
| g/kg | gram/kilogram |
| GSK3β | glycogen synthase kinase 3 β |
| GFP | green fluorescent protein |

| | |
|---|---|
| HAF | hypoxia associated factor |
| HECT | homology to E6AP C terminus |
| HEK | human embryonal kidney |
| HERC2 | HECT and RLD Domain Containing E3 Ubiquitin Protein Ligase 2 |
| HIF | hypoxia-inducible factor |
| □□□ | □□□□□□□□□□ |
| HOIL-1 | Heme-Oxidized IRP2 ubiquitin ligase 1 |
| HOIP | HOIL-1 interacting protein |
| HR | homologous recombination |
| IBR | in-between-RING |
| IFN | interferon |
| IL | interleukin |
| IL-1R | interleukin-1 receptor |
| Leu | Leucine |
| LPS | lipopolysaccharide |
| LUBAC | linear ubiquitin assembly complex |
| Lys | Lysine |
| MAT | Mating type locus (a or $\alpha$) |
| MDC1 | Mediator of DNA damage checkpoint 1 |
| MET-1 | Methionine-1 |
| min | minute |
| MRN | Mre1-Rad50-Nbs1 |
| mRNA | messenger RNA |
| µM/mM | micro-/mili-molar |
| µL/mL | micro-/mili-litre |
| NHEJ | nonhomologous end joining |
| NF-κB | nuclear factor “kappa-light-chain-enhancer” of activated B-cell |
| nM | Nanomolar |
| ns | not significant |
| N-terminal | amino-terminal |
| ODD | oxygen dependent degradation |
| OTU | ovarian tumor proteases |

| | |
|---|---|
| p- | phospho- |
| PAS | per-arnt-sim |
| Phe | Phenylalanine |
| pM | picomolar |
| POI | Protein of interest |
| PPI | protein-protein interaction |
| qPCR | quantitative real time polymerase chain reaction |
| RACK1 | Receptor protein kinase C |
| RBR | RING-between-RING |
| Rcat | required for catalysis |
| rev | reverse |
| RING | really interesting new gene |
| RNA | ribonucleic acid |
| RNF | RING finger protein |
| ROS | reactive oxygen species |
| SDS-PAGE | Sodium-Dodecyl-Sulfate-Polyacrylamide-Gelelectrophoresis |
| TAD | Transactivation Domain |
| Thr | Threonine |
| TLR | Toll-like receptor |
| TNBC | triple negative breast cancer |
| TNF$\alpha$ | tumor necrosis factor alpha |
| TNFR | tumor necrosis factor receptor |
| TRAF | TNFR associated factor |
| Trp | Tryptophane |
| Tyr | Tyrosine |
| Ub | Ubiquitin |
| UBE2N | Ubiquitin-conjugating enzyme E2 N |
| Uev1a | Ubiquitin-conjugating E2 variant 1a |
| WT | Wildtype |
| Y2H | yeast-two-hybrid |

# 10. Supplement

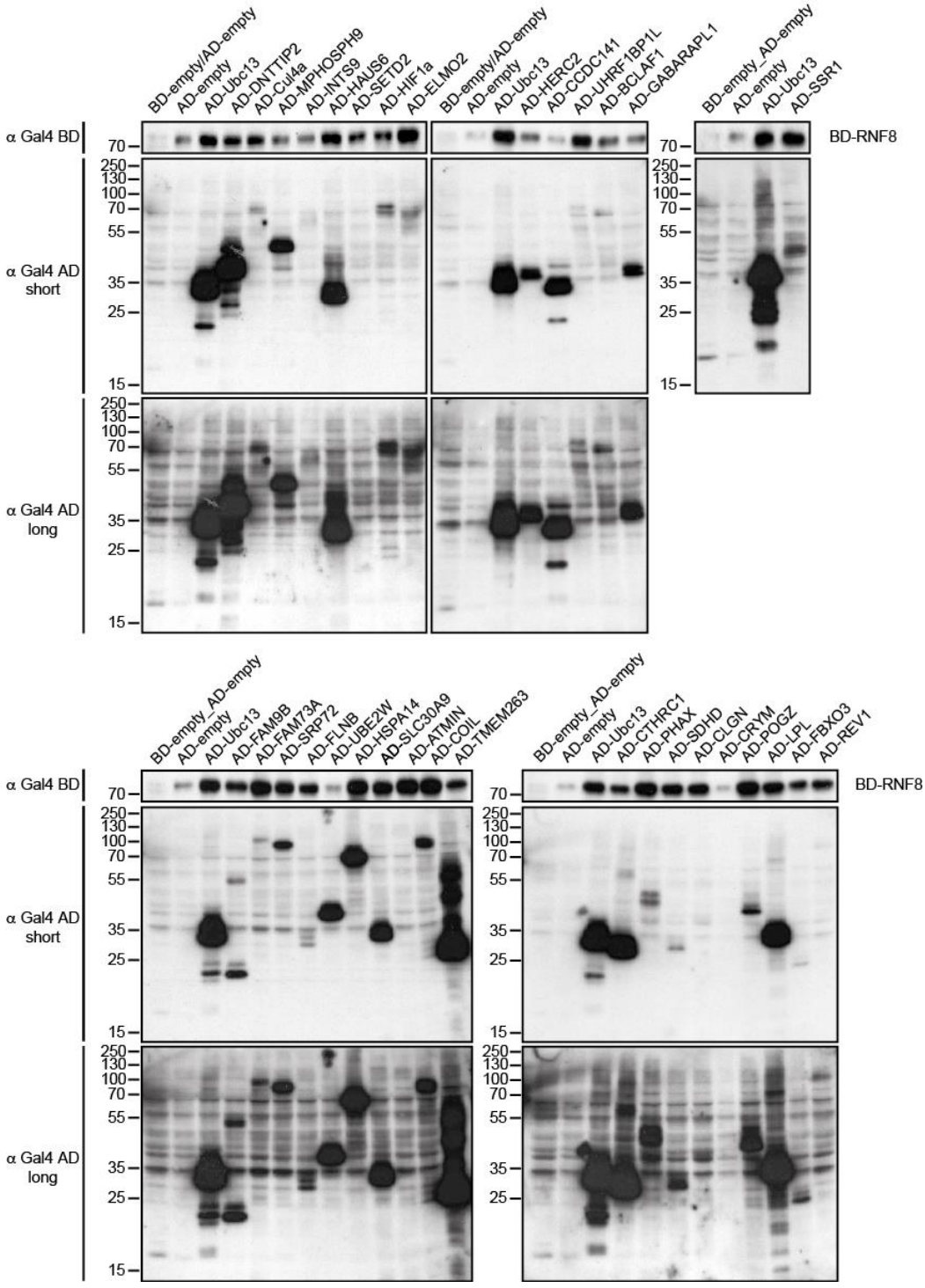


**Supplement 1: Expression levels of BD-RNF8 and the implicated AD-plasmid.** Protein extraction from 34 Y2H assays. RNF8 was used as bait (BD-RNF8) and 34 possible hits identified in the Y2H screen as prey (AD-plasmids as indicated). The expression levels were analyzed by western blot using antibodies against the Gal4 binding domain as well as the Gal4 activating domain.

# 11. Appendix

## 11.1 Publications

Kraft VAN, Bezjian CT, Pfeiffer S, **Ringelstetter L**, Müller C, Zandkarimi F, Merl-Pham J, Bao X, Anastasov N, Kössl J, Brandner S, Daniels JD, Schmitt-Kopplin P, Hauck SM, Stockwell BR, Hadian K, Schick JA. GTP Cyclohydrolase 1/Tetrahydrobiopterin Counteract Ferroptosis through Lipid Remodeling. *ACS Cent Sci.* 2020 Jan 22;6(1):41-53.

Brenke JK, Popowicz GM, Schorpp K, Rothenaigner I, Roesner M, Meininger I, Kalinski C, **Ringelstetter L**, R'kyek O, Jürjens G, Vincendeau M, Plettenburg O, Sattler M, Krappmann D, Hadian K (2018). Targeting TRAF6 E3 ligase activity with a small-molecule inhibitor combats autoimmunity. *J Biol Chem.* 2018 Aug 24;293(34):13191-13203.

## 11.2 Acknowledgement

I would like to thank my doctoral advisor Prof. Michael Groll for his great support, scientific advice and enthusiasm during the last years.

I also want to express my gratitude to my supervisor Dr. Kamyar Hadian, for providing this topic as well as reviewing my thesis. Thank you for all your time and empathy as well as the numerous possibilities to explore new fields. Your encouragement as well as your scientific and non-scientific support is very much appreciated.

Special thanks goes to Jochen Rech for the DNA preparation of yeast samples at the Max-Planck-Institute of Biochemistry.

I would like to thank all my fantastic colleagues of the Hadian group. Special thanks goes to Stefanie Brandner, Lisa Weber and Scarlett Dornauer. Your constant and generous help made (new) life possible. Thank you very much.

Jara Brenke and Kenji Schorpp have always been true superheroes. Thanks for guiding me in so many ways.

Finally, I am deeply grateful to all my family and friends. Mama, Papa, Gabriel, Severin, Alice, Anna, Simone, Steffi, Meike, Conny & Bernd: you made this so easy. Thank you.

Ein besonderer Dank geht an meine Eltern, die mich immer ermutigt und bedingungslos unterstützt haben.
Severin, du bist immer da und hältst mir den Rücken frei. Deine Ruhe und Zuversicht haben mein Leben so viel leichter gemacht.